



1 **Heterogeneous reactions of mineral dust aerosol: implications for**
2 **tropospheric oxidation capacity**

3 Mingjin Tang,^{1,*} Xin Huang,² Keding Lu,³ Maofa Ge,⁴ Yongjie Li,⁵ Peng Cheng,⁶ Tong Zhu,^{3,*}
4 Aijun Ding,² Yuanhang Zhang,³ Sasho Gligorovski,¹ Wei Song,¹ Xiang Ding,¹ Xinhui Bi,¹
5 Xinming Wang^{1,7,*}

6

7 ¹ State Key Laboratory of Organic Geochemistry and Guangdong Key Laboratory of
8 Environmental Protection and Resources Utilization, Guangzhou Institute of Geochemistry,
9 Chinese Academy of Sciences, Guangzhou, China

10 ² Joint International Research Laboratory of Atmospheric and Earth System Sciences
11 (JirLATEST), School of Atmospheric Sciences, Nanjing University, Nanjing, China

12 ³ State Key Joint Laboratory of Environmental Simulation and Pollution Control, College of
13 Environmental Sciences and Engineering, Peking University, Beijing, China

14 ⁴ Beijing National Laboratory for Molecular Sciences, State Key Laboratory for Structural
15 Chemistry of Unstable and Stable Species, Institute of Chemistry, Chinese Academy of
16 Sciences, Beijing, China

17 ⁵ Department of Civil and Environmental Engineering, Faculty of Science and Technology,
18 University of Macau, Avenida da Universidade, Taipa, Macau, China

19 ⁶ Institute of Mass Spectrometer and Atmospheric Environment, Jinan University, Guangzhou,
20 China

21 ⁷ Center for Excellence in Regional Atmospheric Environment, Institute of Urban
22 Environment, Chinese Academy of Sciences, Xiamen 361021, China

23

24 Correspondence: Mingjin Tang (mingjintang@gig.ac.cn), Tong Zhu (tzhu@pku.edu.cn),
25 Xinming Wang (wangxm@gig.ac.cn)



26 **Abstract**

27 Heterogeneous reactions of mineral dust aerosol with trace gases in the atmosphere could
28 directly and indirectly affect tropospheric oxidation capacity, in addition to aerosol
29 composition and physicochemical properties. In this article we provide a comprehensive and
30 critical review of laboratory studies of heterogeneous uptake of OH, NO₃, O₃, and their directly
31 related species as well (including HO₂, H₂O₂, HCHO, HONO, and N₂O₅) by mineral dust
32 particles. Atmospheric importance of heterogeneous uptake as sinks for these species are
33 assessed i) by comparing their lifetimes with respect to heterogeneous reactions with mineral
34 dust to lifetimes with respect to other major loss processes and ii) by discussing relevant field
35 and modelling studies. We have also outlined major open questions and challenges in
36 laboratory studies of heterogeneous uptake by mineral dust and discussed research strategies
37 to address them in order to better understand the effects of heterogeneous reactions with
38 mineral dust on tropospheric oxidation capacity.

39



40 **1 Introduction**

41 **1.1 Mineral dust in the atmospheres**

42 Mineral dust, emitted from arid and semi-arid regions with an annual flux of ~2000 Tg
43 per year, is one of the most abundant types of aerosol particles in the troposphere (Textor et al.,
44 2006; Huneus et al., 2011; Ginoux et al., 2012). After being emitted into the atmosphere,
45 mineral dust aerosol has an average lifetime of a few days in the troposphere and can be
46 transported over several thousand kilometers, thus having important impacts globally
47 (Prospero, 1999; Uno et al., 2009; Huneus et al., 2011). Mineral dust aerosol has a myriad of
48 significant impacts on atmospheric chemistry and climate. For example, dust aerosol particles
49 can influence the radiative balance of the Earth system directly by scattering and absorbing
50 solar and terrestrial radiation (Balkanski et al., 2007; Jung et al., 2010; Lemaitre et al., 2010;
51 Huang et al., 2015b), and indirectly by serving as cloud condensation nuclei (CCN) to form
52 cloud droplets (Koehler et al., 2009; Kumar et al., 2009; Twohy et al., 2009) and ice nucleation
53 particles (INP) to form ice particles (DeMott et al., 2003; Hoose and Moehler, 2012; Murray
54 et al., 2012; Ladino et al., 2013; DeMott et al., 2015). Mineral dust particles are believed to be
55 the dominant ice nucleation particles in the troposphere (Hoose et al., 2010; Creamean et al.,
56 2013; Cziczo et al., 2013), therefore having a large impact on the radiative balance,
57 precipitation, and the hydrological cycle (Rosenfeld et al., 2001; Lohmann and Feichter, 2005;
58 Rosenfeld et al., 2008). In addition, deposition of mineral dust is a major source for several
59 important nutrient elements (e.g., Fe and P) in remote regions such as open ocean waters and
60 the Amazon (Jickells et al., 2005; Mahowald et al., 2005; Mahowald et al., 2008; Boyd and
61 Ellwood, 2010; Nenes et al., 2011; Shi et al., 2012), strongly affecting several biogeochemical
62 cycles and the climate system of the Earth (Jickells et al., 2005; Mahowald, 2011; Schulz et al.,
63 2012). The impacts of mineral dust aerosol on air quality, atmospheric visibility, and public



64 health have also been widely documented (Prospero, 1999; Mahowald et al., 2007; Meng and
65 Lu, 2007; De Longueville et al., 2010; de Longueville et al., 2013; Giannadaki et al., 2014).

66 It is worthy being emphasized that impacts of mineral dust aerosol on various aspects
67 of atmospheric chemistry and climate depend on its mineralogy (Journet et al., 2008; Crowley
68 et al., 2010a; Formenti et al., 2011; Highwood and Ryder, 2014; Jickells et al., 2014; Morman
69 and Plumlee, 2014; Fitzgerald et al., 2015; Tang et al., 2016a), which shows large geographical
70 and spatial variability (Claquin et al., 1999; Ta et al., 2003; Zhang et al., 2003; Jeong, 2008;
71 Nickovic et al., 2012; Scheuven et al., 2013; Formenti et al., 2014; Journet et al., 2014; Scanza
72 et al., 2015).

73 Mineral dust particles can undergo heterogeneous and/or multiphase reactions during
74 their transport (Dentener et al., 1996; Usher et al., 2003a; Crowley et al., 2010a). These
75 reactions will modify the composition of dust particles (Matsuki et al., 2005; Ro et al., 2005;
76 Sullivan et al., 2007; Shi et al., 2008; Li and Shao, 2009; He et al., 2014) and subsequently
77 change their physicochemical properties, including hygroscopicity, CCN and IN activities
78 (Krueger et al., 2003b; Sullivan et al., 2009b; Chernoff and Bertram, 2010; Ma et al., 2012;
79 Tobo et al., 2012; Sihvonen et al., 2014; Wex et al., 2014; Kulkarni et al., 2015), and the
80 solubility of Fe and P, and etc. (Meskhidze et al., 2005; Vlasenko et al., 2006; Duvall et al.,
81 2008; Nenes et al., 2011; Shi et al., 2012; Ito and Xu, 2014). The effects of heterogeneous and
82 multiphase reactions on the hygroscopicity and CCN and IN activities of dust particles have
83 been comprehensively summarized by a very recent review paper (Tang et al., 2016a), and the
84 impacts of atmospheric aging processes on the Fe solubility of mineral dust has also been
85 reviewed (Shi et al., 2012).

86 Heterogeneous reactions of mineral dust in the troposphere can also remove or produce
87 a variety of reactive trace gases, directly and/or indirectly modifying the gas phase
88 compositions of the troposphere and thus changing its oxidation capacity. The global impact



89 of mineral dust aerosol on tropospheric chemistry through heterogeneous reactions was
90 proposed in the mid-1990s by a modelling study (Dentener et al., 1996), which motivated many
91 following laboratory, field, and modelling work (de Reus et al., 2000; Bian and Zender, 2003;
92 Usher et al., 2003a; Bauer et al., 2004; Crowley et al., 2010a; Zhu et al., 2010; Wang et al.,
93 2012; Nie et al., 2014). It should be noted that the regional impact of heterogeneous reactions
94 of mineral dust aerosol was even recognized earlier (Zhang et al., 1994). It has also been
95 suggested that dust aerosol could indirectly impact tropospheric chemistry by affecting
96 radiative fluxes and thus photolysis rates (Liao et al., 1999; Bian and Zender, 2003; Jeong and
97 Sokolik, 2007; Real and Sartelet, 2011).

98 A few minerals (e.g., TiO_2) with higher refractive indices, compared to stratospheric
99 sulfuric acid particles, have been proposed as potentially suitable materials (Pope et al., 2012;
100 Tang et al., 2014e; Weisenstein et al., 2015) instead of sulfuric acid and its precursors, to be
101 delivered into the stratosphere in order to scatter more solar radiation back into space, as one
102 of solar radiation management methods for climate engineering (Crutzen, 2006).
103 Heterogeneous uptake of reactive trace gases by minerals is also of interest in this aspect for
104 assessment of impacts of particle injection on stratospheric chemistry and especially
105 stratospheric ozone (Pope et al., 2012; Tang et al., 2014e; Tang et al., 2016b). In addition, some
106 minerals, such as CaCO_3 and TiO_2 , are widely used as raw materials in construction, and their
107 heterogeneous interactions with reactive trace gases can be important for local outdoor and
108 indoor air quality (Langridge et al., 2009; Raff et al., 2009; Ammar et al., 2010; Baergen and
109 Donaldson, 2016; George et al., 2016) and deterioration of construction surfaces (Lipfert, 1989;
110 Webb et al., 1992; Striegel et al., 2003; Walker et al., 2012).

111 **1.2 An introduction to heterogeneous kinetics**

112 The rates of atmospheric heterogeneous reactions are usually described or
113 approximated as pseudo-first-order reactions. The pseudo-first-order removal rate of a trace



114 gas (X), $k_1(X)$, due to the heterogeneous reaction with mineral dust, depends on its average
115 molecular speed, $c(X)$, the surface area concentration of mineral dust aerosol, S_a , and the uptake
116 coefficient, γ , given by Eq. (1) (Crowley et al., 2010a; Kolb et al., 2010; Ammann et al., 2013;
117 Tang et al., 2014b):

$$118 \quad k_1(X) = 0.25 \cdot c(X) \cdot S_a \cdot \gamma \quad (1)$$

119 The uptake coefficient is the net probability that a molecule X is actually removed from the gas
120 phase upon collision with the surface, equal to the ratio of number of molecules removed from
121 the gas phase to the total number of gas-surface collisions (Crowley et al., 2010a).

122 Heterogeneous reaction of a trace gas (X) will lead to depletion of X close to the surface,
123 and thus the effective uptake coefficient, γ_{eff} , will be smaller than the true uptake coefficient, γ ,
124 as described by Eq. (2) (Crowley et al., 2010a; Davidovits et al., 2011; Tang et al., 2014b):

$$125 \quad \frac{1}{\gamma_{\text{eff}}} = \frac{1}{\gamma} + \frac{1}{\Gamma_{\text{diff}}} \quad (2)$$

126 where Γ_{diff} represents the gas phase diffusion limitation. For the uptake onto spherical particles,
127 Eq. (3) (the Fuchs-Sutugin equation) can be used to calculate Γ_{diff} (Tang et al., 2014b; Tang et
128 al., 2015):

$$129 \quad \frac{1}{\Gamma_{\text{diff}}} = \frac{0.75+0.286Kn}{Kn \cdot (Kn+1)} \quad (3)$$

130 where Kn is the Knudsen number, given by Eq. (4)

$$131 \quad Kn = \frac{2\lambda(X)}{d_p} = \frac{6D(X)}{c(X) \cdot d_p} \quad (4)$$

132 where $\lambda(X)$, $D(X)$ and d_p are the mean free path of X, the gas phase diffusion coefficient of X,
133 and the particle diameter, respectively. Experimentally measured gas phase diffusion
134 coefficients of trace gases with atmospheric relevance have been recently compiled and
135 evaluated (Tang et al., 2014b; Tang et al., 2015); if not available, they can be estimated using
136 Fuller's semi-empirical method (Fuller et al., 1966; Tang et al., 2015). A new method has also
137 been proposed to calculate Kn without the knowledge of $D(X)$, given by Eq. (5):



138
$$Kn = \frac{2}{d_p} \cdot \frac{\lambda_p}{P} \quad (5)$$

139 where P is the pressure in atm and λ_p is the pressure-normalized mean free path which is equal
140 to 100 nm·atm (Tang et al., 2015).

141 **1.3 Scope of this review**

142 Usher et al. (2003a) provided the first comprehensive review in this field, and
143 heterogeneous reactions of mineral dust with a myriad of trace gases, including nitrogen oxides,
144 SO₂, O₃, and some organic compounds are included. After that, the IUPAC Task Group on
145 Atmospheric Chemical Kinetic Data Evaluation published the first critical evaluation of kinetic
146 data for heterogeneous reactions of solid substrates including mineral dust particles (Crowley
147 et al., 2010a), and kinetic data for heterogeneous uptake of several trace gases (including O₃,
148 H₂O₂, NO₂, NO₃, HNO₃, N₂O₅, and SO₂) onto mineral dust have been recommended. It should
149 be pointed out that in addition to this and other review articles published by Atmospheric
150 Chemistry and Physics, the IUPAC task group keeps updating recommended kinetic data
151 online (<http://iupac.pole-ether.fr/>). We note that a few other review papers and monographs
152 have also mentioned atmospheric heterogeneous reactions of mineral dust particles (Cwiertny
153 et al., 2008; Zhu et al., 2011; Chen et al., 2012; Rubasinghege and Grassian, 2013; Shen et al.,
154 2013; Burkholder et al., 2015; Ge et al., 2015; George et al., 2015; Akimoto, 2016), in a less
155 comprehensive manner compared to Usher et al. (2003a) and Crowley et al. (2010). For
156 example, Cwiertny et al. (2008) reviewed heterogeneous reactions and heterogeneous
157 photochemical reactions of O₃ and NO₂ with mineral dust. Atmospheric heterogeneous
158 photochemistry was summarized by Chen et al. (2012) for TiO₂ and by George et al. (2015)
159 for other minerals. Heterogeneous reactions of mineral dust with a few volatile organic
160 compounds (VOCs), such as formaldehyde, acetone, methacrolein, methyl vinyl ketone, and
161 organic acids, have been covered by a review article on heterogeneous reactions of VOCs (Shen
162 et al., 2013). The NASA-JPL data evaluation panel has compiled and evaluated kinetic data for



163 heterogeneous reactions with alumina (Burkholder et al., 2015). In a very recent paper, Ge et
164 al. (2015) summarized previous studies on heterogeneous reactions of mineral dust with NO₂,
165 SO₂, and monocarboxylic acids, with work conducted by scientists in China emphasized. In his
166 monograph entitled Atmospheric Reaction Chemistry, Akimoto (2015) briefly discussed some
167 heterogeneous reactions of mineral dust particles in the troposphere. Roles heterogeneous
168 chemistry of aerosol particles (including mineral dust) play in haze formation in China were
169 outlined (Zhu et al., 2011), and effects of surface adsorbed water and thus relative humidity
170 (RH) on heterogeneous reactions of mineral dust have also been discussed by a recent feature
171 article (Rubasinghege and Grassian, 2013).

172 After the publication of the two benchmark review articles (Usher et al., 2003a;
173 Crowley et al., 2010a), much advancement has been made in this field. For example,
174 heterogeneous uptake of HO₂ radicals by mineral dust particles had not been explored at the
175 time when Crowley et al. (2010a) published the IUPAC evaluation, and in the last few years
176 this reaction has been investigated by two groups (Bedjanian et al., 2013b; Matthews et al.,
177 2014). A large number of new studies on the heterogeneous reactions of mineral dust with H₂O₂
178 (Wang et al., 2011; Zhao et al., 2011b; Romanias et al., 2012b; Yi et al., 2012; Zhou et al.,
179 2012; Romanias et al., 2013; Zhao et al., 2013; El Zein et al., 2014; Zhou et al., 2016) and N₂O₅
180 (Tang et al., 2012; Tang et al., 2014a; Tang et al., 2014c; Tang et al., 2014e) have emerged.
181 Therefore, a review on atmospheric heterogeneous reaction of mineral dust is both timely and
182 necessary.

183 Furthermore, the novelty of our current review, which distinguishes it from previous
184 reviews in the same/similar fields (Usher et al., 2003a; Cwiertny et al., 2008; Crowley et al.,
185 2010a; Zhu et al., 2011; Chen et al., 2012; Shen et al., 2013; Ge et al., 2015; George et al.,
186 2015), is the fact that atmospheric relevance and significance of laboratory studies are
187 illustrated, discussed, and emphasized. We hope that this paper will be useful not only for those



188 whose expertise is laboratory work but also for experts in field measurements and atmospheric
189 modelling. The following approaches are used to achieve this goal: 1) lifetimes of reactive trace
190 gases with respect to heterogeneous uptake by mineral dust, calculated using preferred uptake
191 coefficients and typical mineral dust mass concentrations, are compared to their lifetimes in
192 the troposphere (discussed in Section 2.1) in order to discuss the significance of heterogeneous
193 reactions as atmospheric sinks for these trace gases; 2) atmospheric importance of these
194 heterogeneous reactions are further discussed by referring to representative box, regional, and
195 global modelling studies reported previously; 3) we also describe two of the largest challenges
196 in the laboratory studies of heterogeneous reactions of mineral dust particles (Section 2.2), and
197 explain why reported uptake coefficients show large variability and how we interpret and use
198 these kinetic data. In fact, the major expertise of a few coauthors of this review paper is field
199 measurements and/or modelling studies, and their contribution should largely increase the
200 readability of this paper for the entire atmospheric chemistry community regardless of the
201 academic background of individual readers.

202 OH, NO₃, and O₃ are the most important gas phase oxidants in the troposphere, and
203 their contribution to tropospheric oxidation capacity has been well recognized (Brown and
204 Stutz, 2012; Stone et al., 2012). HO₂ radicals are closely linked with OH radicals (Stone et al.,
205 2012). H₂O₂, HCHO and HONO are important precursors for OH radicals in the troposphere
206 (Stone et al., 2012), and they may also be important oxidants in the aqueous phase (Seinfeld
207 and Pandis, 2006). Tropospheric N₂O₅ is found to be in dynamic equilibrium with NO₃ radicals
208 (Brown and Stutz, 2012). Therefore, in order to provide a comprehensive view of implications
209 of heterogeneous reactions of mineral dust particles for tropospheric oxidation capacity, not
210 only heterogeneous uptake of OH, NO₃, and O₃ but also heterogeneous reactions of HO₂, H₂O₂,
211 HCHO, HONO, and N₂O₅ are included. Cl atoms (Spicer et al., 1998; Osthoff et al., 2008;
212 Thornton et al., 2010; Phillips et al., 2012; Liao et al., 2014; Wang et al., 2016) and stable



213 Criegee radicals (Mauldin III et al., 2012; Welz et al., 2012; Percival et al., 2013; Taatjes et al.,
214 2013) are proposed to be potentially important oxidants in the troposphere, though their
215 atmospheric significance is to be systematically assessed (Percival et al., 2013; Taatjes et al.,
216 2014; Simpson et al., 2015). In addition, their heterogeneous reactions with mineral dust have
217 seldom been explored. Therefore, heterogeneous uptake of Cl atoms (and their precursors such
218 as ClNO₂) and stable Criegee radicals by mineral dust is not included here.

219 In Section 2, a brief introduction to tropospheric chemistry of OH, HO₂, H₂O₂, O₃,
220 HCHO, HONO, NO₃, and N₂O₅ (8 species in total) is provided first. After that, we describe
221 two major challenges in laboratory studies of heterogeneous reactions of mineral dust particles,
222 and then discuss their implications in reporting and interpreting kinetic data. Following this in
223 Section 3, we review previous laboratory studies of heterogeneous reactions of mineral dust
224 particles with these eight reactive trace gases. Uncertainties for each individual reactions are
225 discussed, and future work required to reduce these uncertainties is suggested. In addition,
226 atmospheric importance of these reactions is discussed by 1) comparing their lifetimes with
227 respect to heterogeneous uptake to typical lifetimes in the troposphere and 2) discussing
228 representative modelling studies at various spatial and temporal scales. Finally in Section 4 we
229 outline key challenges which preclude better understanding of impacts of heterogeneous
230 reactions of mineral dust on tropospheric oxidation capacity and discuss how they can be
231 addressed by future work.

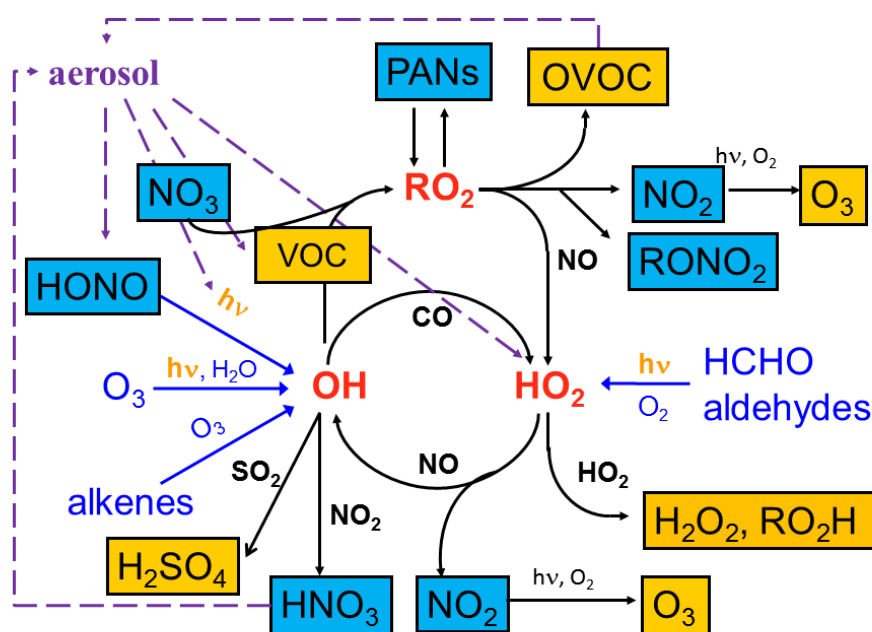
232 **2 Background**

233 In first part of this section we provide a brief introduction of production and removal
234 pathways, chemistry, and lifetimes of OH, HO₂, H₂O₂, O₃, HCHO, HONO, NO₃, and N₂O₅ in
235 the troposphere. In the second part we describe two of the largest challenges in laboratory
236 investigation of heterogeneous reactions of mineral dust particles and discuss their implications
237 for reporting, interpreting, and using uptake coefficients.



238 **2.1 Sources and sinks of tropospheric oxidants**

239 Figure 1 shows a simplified schematic diagram of atmospheric chemistry of major free
 240 radicals in the troposphere. Sources, sinks, and atmospheric lifetimes of these radicals and their
 241 important precursors are discussed below.



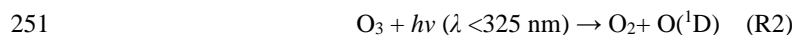
242

243 **Figure 1.** Simplified schematic diagram of chemistry of major free radicals in the troposphere.

244 **2.1.1.1 OH, HO₂, and H₂O₂**

245 Large amounts of OH ($10^6 - 10^7$ molecule cm^{-3}) and HO₂ radicals ($10^8 - 10^9$ cm^{-3}) have
 246 been observed and predicted for the lower troposphere (Stone et al., 2012). The first major
 247 primary source of OH radicals in the troposphere is the reaction of water vapor with O(¹D)
 248 (R1), which is produced from photolysis of O₃ by UV radiation with wavelengths smaller than
 249 325 nm (R2) (Atkinson et al., 2004; Burkholder et al., 2015):





252 In polluted urban areas, another two primary sources of OH and HO₂ radicals, i.e. photolysis
253 of HONO and HCHO, become significant (Seinfeld and Pandis, 2006) and sometimes even
254 dominate the primary production of OH (Su et al., 2008):



259 Photolysis of higher oxygenated volatile organic compounds (OVOCs) such as di-carbonyl
260 compounds has also been suggested as important primary sources for HO_x radicals in
261 megacities in China (Lu et al., 2012; Lu et al., 2013) and Mexico (Dusanter et al., 2009). Under
262 twilight conditions as well as during winter time, ozonolysis of alkenes and photolysis of
263 OVOCs have been found to be dominant primary sources of OH and HO₂ (Geyer et al., 2003;
264 Heard et al., 2004; Kanaya et al., 2007b; Edwards et al., 2014; Lu et al., 2014).

265 After initiated by primary production channels described above, OH radicals further
266 react with volatile organic compounds (VOCs) to generate organic peroxy radicals (RO₂). RO₂
267 radicals are then converted to HO₂ radicals by reacting with NO (R5) and the produced HO₂
268 radicals are finally recycled back to OH via reaction with NO (R6).



271 Due to these chain reactions, ambient OH levels are sustained and emitted reductive trace gas
272 compounds (e.g., VOCs and NO) are catalytically oxidized (Seinfeld and Pandis, 2006). These
273 chain reactions are terminated by reaction of OH with NO₂ (R7, in which M is the third-body
274 molecule) at high NO_x conditions and by cross reaction of HO₂ with RO₂ and self-reaction of
275 HO₂ radicals (R8) at low NO_x conditions.



278 In recent years, a new OH regeneration mechanism, which has not been completely elucidated
279 so far, has been identified for low NO_x environments including both forested (Lelieveld et al.,
280 2008) and rural areas (Hofzumahaus et al., 2009; Lu et al., 2012). This new mechanism is found
281 to stabilize the observed OH-*j*(O¹D) relationships and enables a type of maximum efficiency
282 of OH sustainment under low NO_x conditions (Rohrer et al., 2014).

283 Table 1 summarizes representative lifetimes of OH and HO₂ radicals in the troposphere
284 as determined by previous field campaigns. The OH lifetime is an important parameter to
285 characterize HO_x chemistry as well as VOC reactivity in the troposphere. As a result, it has
286 been widely measured at different locations using a variety of experimental methods (Sinha et
287 al., 2008; Ingham et al., 2009), as discussed by a very recent paper (Yang et al., 2016b). OH
288 lifetimes in clean environments, like open ocean and remote continental areas, are dominated
289 by reactions with CO, CH₄, and HCHO, summed up to values of about 0.5-1 s (Ehhalt, 1999;
290 Brauers et al., 2001). OH lifetimes in forested areas, mainly contributed by oxidation of
291 biogenic VOCs, are typically in the range of 0.01-0.05 s (Ingham et al., 2009; Nölscher et al.,
292 2012). In urban areas, OH lifetimes are determined by anthropogenically emitted hydrocarbons,
293 NO_x, CO, and biogenic VOCs as well, and they are typically smaller than 0.1 s (Ren et al.,
294 2003; Mao et al., 2010b; Lu et al., 2013).

295 Compared to OH radicals, lifetimes of HO₂ radicals have been much less investigated
296 and are mainly determined by ambient NO concentrations when NO is larger than 10 pptv
297 (parts per trillion by volume). Therefore, the lower limit of HO₂ lifetimes, on the order of 0.1 s,
298 often appear in polluted urban areas (Ren et al., 2003; Kanaya et al., 2007a; Lu et al., 2012).
299 The upper limit of HO₂ lifetimes, up to 1000-2000 s, is often observed in clean regions and
300 sometimes also in urban areas during nighttime (Holland et al., 2003; Lelieveld et al., 2008;



301 Whalley et al., 2011). In addition, heterogeneous uptake of HO₂ radicals have been frequently
 302 considered in the budget analysis of HO_x radicals for marine and polluted urban regions
 303 (Abbatt et al., 2012).

304

305 **Table 1.** Summary of typical lifetimes of OH, HO₂, NO₃ and N₂O₅ in the troposphere reported
 306 by field measurements.

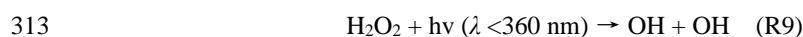
Time	Location	Lifetimes	Reference
OH radicals			
OCT-NOV 1996	Tropical Atlantic Ocean	1 s	(Brauers et al., 2001)
AUG 1994	Mecklenburg Vorpommern, Germany	0.5 s	(Ehhalt, 1999)
JUL-AUG 1998	Pabstthum (rural Berlin), Germany	0.15-0.5 s	(Mihelcic et al., 2003)
AUG-SEP 2000	Houston, US	0.08-0.15 s	(Mao et al., 2010b)
JUN-AUG 2001	New York, US	0.04-0.06 s	(Ren et al., 2003)
AUG 2007	Tokyo, Japan	0.01-0.1 s	(Chatani et al., 2009)
JUL 2006	Backgarden (rural Guangzhou), China	0.008-0.1 s	(Lou et al., 2010)
AUG 2006	Yufa (rural Beijing), China	0.01-0.1s	(Lu et al., 2013)
APR-MAY 2008	Borneo, Malaysia	0.015-0.1 s	(Ingham et al., 2009)
JUL-AUG 2010	Hyytiala, Finland	0.01-0.5 s	(Nölscher et al., 2012)
HO ₂ radicals			
JUL-AUG 1998	Pabstthum (rural Berlin), Germany	3-500 s	(Holland et al., 2003)
JUN-AUG 2001	New York, US	0.1-1.5 s	(Ren et al., 2003)
JUL-AUG 2004	Tokyo, Japan	0.05-1000 s	(Kanaya et al., 2007a)
JUL 2006	Backgarden (rural Guangzhou), China	0.1-500 s	(Lu et al., 2012)
AUG 2006	Yufa (rural Beijing), China	0.06-500 s	(Lu et al., 2013)
OCT 2005	Suriname	500-1000 s	(Lelieveld et al., 2008)
APR-MAY 2008	Borneo, Malaysia	20-2000 s	(Whalley et al., 2011)



NO ₃ radicals			
OCT 1996	Helgoland, Germany	10-1000 s	(Martinez et al., 2000)
JUL-AUG 1998	Berlin, Germany	10-500 s	(Geyer et al., 2001)
JUL-AUG 2002	US east coast	typically a few min, up to 20 min	(Aldener et al., 2006)
MAY 2008	Klein Feldberg, Germany	up to ~1500 s	(Crowley et al., 2010b)
AUG-SEP 2011	Klein Feldberg, Germany	up to 1 h, with an average value of ~200 s	(Sobanski et al., 2016)
N ₂ O ₅			
OCT 1996	Helgoland, Germany	hundred to thousand seconds	(Martinez et al., 2000)
JAN 2004	Contra Costa, California, US	600-1800 s	(Wood et al., 2005)
JUL-AUG 2002	US east coast	up to 60 min	(Aldener et al., 2006)
NOV 2009	Fairbank, Alaska, US	~6 min on average	(Huff et al., 2011)
NOV-DEC 2013	Hong Kong, China	from <0.1 h to 13 h	(Brown et al., 2016)

307

308 Formation and removal of gas phase H₂O₂ in the troposphere is closely linked with the
 309 HOx radical chemistry. Tropospheric H₂O₂ is mainly produced from self-reaction of HO₂
 310 radicals (R8) and this process is further enhanced by the presence of water vapor (Stockwell,
 311 1995). In addition to dry and wet deposition, another two pathways, i.e. photolysis (R9) and
 312 the reaction with OH (R10), dominate the removal of H₂O₂ in the troposphere:



315 Typical $J(\text{H}_2\text{O}_2)$ daily maximum values are $\sim 7.7 \times 10^{-6} \text{ s}^{-1}$ for solar zenith angle of 0°
 316 and $\sim 6.0 \times 10^{-6} \text{ s}^{-1}$ in the northern mid-latitude (Stockwell et al., 1997), corresponding to
 317 $\tau_{\text{phot}}(\text{H}_2\text{O}_2)$ (H₂O₂ lifetimes with respect to photolysis) of 33-56 h (or 1.5-2 days). The rate
 318 constant for the bimolecular reaction of H₂O₂ with OH radicals is $1.7 \times 10^{-12} \text{ cm}^3 \text{ molecule}^{-1} \text{ s}^{-1}$
 319 at room temperature, and its temperature dependence is quite small (Atkinson et al., 2004).



320 Concentrations of OH radicals in the troposphere are usually in the range of $(1-10)\times 10^6$
321 molecule cm^{-3} , and thus $\tau_{\text{OH}}(\text{H}_2\text{O}_2)$ (H_2O_2 lifetimes with respect to reaction with OH radicals)
322 are estimated to be around 16-160 h. Dry deposition rates of H_2O_2 were determined to be ~ 5
323 cm s^{-1} (Hall and Claiborn, 1997), and an assumed boundary height of 1 km gives $\tau_{\text{dry}}(\text{H}_2\text{O}_2)$
324 (H_2O_2 lifetimes with respect to dry deposition) of 5-6 h. Therefore, dry deposition is a major
325 sink for near surface H_2O_2 . We do not estimate H_2O_2 lifetimes with respect to wet deposition
326 because wet deposition rates depend on amount of precipitation which shows large spatial and
327 temporal variation. Heterogeneous uptake of H_2O_2 by ambient aerosols as well as fog and rain
328 droplets is also considered to be a significant sink for H_2O_2 , especially when the ambient SO_2
329 concentrations are high (de Reus et al., 2005; Hua et al., 2008).

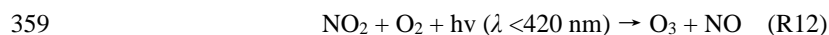
330 As mentioned previously, HONO and HCHO are two important precursors for OH
331 radicals, and therefore their removal (as well as production) significantly affects tropospheric
332 oxidation capacity. The typical $J(\text{HONO})$ daily maximum value for the northern mid-latitude
333 is $\sim 1.63\times 10^{-3} \text{ s}^{-1}$ (Stockwell et al., 1997), corresponding to $\tau_{\text{phot}}(\text{HONO})$ of about 10 min. This
334 is supported by field measurements which suggest that lifetimes of HONO due to photolysis
335 during the daytime are typically in the range of 10-20 min (Alicke et al., 2003; Li et al., 2012).
336 The second order rate constant for the reaction of HONO with OH radicals is $6.0\times 10^{-12} \text{ cm}^3$
337 molecule $^{-1} \text{ s}^{-1}$ at 298 K (Atkinson et al., 2004), giving $\tau_{\text{OH}}(\text{HONO})$ of ~ 280 min (~ 4.6 h) if OH
338 concentration is assumed to be 1×10^7 molecule cm^{-3} . Dry deposition velocities of HONO
339 reported by previous work show large variability, ranging from 0.077 to 3 cm s^{-1} (Harrison and
340 Kitto, 1994; Harrison et al., 1996; Stutz et al., 2002), and thus $\tau_{\text{dry}}(\text{HONO})$ are estimated to be
341 in the range of ~ 9 h to several days if a boundary height of 1 km is assumed. Therefore,
342 photolysis is the main sink for HONO in the troposphere and the contribution from dry
343 deposition and reaction with OH is quite minor.



344 The second order rate constant for the reaction of HCHO with OH radicals is 8.5×10^{-12}
345 $\text{cm}^3 \text{ molecule}^{-1} \text{ s}^{-1}$ at 298 K (Atkinson et al., 2006), and $\tau_{\text{OH}}(\text{HCHO})$ is calculated to be ~200
346 min (~3.3 h) if OH concentration is assumed to be $1 \times 10^7 \text{ molecule cm}^{-3}$. The typical $J(\text{HCHO})$
347 daily maximum value for the northern mid-latitude is $\sim 5.67 \times 10^{-5} \text{ s}^{-1}$ (Stockwell et al., 1997),
348 giving $\tau_{\text{phot}}(\text{HCHO})$ of about 300 min (~5 h). The dry deposition velocity for HCHO was
349 measured to be 1.4 cm s^{-1} (Seyfioglu et al., 2006), corresponding to $\tau_{\text{dry}}(\text{HCHO})$ of ~20 h if the
350 boundary layer height is assumed to be 1 km. To summarize, lifetimes of HCHO in the
351 troposphere are estimated to be a few hours, with photolysis and reaction with OH radicals
352 being major sinks.

353 2.1.2 O₃

354 After being emitted, NO is converted to NO₂ in the troposphere through its reactions
355 with O₃ (R11) and peroxy radicals (R5, R6). NO₂ is further photolyzed to generate O₃ (R12),
356 and NO oxidation processes through R5 and R6 are the reason for O₃ increase in the
357 troposphere (Wang and Jacob, 1998).



360 Tropospheric O₃ is mainly destroyed via its photolysis (R1) and the subsequent reaction of O¹D
361 with H₂O (R2). Other important removal pathways include dry deposition, reaction with NO₂
362 (to produce NO₃ radicals) (R13), and ozonolysis of alkenes, etc.



364 In addition, the loss of NO₂ through reaction with OH (R7) and the loss of peroxy radicals
365 through their self-reactions (R8) would be a significant term of O₃ losses in large scales.
366 Therefore, it is anticipated that both the formation and destruction of O₃ is closely related with
367 gas phase HOx and NOx radical chemistry.



368 Several processes remove O₃ from the troposphere. The first one is the photolysis of O₃
369 to produce O¹D (R1) and the subsequent reaction of O¹D with H₂O (R2); therefore, the removal
370 rate of O₃ through this pathway depends on solar radiation and RH. $\tau_{\text{pho}}(\text{O}_3)$ is typically in the
371 range of 1.8-10 days in the troposphere (Stockwell et al., 1997). Ozonolysis of alkenes is
372 another significant sink for O₃ under high VOCs conditions, and $\tau_{\text{alkene}}(\text{O}_3)$ with respect to
373 reaction with alkenes are estimated to be 3-8 h for urban and forested areas (Shirley et al., 2006;
374 Kanaya et al., 2007b; Whalley et al., 2011; Lu et al., 2013; Lu et al., 2014). O₃ lifetimes in the
375 remote troposphere are primarily determined by O₃ photolysis (and the subsequent reaction of
376 O¹D with H₂O) and reactions of O₃ with HO₂ and OH. For typical conditions ($j(\text{O}^1\text{D})$, H₂O,
377 HO₂, OH, temperature, and pressure) over northern mid-latitude oceans, O₃ lifetimes are
378 calculated to be a few days in summer, 1-2 weeks in spring/autumn, and about a month for in
379 winter, using the GEOS-Chem model (to be published). O₃ dry deposition has been extensively
380 studied and as a rule of thumb, 1 cm s⁻¹ is taken as its dry deposition rate (Wesely and Hicks,
381 2000). Consequently, $\tau_{\text{dry}}(\text{O}_3)$ is calculate to be ~28 h, assuming a boundary height of 1 km.
382 Reactions with NO and NO₂ will further contribute to the removal of O₃ in the troposphere at
383 night. The second-order rate constants are 1.9×10^{-14} cm³ molecule⁻¹ s⁻¹ for the reaction of O₃
384 with NO and 3.5×10^{-17} cm³ molecule⁻¹ s⁻¹ for its reaction with NO₂ at 298 K (Atkinson et al.,
385 2004), and O₃ lifetimes are calculated to be ~29 h and ~32 h in the presence of 20 pptv NO and
386 10 ppbv (parts per billion by volume) NO₂, respectively.

387 Moreover, heterogeneous processes may also strongly influence the budget of O₃
388 through impacts on sources and sinks of HOx and NOx (Dentener et al., 1996; Jacob, 2000;
389 Zhu et al., 2010), the production of halogen radicals (Thornton et al., 2010; Phillips et al., 2012;
390 Wang et al., 2016), and possibly also direct removal of O₃ due to heterogeneous uptake (de
391 Reus et al., 2000).



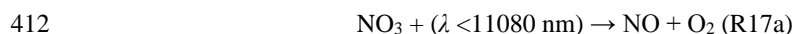
392 **2.1.3 NO₃ radicals (and N₂O₅)**

393 Oxidation of NO₂ by O₃ (R13) is the dominant source for NO₃ radicals in the
394 troposphere. NO₃ radicals further react with NO₂ to form N₂O₅ (R14), which can thermally
395 dissociate back to NO₃ and NO₂ (R15) (Wayne et al., 1991; Brown and Stutz, 2012).



399 The equilibrium between NO₃ and N₂O₅ is usually reached within several seconds under typical
400 tropospheric conditions. Therefore, NO₃ radicals are considered to be in dynamic equilibrium
401 with N₂O₅, as confirmed by a number of field measurements (Brown and Stutz, 2012, and
402 references therein). As a results, NO₃ and N₂O₅ are discussed together here. Recently reactions
403 of Criegee radicals with NO₂ are proposed as another source for NO₃ radicals (Ouyang et al.,
404 2013), though atmospheric significance of this source has not been systematically assessed yet
405 (Sobanski et al., 2016).

406 Photolysis of NO₃ (R17) and its reaction with NO (R16) are both very fast (Wayne et
407 al., 1991), and atmospheric chemistry of NO₃ (and thus N₂O₅) is only important during
408 nighttime, though the daytime presence of NO₃ and N₂O₅ in the troposphere has also been
409 reported (Brown and Stutz, 2012). Therefore, for a sink to be important for NO₃ or N₂O₅, the
410 lifetime with respect to this sink should be comparable to or shorter than half one day.



414 The predominant sinks for tropospheric NO₃ and N₂O₅ include reactions with
415 unsaturated volatile organic compounds (VOCs), reaction with dimethyl sulfite in the marine
416 and coastal troposphere, and heterogeneous uptake by aerosol particles and cloud droplets



417 (Brown and Stutz, 2012). The gas phase reaction of N_2O_5 with water vapor was investigated
418 by a laboratory study (Wahner et al., 1998), and several field measurements have suggested
419 that this reaction is unlikely to be significant in the troposphere (Brown et al., 2009; Crowley
420 et al., 2010b; Brown and Stutz, 2012). Lifetimes of NO_3 and N_2O_5 during nighttime depend on
421 a variety of atmospheric conditions (including concentrations of VOCs and aerosols, aerosol
422 composition and mixing state, and RH etc.) (Brown and Stutz, 2012), exhibiting large spatial
423 and temporal variations. As shown in Table 1, NO_3 lifetimes typically range from tens of
424 seconds to 1 h, while N_2O_5 lifetimes are usually longer, spanning from <10 min to several hours.

425 **2.2 Laboratory studies of atmospheric heterogeneous reactions of mineral dust** 426 **particles**

427 Kinetics of heterogeneous reactions can be determined by measuring the decay and/or
428 production rates of trace gases in the gas phase (Hanisch and Crowley, 2001; Usher et al.,
429 2003b; Liu et al., 2008a; Vlasenko et al., 2009; Pradhan et al., 2010a; Tang et al., 2012; Zhou
430 et al., 2014). Alternatively, reaction rates can also be measured by detecting changes in particle
431 composition (Goodman et al., 2000; Sullivan et al., 2009a; Li et al., 2010; Tong et al., 2010;
432 Ma et al., 2012; Kong et al., 2014). A number of experimental techniques have been developed
433 and utilized to investigate heterogeneous reactions of mineral dust particles, as summarized in
434 Table 1. It should be emphasized that this list is far from being complete and only techniques
435 mentioned in this review paper are included. These techniques can be classified into three
436 groups according to the way particles under investigation exist: 1) particle ensembles deposited
437 on a substrate, 2) an ensemble of particles as an aerosol, and 3) single particles, either levitated
438 or deposited on a substrate. Detailed description of these techniques can be found in several
439 previous review articles and monographies (Usher et al., 2003a; Cwierny et al., 2008; Crowley
440 et al., 2010a; Kolb et al., 2010; Akimoto, 2016) and thus is not repeated here. Instead, in this
441 paper we intend to discuss two critical issues in determining and reporting uptake coefficients



442 for heterogeneous reactions of mineral dust particles, i.e. 1) surface area available for
443 heterogeneous uptake and 2) time dependence of heterogeneous kinetics.

444 For experiments in which single particles are used, usually surface techniques,
445 including Raman spectroscopy (Liu et al., 2008b; Zhao et al., 2011a), scanning electron
446 microscopy (SEM) (Krueger et al., 2003a; Laskin et al., 2005b), and secondary ion mass
447 spectroscopy (SIMS) (Harris et al., 2012), can be utilized to characterize their compositional
448 and morphological changes simultaneously. Nevertheless, it is still non-trivial to derive
449 quantitative information for most of surface techniques. In addition to being deposited on a
450 substrate, single particles can also be levitated by an electrodynamic balance (Lee and Chan,
451 2007; Pope et al., 2010) or optical levitation (Tong et al., 2011; Krieger et al., 2012; Rkiouak
452 et al., 2014), and Raman spectroscopy can be used to measure the compositional changes of
453 levitated particles (Lee et al., 2008; Tang et al., 2014a).

454

455 **Table 2:** Abbreviations of experimental techniques used by previous laboratory studies to
456 investigate heterogeneous reactions of mineral dust. Only techniques mentioned in this review
457 paper are included.

abbreviation	full name
AFT	aerosol flow tube
CIMS	chemical ionization mass spectrometry
CLD	chemiluminescence detector
CRDS	cavity ring-down spectroscopy
CRFT	coated rod flow tube
CWFT	coated wall flow tube
DRIFTS	diffuse reflectance infrared Fourier transform spectroscopy
EC	environmental chamber
KC	Knudsen cell reactor
IC	ion chromatography
LIF	laser induced fluorescence
MS	mass spectrometry



T-FTIR

transmission FTIR

458

459 **2.2.1 Surface area available for heterogeneous uptake**

460 As described by Eq. (1), surface area concentration is required to derive uptake
461 coefficients from measured pseudo first order reaction rates. However, it can be a difficult task
462 to obtain surface area concentrations for particles. In fact, variation in estimated surface area
463 available for heterogeneous uptake is one of the main reasons why large differences in uptake
464 coefficients have been reported by different groups for the same reaction system of interest.

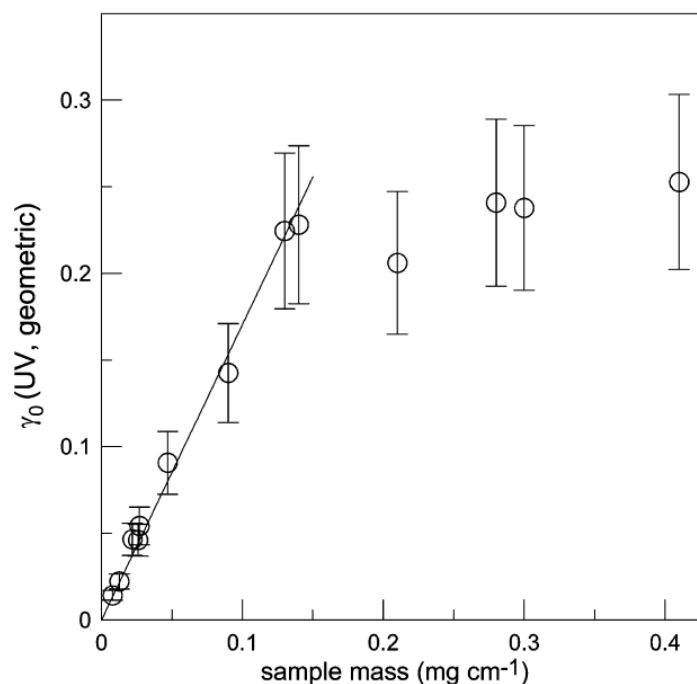
465 For experiments in which aerosol particles are used, surface area concentrations are
466 typically derived from size distribution measured using an aerodynamic particle sizer (APS) or
467 scanning mobility particle sizer (SMPS). Because of the non-sphericity of mineral dust
468 particles, it is not straightforward to convert aerodynamic and mobility diameters to surface
469 area. In some aerosol chamber studies, surface areas available for heterogeneous uptake are
470 assumed to be equal to the BET surface areas of dust particles introduced into the chamber
471 (Mogili et al., 2006b; Mogili et al., 2006a; Chen et al., 2011b). Some dust particles are porous,
472 making their BET surface areas much larger than the corresponding geometrical surface areas.
473 $\gamma(\text{N}_2\text{O}_5)$ for airborne SiO_2 particles reported by two previous studies (Mogili et al., 2006b;
474 Wagner et al., 2009) differed by almost two orders of magnitude. Tang et al. (2014a) suggested
475 that such a large difference is mainly due to the fact that different methods were used to
476 calculate surface area available for heterogeneous uptake. Specifically, Mogili et al. (2006a)
477 used the BET surface area, while Wagner et al. (2009) used Stoke diameters derived from APS
478 measurements to calculate the surface area. Tang et al. (2014a) further found that if the same
479 method is used to calculate surface area concentrations, $\gamma(\text{N}_2\text{O}_5)$ reported by the two studies
480 (Mogili et al., 2006b; Wagner et al., 2009) agree fairly well.

481 This issue becomes even more severe for experiments using mineral dust particles
482 deposited on a substrate. In these experiments the surface area available for heterogeneous



483 uptake is assumed to be either the projected area of dust particles (equal to the geometrical
484 surface area of the sample holder) or the BET surface area of the dust sample. Multiple layers
485 of powdered dust samples are typically deposited on a substrate. Consequently, it is not
486 uncommon that the BET surface area is several orders of magnitude larger than the projected
487 area (Nicolas et al., 2009; Liu et al., 2010; Tong et al., 2010). The surface area actually available
488 for heterogeneous uptake falls between the two extreme cases and varies for different studies.
489 For a very fast heterogeneous reaction it is likely that only the topmost few layers of a powdered
490 sample are accessible for the reactive trace gases, whereas more underlying layers become
491 available for slower uptake processes. Therefore, uptake coefficients reported by experiments
492 using aerosol samples, if available, are preferred and used in this study to estimate the
493 atmospheric importance of heterogeneous reactions. We note that a similar strategy has also
494 been adopted by the IUPAC task group (Crowley et al., 2010a).

495 In theory, transport of gaseous molecules within the interior space of the powdered
496 sample coupled to reaction with particle surface can be described by mathematical models. The
497 KML (Keyser-Moore-Leu) model initially developed to describe diffusion and reaction of
498 gaseous molecules in porous ice (Keyser et al., 1991; Keyser et al., 1993) has been used to
499 derive uptake coefficients for heterogeneous reactions of mineral dust particles. One major
500 drawback of the KML model (and other models with similar principles but different
501 complexities) is that it can be difficult to measure or accurately calculate diffusion constants of
502 reactive trace gases through powdered samples (Underwood et al., 2000).



503

504 **Figure 2.** Projected area based uptake coefficients of H₂O₂ on irradiated TiO₂ particles as a
505 function of TiO₂ sample mass (per cm length of the support tube onto which TiO₂ particles
506 were deposited). Reprinted with permission from (Romanias et al., 2012b). Copyright 2012
507 American Chemical Society.

508

509 Grassian and coworkers developed a simple method to calculate surface area available
510 for heterogeneous uptake (Underwood et al., 2000; Li et al., 2002). If the thickness of a
511 powdered sample is smaller than the interrogation depth of the reactive trace gas (i.e. depth of
512 the sample which can actually be reached by the reactive trace gas), all the particles should be
513 accessible for heterogeneous uptake. In this case, uptake coefficients calculated using the
514 projected area should exhibit a linear mass dependence. The linear mass dependent (LMD)
515 regime can be experimentally determined, with an example shown in Figure 2. Figure 2
516 suggests that when the TiO₂ sample mass is <0.15 mg cm⁻¹, the projected area based uptake

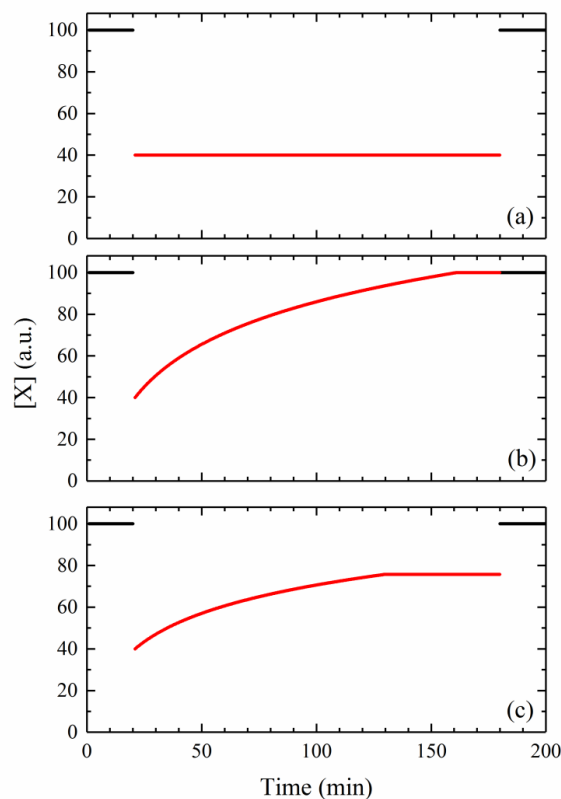


517 coefficients depend linearly on the sample mass. If measurements are carried out within the
518 LMD regime, surfaces of all the particles are available for heterogeneous uptake and the BET
519 surface area should be used to calculate uptake coefficients (Underwood et al., 2000; Romanias
520 et al., 2012b; Bedjanian et al., 2013b).

521 Another way to circumvent the problem due to diffusion within interior space of
522 powdered samples is to use particles less than one layer (Hoffman et al., 2003a; Hoffman et al.,
523 2003b). This experimental strategy was used to investigate heterogeneous reactions of NaCl
524 with HNO₃, N₂O₅, and ClONO₂, and a mathematical model was developed to calculate the
525 effective surface area exposed to reactive trace gases (Hoffman et al., 2003a; Hoffman et al.,
526 2003b). Nevertheless, to our knowledge this method has not yet be used by laboratory studies
527 of heterogeneous reaction of mineral dust particles.

528 **2.2.2 Time dependence of heterogeneous kinetics**

529 When exposed to reactive trace gases, mineral dust surface may become deactivated
530 and thus gradually lose its heterogeneous reactivity. Figure 3 shows three representative
531 examples of decays of a reactive trace gas, X, after exposure to mineral dust particles. For the
532 case shown in Figure 3a, no surface active sites are consumed and the uptake rate is
533 independent of reaction time. Figure 3b displays another case in which surface reactive sites
534 may be consumed and heterogeneous uptake will cease after some exposure. In addition, as
535 shown in Figure 3c, an initial large uptake rate gradually decreases with time to a non-zero
536 constant value for longer exposure (i.e. the heterogeneous reaction reaches a “steady state”).



537

538 **Figure 3.** Synthetic data of the decay of a trace gas, X, due to heterogeneous reaction when it
539 is exposed to mineral dust particles from 20 to 180 min: a) not surface deactivation; b) complete
540 surface deactivation; c) partial surface deactivation. Black curves represent the concentration
541 of X without exposure to mineral dust particles (i.e. initial [X]), and red curves represent the
542 evolution of measured [X] during exposure of X to mineral dust particles.

543

544 In atmospheric chemistry community, heterogeneous reactions are usually treated as
545 pseudo-first-order processes (with respect to reactive trace gases), as implied by Eq. (1).
546 However, deactivation of mineral dust surfaces has been reported for a variety of trace gases
547 by experiments using particle ensembles deposited on a substrate (Underwood et al., 2001;



548 Hanisch and Crowley, 2003a; Ndour et al., 2009; Tang et al., 2010; Zhou et al., 2012; Romanias
549 et al., 2013; Liu et al., 2015). Therefore, uptake coefficients are normally set to be time
550 dependent (instead of assuming to be a constant), such that Eq. (1) is still valid for time
551 dependent heterogeneous kinetics. Many studies (Michel et al., 2003; Seisel et al., 2005;
552 Karagulian et al., 2006; Wang et al., 2011; El Zein et al., 2014) have reported initial and/or
553 steady-state uptake coefficients (γ_0 and γ_{ss} , respectively). What makes interpreting reported
554 uptake coefficients more difficult is that even for the same heterogeneous reaction, γ_0 and γ_{ss}
555 may exhibit dependence on experimental conditions (e.g., dust sample mass, trace gas
556 concentration, temperature, and etc.). For example, it takes less time for a reaction to reach
557 steady-state when higher concentrations are used for the same reactive trace gas. In many cases,
558 surface may be completely deactivated given sufficient reaction time. Furthermore, γ_0 is usually
559 reported as the first measurable uptake coefficient, which largely depends on the response time
560 (and time resolution) of the instrument used to detect the trace gas.

561 In aerosol flow tube experiments, on the other hand, exposure time of mineral dust
562 aerosol particles to trace gases are very short (typically <1 min). Therefore, significant surface
563 deactivation is not observed and decays of trace gases can usually be well described by pseudo-
564 first-order kinetics with time independent uptake coefficients (Vlasenko et al., 2006; Pradhan
565 et al., 2010a; Tang et al., 2012; Matthews et al., 2014).

566 Ideally laboratory studies of heterogeneous reactions should be carried out at or at least
567 close to atmospherically relevant conditions, such that experimental results can be directly used.
568 However, due to experimental challenges, laboratory studies are usually performed at much
569 shorter time scales (from <1 min to a few hours, compared to average residence time of several
570 days for mineral dust aerosol) and with much higher trace gas concentrations. Alternatively,
571 measurements can be conducted over a wide range of experimental conditions in order that
572 fundamental physical and chemical processes can be deconvoluted and corresponding rate



573 constants can be determined (Kolb et al., 2010; Davidovits et al., 2011; Pöschl, 2011). With
574 more accurate kinetic data, kinetic models which integrate these fundamental processes can be
575 constructed and applied to predict uptake coefficients for atmospherically relevant condition
576 (Ammann and Poschl, 2007; Pöschl et al., 2007; Shiraiwa et al., 2012; Berkemeier et al., 2013).
577 Unfortunately, measurements of this type are resource-demanding. In practice laboratory
578 studies of heterogeneous kinetics are usually carried out under very limited experimental
579 conditions. Therefore, there is a great need to invest more resource in fundamental laboratory
580 research.

581 **3 Heterogeneous reactions of mineral dust particles with tropospheric** 582 **oxidants and their direct precursors**

583 The importance of a heterogeneous reaction for removal of a trace gas, X, is determined
584 by the uptake coefficient and the aerosol surface area concentration, as suggested by Eq. (1). It
585 also depends on the rates of other removal processes in competition, although it is not
586 uncommon that this aspect has not been fully taken into account. In this section, previous
587 laboratory studies of heterogeneous reactions of mineral dust particles with OH, HO₂, H₂O₂,
588 O₃, HCHO, HONO, NO₃, and N₂O₅ are summarized, analyzed, and discussed. After that,
589 lifetimes of each trace gases with respect to their heterogeneous reactions with mineral dust are
590 calculated, using uptake coefficients listed in Table 2, followed by discussion of relative
591 importance of heterogeneous reactions for their removal in the troposphere. In addition, we
592 also discuss representative modeling studies to further demonstrate and illustrate the
593 importance of these heterogeneous reactions.

594 Uptake coefficients which are used in this paper to calculate lifetimes with respect to
595 heterogeneous reactions with mineral dust particles are shown in Table 2. The IUPAC Task
596 Group on Atmospheric Chemical Kinetic Data Evaluation has been compiling and evaluating
597 kinetic data for atmospheric heterogeneous reactions (Crowley et al., 2010a), and preferred



598 uptake coefficients are also recommended. It should be noted that uptake coefficients listed in
599 Table 2 do not intend to compete with those recommended by the IUPAC task group. Instead,
600 some of our values are largely based on their recommended values if available and proper.

601

602 **Table 3:** Uptake coefficients used in this work to calculate lifetimes of OH, HO₂, H₂O₂, O₃,
603 HCHO, HONO, NO₃, and N₂O₅ with respect to heterogeneous reactions with mineral dust
604 aerosol.

species	uptake coefficient	species	uptake coefficient
OH	0.2	HCHO	1×10 ⁻⁵
HO ₂	0.038	HONO	1×10 ⁻⁶
H ₂ O ₂	1×10 ⁻³	NO ₃	0.018
O ₃	4.5×10 ⁻⁶	N ₂ O ₅	0.020

605

606 The pseudo-first-order loss rate depends on the aerosol surface area concentration,
607 which depends on aerosol number concentration and its size distribution. Although particle
608 sizing instruments such as aerodynamic particle sizer (APS) and scanning particle mobility
609 sizer (SMPS) are commercially available, particle mass concentrations are still more widely
610 measured and reported. Therefore, it is convenient to calculate lifetimes based on mass
611 concentration instead of surface area concentration. This calculation requires information of
612 particle size and density. For simplicity dust aerosol particles are assumed to have an average
613 particles diameter of 1 μm and a density of 2.7 g cm⁻³. Consequently, the lifetime of X with
614 respect to its heterogeneous reaction with mineral dust, τ_{het}(X), can be described by Eq. (6)
615 (Wagner et al., 2008; Tang et al., 2010; Tang et al., 2012):

616

$$\tau_{het}(X) = \frac{1.8 \times 10^8}{\gamma_{eff}(X) \cdot c(X) \cdot L} \quad (6)$$

617 where γ_{eff}(X) is the effective uptake coefficient of X, c(X) is the average molecular speed of X
618 (cm s⁻¹), and L is the mineral dust loading (i.e. mass concentration) in μg m⁻³. Mass



619 concentrations of mineral dust aerosol particles in the troposphere show high variability,
620 ranging from a few $\mu\text{g m}^{-3}$ in background regions such as north Atlantic to $>1000 \mu\text{g m}^{-3}$ during
621 extreme dust storms (Prospero, 1979; Zhang et al., 1994; de Reus et al., 2000; Gobbi et al.,
622 2000; Alfaro et al., 2003). To take into account this spatial and temporal variation, mass
623 concentrations of 10, 100, and $1000 \mu\text{g m}^{-3}$ are used in this paper to assess atmospheric
624 significance of heterogeneous reactions with mineral dust for the removal of trace gases.

625 **3.1 OH and HO₂ radicals**

626 **3.1.1 OH radicals**

627 Heterogeneous uptake of OH radicals by mineral dust particles was first investigated
628 using a coated wall flow tube with detection of OH radicals by electron paramagnetic resonance
629 (EPR) (Gershenzon et al., 1986). The uptake coefficient was reported to be 0.04 ± 0.02 for Al_2O_3
630 and 0.0056 ± 0.0020 for SiO_2 , independent of temperature in the range of 253–348 K
631 (Gershenzon et al., 1986). Using laser induced fluorescence (LIF), Suh et al. (2000) measured
632 concentration changes of OH radicals after the gas flow was passed through a wire screen
633 loaded with TiO_2 (anatase or rutile), $\alpha\text{-Al}_2\text{O}_3$, or SiO_2 under dry conditions. It is shown that the
634 uptake coefficients, $\gamma(\text{OH})$, increased with temperature from ~ 310 K to ~ 350 K for all the three
635 oxides, being $(2\text{--}4) \times 10^{-4}$ for TiO_2 , $(2\text{--}4) \times 10^{-3}$ for SiO_2 , and $(5\text{--}6) \times 10^{-3}$ for $\alpha\text{-Al}_2\text{O}_3$ (Suh et al.,
636 2000). Unfortunately, most of the results reported by Suh et al. (2000) are only presented
637 graphically. In an earlier study (Bogart et al., 1997), $\gamma(\text{OH})$ was reported to be 0.41 ± 0.04 at
638 300 K on deposited SiO_2 films, decreasing with temperature. $\text{OH}(\text{X}^2\text{II})$ radicals used by Bogart
639 et al. were generated in a 20:80 tetraethoxysilane/ O_2 plasmas and their atmospheric relevance
640 is not very clear; therefore, this study is not included in Table 1 or further discussed.

641 The average $\gamma(\text{OH})$ was determined to be 0.20 for Al_2O_3 at room temperature under dry
642 conditions (Bertram et al., 2001), using a coated wall flow tube coupled to chemical ionization
643 mass spectrometry (CIMS). In a following study, the RH dependence of $\gamma(\text{OH})$ on SiO_2 and



644 Al_2O_3 at room temperature was investigated (Park et al., 2008). It is found that $\gamma(\text{OH})$ increased
645 from 0.032 ± 0.007 at 0% RH to 0.098 ± 0.022 at 33% RH for SiO_2 and from 0.045 ± 0.005 at 0%
646 RH to 0.084 ± 0.012 at 38% RH for Al_2O_3 (Park et al., 2008).



647 **Table 4:** Summary of previous laboratory studies on heterogeneous reactions of mineral dust with OH and HO₂ radicals

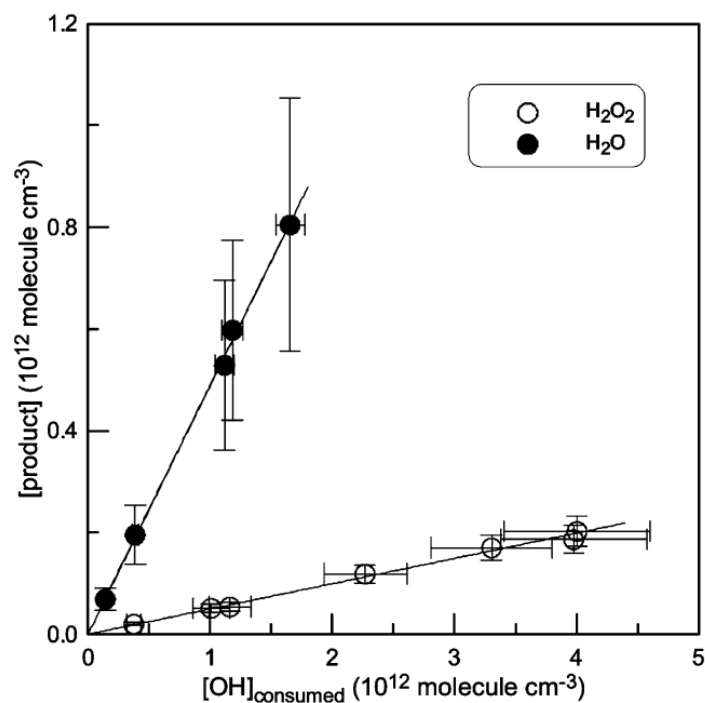
Trace gases	Dust	Reference	T (K)	Concentration (molecule cm ⁻³)	Uptake coefficients	Techniques
OH	TiO ₂	Suh et al., 2000	308 to 350	~4×10 ¹²	(2-4)×10 ⁻⁴ , increasing with temperature	LIF
	SiO ₂	Gershenson et al., 1986	253-343	<2×10 ¹²	0.0056±0.002, independent of temperature	CWFT-EPR
		Suh et al., 2000	308 to 350	~4×10 ¹²	(2-4)×10 ⁻³ , increasing with temperature	LIF
	Al ₂ O ₃	Park et al., 2008	room temperature	~4×10 ¹¹	0.032±0.007 at 0% RH and 0.098±0.022 at 33% RH	CWFT-CIMS
		Gershenson et al., 1986	253-343	<2×10 ¹²	0.04±0.02, independent of temperature	CWFT-EPR
		Suh et al., 2000	308 to 350	~4×10 ¹²	(5-6)×10 ⁻³ , increasing with temperature	LIF
	ATD	Bertram et al., 2001	room temperature	(1-100)×10 ⁹	0.20	CWFT-CIMS
		Park et al., 2008	room temperature	~4×10 ¹¹	0.045±0.005 at 0%RH and 0.084±0.012 at 38% RH	CWFT-CIMS
		Bedjanian et al., 2013a	275-320	(0.4-5.2)×10 ¹²	0.20 at 0% RH, showing a negative RH dependence but no dependence on temperatures	CRFT-MS
	HO ₂	ATD	Bedjanian et al., 2013b	275-320	(0.35-3.3)×10 ¹²	0.067±0.004 at 0% RH, showing a negative RH dependence (0.02-94%) but no dependence on temperature.
		Matthews et al., 2014	291±2	(3-10)×10 ⁸	0.018±0.006 when HO ₂ concentration was 3×10 ⁸ molecule cm ⁻³ and 0.031±0.008 when HO ₂ concentration was 3×10 ⁸ molecule cm ⁻³ . No RH (5-76%) dependence was observed.	AFT-FAGE



649 Recently a coated rod flow tube was used to investigate uptake of OH radicals by
650 Arizona test dust (ATD) particles (Bedjanian et al., 2013a) as a function of temperature (275-
651 320 K) and RH (0.03-25.9%). Gradual surface deactivation was observed, and the initial uptake
652 coefficient was found to be independent of temperature and decrease with increasing RH, given
653 by Eq. (7):

$$654 \quad \gamma_0 = 0.2/(1 + RH^{0.36}) \quad (7)$$

655 with an estimated uncertainty of $\pm 30\%$. Please note that uptake coefficients reported by
656 Bedjanian et al. (2013a) are based on the geometrical area of the rod coated with ATD particles
657 and thus should be considered as the upper limit. No effect of UV radiation, with $J(\text{NO}_2)$ up to
658 0.012 s^{-1} , was observed (Bedjanian et al., 2013a). In addition, H_2O and H_2O_2 were found to be
659 the major and minor products in the gas phase respectively (Bedjanian et al., 2013a), as shown
660 in Figure 4.



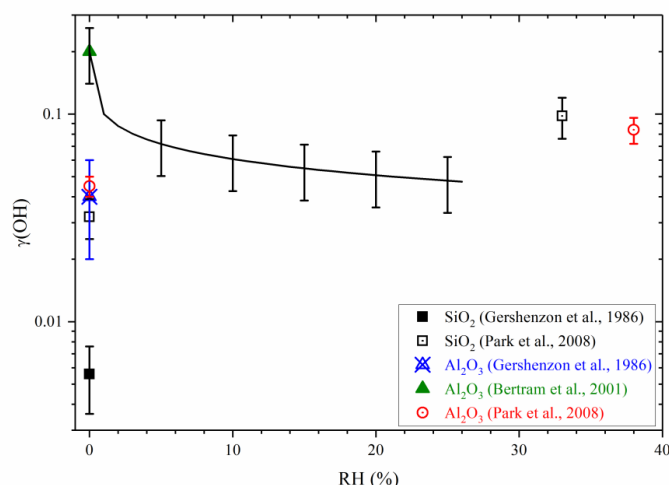
661



662 **Figure 4.** Concentrations of H₂O (solid circles) and H₂O₂ (open circles) produced in the gas
663 phase due to heterogeneous reaction of OH radicals with ATD particles. Reprinted with
664 permission from Bedjanian et al. (2013a). Copyright 2013 American Chemical Society.

665

666 As shown in Figure 5, $\gamma(\text{OH})$ reported by previous flow tube studies, except that onto
667 SiO₂ particles reported by Gershenzon et al. (1986), show reasonably good agreement,
668 considering that different minerals were used. Reported $\gamma(\text{OH})$ are larger than 0.02 in general,
669 suggesting that mineral dust exhibits relatively large reactivity towards OH radicals.
670 Discrepancies are also identified from data presented in Figure 5, with the most evident one
671 being the effect of RH. Park et al. (2008) found that $\gamma(\text{OH})$ increased significantly with RH for
672 both SiO₂ and Al₂O₃, while Bedjanian et al. (2013b) suggested that $\gamma(\text{OH})$ showed a negative
673 dependence on RH. It is not clear yet whether different minerals used by these two studies can
674 fully account for the different RH dependence observed. Furthermore, a positive dependence
675 of $\gamma(\text{OH})$ on temperature was found by Suh et al. (2000) for TiO₂, α -Al₂O₃, and SiO₂, while
676 Bogart et al. (1997) reported a negative temperature effect for deposited SiO₂ film and no
677 significant dependence on temperature was found for ATD (Bedjanian et al., 2013a).



678



679 **Figure 5.** Uptake coefficients of OH radicals for different minerals at room temperature, as
680 reported by different studies. The plotted RH dependence of $\gamma(\text{OH})$ for ATD (solid curve) is
681 based on the parameterization reported by Bedjanian et al. (2013a), i.e. Eq. (7).

682

683 A $\gamma(\text{OH})$ value of 0.2, reported by Bedjanian et al. (2013a) for ATD, is used in our
684 present work to evaluate the importance of heterogeneous uptake of OH radicals by mineral
685 dust aerosol. According to Eq. (6), dust mass loadings of 10, 100, and 1000 $\mu\text{g m}^{-3}$ correspond
686 to $\tau_{\text{het}}(\text{OH})$ of ~ 25 min, 150 s, and 15 s with respect to heterogeneous uptake by mineral dust.
687 As discussed in Section 2.1.1, lifetimes of tropospheric OH are in the range of 1 s or less in
688 very clean regions and < 0.1 s in polluted and forested areas, much shorter than $\tau_{\text{het}}(\text{OH})$. Even
689 if $\gamma(\text{OH})$ is assumed to be 1, for uptake by 1 μm particles $\gamma_{\text{eff}}(\text{OH})$ is calculated to be 0.23,
690 which is only 15% larger than what we use to calculate $\tau_{\text{het}}(\text{OH})$. Therefore, it can be concluded
691 that heterogeneous reaction with mineral dust aerosol is not a significant sink for OH radicals
692 in the troposphere.

693 3.1.2 HO₂ radicals

694 To the best of our knowledge, only two previous studies have investigated
695 heterogeneous uptake of HO₂ radicals by mineral dust particles. Bedjanian et al. (2013b) used
696 a coated rod flow tube to study the interaction of HO₂ radicals with ATD film as a function of
697 temperature and RH. Surface deactivation was observed, and γ_0 , based on the geometrical area
698 of dust films, was determined to be 0.067 ± 0.004 under dry conditions (Bedjanian et al., 2013b).
699 The initial uptake coefficient, independent of temperature, was found to decrease with RH,
700 given by Eq. (8):

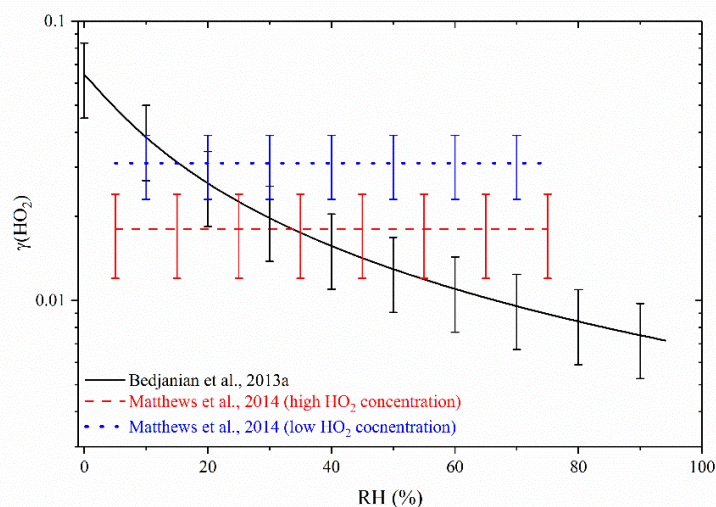
$$701 \quad \gamma_0 = 1.2 / (18.7 + RH^{1.1}) \quad (8)$$

702 with an estimated uncertainty of $\pm 30\%$. UV radiation, with $J(\text{NO}_2)$ ranging from 0 to 0.012 s^{-1} ,
703 did not affect uptake kinetics significantly. In addition, the yield of H₂O₂(g), defined as the



704 ratio of formed $\text{H}_2\text{O}_2(\text{g})$ molecules to consumed HO_2 radicals, was determined to be <5%
705 (Bedjanian et al., 2013b).

706 In the second study (Matthews et al., 2014), an aerosol flow tube was deployed to
707 measure $\gamma(\text{HO}_2)$ onto ATD aerosol particles at 291 ± 2 K, with HO_2 detection via the
708 fluorescence assay by gas expansion technique. No significant effect of RH in the range of 5-
709 76% was observed, and $\gamma(\text{HO}_2)$ was reported to be 0.031 ± 0.008 for $[\text{HO}_2]$ of 3×10^8 molecule
710 cm^{-3} and 0.018 ± 0.006 for $[\text{HO}_2]$ of 1×10^9 molecule cm^{-3} (Matthews et al., 2014). In addition,
711 $\gamma(\text{HO}_2)$ was found to decrease with increasing reaction time. The negative dependence of $\gamma(\text{HO}_2)$
712 on $[\text{HO}_2]$ and reaction time implies that ATD surface is gradually deactivated upon exposure
713 to HO_2 radicals, as directly observed by Bedjanian et al. (2013a).



714

715 **Figure 6.** RH dependence of $\gamma(\text{HO}_2)$ for ATD reported by two previous studies. Solid curve,
716 reported by Bedjanian et al. (2013b) with initial $[\text{HO}_2]$ in the range of $(0.35\text{-}3)\times 10^{12}$ molecule
717 cm^{-3} ; dashed and dotted curve, reported by Matthews et al. (2014) with initial $[\text{HO}_2]$ of 1×10^9
718 and 3×10^8 molecule cm^{-3} , respectively. Numerical data for $\gamma(\text{HO}_2)$ at different RH were not
719 provided by Matthews et al. (2014), and thus in this figure we plot their reported average $\gamma(\text{HO}_2)$



720 together with their estimated uncertainties. The plotted RH dependence of $\gamma(\text{HO}_2)$ reported by
721 Bedjanian et al. (2013b) is based on their proposed parameterization, i.e. Eq. (8).

722

723 Figure 6 shows the effect of RH on $\gamma(\text{HO}_2)$ for ATD particles. A quick look at Figure 6
724 could lead to the impression that $\gamma(\text{HO}_2)$ reported by two previous studies (Bedjanian et al.,
725 2013b; Matthews et al., 2014) agree relatively well, especially considering that two very
726 different experimental techniques were used. Nevertheless, Matthews et al. (2014), who
727 conducted their measurements with initial $[\text{HO}_2]$ which are 3-4 orders of magnitude lower than
728 those used by Bedjanian et al. (2013a), found a significant negative dependence of $\gamma(\text{HO}_2)$ on
729 initial $[\text{HO}_2]$. If this trend can be further extrapolated to higher initial $[\text{HO}_2]$, one may expect
730 that if carried out with initial $[\text{HO}_2]$ similar to those used by Bedjanian et al. (2013a), Matthews
731 et al. (2014) may find much smaller $\gamma(\text{HO}_2)$. In addition, these two studies also suggest very
732 different RH effects, as evident from Figure 6. We also note that ATD is the only one type of
733 mineral dust onto which heterogeneous uptake of HO_2 radicals was investigated, and the effect
734 of mineralogy is not clear at all yet. Therefore, our understanding of heterogeneous reactions
735 of HO_2 radicals with mineral dust particles is very limited.

736 Apart from these included in Table 4, the uptake of HO_2 by analogues of meteoric
737 smoke particles was also examined at room temperature (James et al., 2017), using an aerosol
738 flow tube. At $(10 \pm 1)\%$ RH, the uptake coefficient was determined to be 0.069 ± 0.012 for olivine
739 (MgFeSiO_4), 0.073 ± 0.004 for fayalite (Fe_2SiO_4), and 0.0043 ± 0.0004 for forsterite (Mg_2SiO_4),
740 respectively. It appears that meteoric smoke particles which do not contain Fe, these which
741 contain Fe show much larger heterogeneous reactivity towards HO_2 radicals. The experimental
742 result indicates a catalytic role of Fe in HO_2 uptake, as supported by electronic structure
743 calculations (James et al., 2017). Though its tropospheric relevance is limited, this study



744 provides valuable mechanistic insights into heterogeneous reaction of mineral dust with HO₂
745 radicals.

746 For reasons discussed in Section 2.2.1, $\gamma(\text{HO}_2)$ reported by Matthews et al. (2014) using
747 aerosol samples are used to calculate $\tau_{\text{het}}(\text{HO}_2)$ with respect to uptake onto mineral dust.
748 Another reason that the data reported by Matthews et al. (2014) are preferred is that [HO₂] used
749 in this study were low enough to be of direct atmospheric relevance. As a result, $\gamma(\text{HO}_2)$
750 measured at lower initial [HO₂] (3×10^8 molecule cm⁻³), equal to 0.031 ± 0.008 , is adopted in our
751 current work to assess the significance of HO₂ uptake by mineral dust. Using Eq. (6), $\tau_{\text{het}}(\text{HO}_2)$
752 is estimated to be 2.2, 22, and 222 min for dust mass concentrations of 1000, 100, and 10 $\mu\text{g m}^{-3}$,
753 respectively. Typical HO₂ lifetimes in the troposphere, as summarized in Table 1, show large
754 variability, ranging from <1 s (Ren et al., 2003) to >30 min (Whalley et al., 2011). Therefore,
755 dust aerosol with moderate mass concentrations could be a significant tropospheric HO₂ sink
756 except regions with very high NO levels.

757 The importance of heterogeneous uptake as a HO₂ sink in the troposphere has also been
758 demonstrated by several more sophisticated modelling studies. For example, it is found that
759 while standard gas phase chemical mechanism used by the GEOS-Chem model would
760 overestimate HO₂ and H₂O₂ concentrations observed in the Arctic troposphere in the spring,
761 including heterogeneous reaction of HO₂ with an average $\gamma(\text{HO}_2)$ of >0.1 in the model could
762 better reproduce the measured concentrations and vertical profiles of HO₂ and H₂O₂ (Mao et
763 al., 2010a). Though not directly relevant for mineral dust aerosol, this study provided strong
764 evidence that heterogeneous uptake can be an important but yet not fully recognized sink for
765 tropospheric HO₂ radicals (Mao et al., 2010a). Using a global tropospheric model, Macintyre
766 and Evans (2011) analyzed the sensitivity of model output to $\gamma(\text{HO}_2)$ values used in the model.
767 A global average $\gamma(\text{HO}_2)$ of 0.028 was derived from available laboratory studies (Macintyre
768 and Evans, 2011), and large regional differences in modelled O₃ were observed between



769 simulations using $\gamma(\text{HO}_2)$ parameterization developed by Macintyre and Evans (2011) and
770 those using a constant $\gamma(\text{HO}_2)$ of 0.2. This results highlights the importance of accurate
771 determination of $\gamma(\text{HO}_2)$ under different tropospheric conditions (e.g., aerosol composition, RH,
772 and temperature).

773 The impact of HO_2 uptake by mineral dust has also been investigated by several
774 modelling studies. For example, an observation constrained box model study (Matthews et al.,
775 2014) suggested that heterogeneous reaction with mineral dust could result in >10% reduction
776 in HO_2 concentrations in Cape Verde, using a $\gamma(\text{HO}_2)$ of 0.038. A WRF-Chem simulation,
777 using $\gamma(\text{HO}_2)$ reported by Bedjanian et al. (2013a), showed that heterogeneous uptake by
778 mineral dust could reduce HO_2 concentrations by up to 40% over northern India during a pre-
779 monsoon dust storm (Kumar et al., 2014).

780 One may assume that heterogeneous reaction of HO_2 with aerosol particles leads to the
781 formation of H_2O_2 (Graedel et al., 1986; Thornton and Abbatt, 2005). A second channel
782 without H_2O_2 formation, i.e. simple decomposition of HO_2 radicals to H_2O and O_2 , may also
783 be important (Bedjanian et al., 2013b; Mao et al., 2013a). Atmospheric impacts can be very
784 different for these two mechanisms. While the second pathway represents a net sink for HO_2
785 in the troposphere, the first channel only converts HO_2 to H_2O_2 via heterogeneous reaction and
786 is thus of limited efficacy as a net sink for HO_x because H_2O_2 can undergo photolysis to
787 generate OH radicals.

788 The relative importance of these two mechanisms has been explored by modelling
789 studies. Mao et al. (2010a) found that only including the first reaction channel (with H_2O_2
790 production) will overestimate H_2O_2 in the Arctic, while only considering the second channel
791 (without H_2O_2 production) would cause underestimation of H_2O_2 . Consequently, it seems that
792 both channels have non-negligible contributions in the troposphere (Mao et al., 2010a).
793 Significant differences in modelled OH, HO_2 , O_3 , and sulfate concentrations have been found



794 by a global model study when including two mechanisms separately (Macintyre and Evans,
795 2011). One experimental study (Bedjanian et al., 2013b) measured gas phase products for
796 heterogeneous reaction of HO₂ radicals with ATD particles and found that gaseous H₂O₂
797 formed in this reaction is minor but probably non-negligible. Considering the importance of
798 mechanisms of heterogeneous reaction of HO₂ with mineral dust, further experimental work is
799 required. Furthermore, mineralogy and RH may also impact the yield of H₂O₂(g), but these
800 effects are not clear yet.

801 **3.2 H₂O₂**

802 Pradhan et al. (2012a, 2012b) utilized an aerosol flow tube to investigate heterogeneous
803 interaction of H₂O₂ with airborne TiO₂, Gobi dust, and Saharan dust particles at 295±2 K, and
804 H₂O₂ was detected by CIMS. A negative dependence of $\gamma(\text{H}_2\text{O}_2)$ on RH was observed for TiO₂,
805 with $\gamma(\text{H}_2\text{O}_2)$ decreasing from $(1.53\pm 0.11)\times 10^{-3}$ at 15% RH to $(6.47\pm 0.74)\times 10^{-4}$ at 40% RH and
806 $(5.04\pm 0.58)\times 10^{-4}$ at 70% RH (Pradhan et al., 2010a). In contrast, H₂O₂ uptake kinetics
807 displayed positive dependence on RH for Gobi and Saharan dust, with $\gamma(\text{H}_2\text{O}_2)$ increasing from
808 $(3.33\pm 0.26)\times 10^{-4}$ at 15% RH to $(6.03\pm 0.42)\times 10^{-4}$ at 70% RH for Gobi dust and from
809 $(6.20\pm 0.22)\times 10^{-4}$ at 15% RH to $(9.42\pm 0.41)\times 10^{-4}$ at 70% RH for Saharan dust (Pradhan et al.,
810 2010b). It appears that heterogeneous reactivity of Saharan dust towards H₂O₂ is significantly
811 higher than Gobi dust.

812 Heterogeneous interaction of gaseous H₂O₂ with SiO₂ and α -Al₂O₃ particles was
813 investigated at 298±1 K, using transmission FTIR to probe particle surfaces and a HPLC-based
814 offline technique to measure gaseous H₂O₂ (Zhao et al., 2011b). It is found that most of H₂O₂
815 molecules were physisorbed on SiO₂ surface and a small amount of molecularly adsorbed H₂O₂
816 underwent thermal decomposition. In contrast, catalytic decomposition occurred to a large
817 fraction of H₂O₂ uptaken by α -Al₂O₃, though some H₂O₂ molecules were also physisorbed on
818 the surface (Zhao et al., 2011b). The uptake coefficient, based on the BET surface area, was



819 found to be independent of initial H_2O_2 concentrations (1.27-13.8 ppmv) while largely affected
820 by RH (Zhao et al., 2011b). $\gamma(\text{H}_2\text{O}_2)$ decreased from $(1.55\pm 0.14)\times 10^{-8}$ at 2% RH to
821 $(0.81\pm 0.11)\times 10^{-8}$ at 21% RH for SiO_2 particles, and further increase in RH (up to 76%) did not
822 affect the uptake kinetics (Zhao et al., 2011b). A similar dependence of $\gamma(\text{H}_2\text{O}_2)$ on RH was
823 also observed for $\alpha\text{-Al}_2\text{O}_3$: $\gamma(\text{H}_2\text{O}_2)$ decreased from $(1.21\pm 0.04)\times 10^{-7}$ at 2% RH to
824 $(0.84\pm 0.07)\times 10^{-7}$ at 21% RH, and the effect of RH was not significant for RH in the range of
825 21-76% (Zhao et al., 2011b). Compared to SiO_2 , $\alpha\text{-Al}_2\text{O}_3$ appears to be much more reactive
826 towards H_2O_2 .

827 In a following study, using the same experimental setup, Zhao et al. (2013) explored
828 heterogeneous interaction of H_2O_2 with fresh, HNO_3 -processed, and SO_2 -processed CaCO_3
829 particles. The uptake of H_2O_2 on fresh CaCO_3 particles was drastically reduced with increasing
830 RH, indicating that H_2O_2 and H_2O compete for surface reactive sites. In addition, about 85-90%
831 of H_2O_2 molecules uptaken by fresh CaCO_3 particles undergo decomposition (Zhao et al.,
832 2013). Unfortunately no uptake coefficients were reported (Zhao et al., 2013). Pretreatment of
833 CaCO_3 particles with HNO_3 or SO_2 can significantly affect their heterogeneous reactivity
834 towards H_2O_2 . The effect of HNO_3 pretreatment increases with surface coverage of nitrate
835 (formed on CaCO_3 particles), showing an interesting dependence on RH. Pretreatment of
836 CaCO_3 with HNO_3 reduced its heterogeneous reactivity by 30-85% at 3% RH, while it led to
837 enhancement of reactivity towards H_2O_2 by 20-60% at 25% RH, a factor of 1-3 at 45% RH,
838 and a factor of 3-8 at 75% RH (Zhao et al., 2013). At low RH, formation of $\text{Ca}(\text{NO}_3)_2$ on the
839 surface could deactivate CaCO_3 ; however, $\text{Ca}(\text{NO}_3)_2$ may exit as an aqueous film at higher RH
840 (Krueger et al., 2003b; Liu et al., 2008b), consequently leading to large enhancement of H_2O_2
841 uptake. Compared to fresh CaCO_3 , SO_2 -processed particles always exhibit much higher
842 reactivity towards H_2O_2 , and enhancement factors, increasing with RH, were observed to fall
843 into the range of 3-10 (Zhao et al., 2013).



844 Heterogeneous uptake of H₂O₂ by several oxides was investigated at 298 K using a
845 Knudsen cell reactor with H₂O₂ measured by a quadrupole mass spectrometer (Wang et al.,
846 2011). $\gamma_0(\text{H}_2\text{O}_2)$, based on the BET surface area of sample powders, was determined to be
847 $(1.00 \pm 0.11) \times 10^{-4}$ for $\alpha\text{-Al}_2\text{O}_3$, $(1.66 \pm 0.23) \times 10^{-4}$ for MgO, $(9.70 \pm 1.95) \times 10^{-5}$ for Fe₂O₃, and
848 $(5.22 \pm 0.90) \times 10^{-5}$ for SiO₂, respectively (Wang et al., 2011). Surface deactivation occurred for
849 all the surfaces, though complete surface saturation was only observed for SiO₂ after extended
850 H₂O₂ exposure. This may indicate that the uptake of H₂O₂ by $\alpha\text{-Al}_2\text{O}_3$, MgO, and Fe₂O₃ are of
851 catalytic nature to some extent (Wang et al., 2011).

852 Continuous wave CRDS was employed to detect the depletion of H₂O₂ and formation
853 of HO₂ radicals in the gas phase above TiO₂ films which were exposed to gaseous H₂O₂ and
854 illuminated by a light-emitting diode at 375 nm (Yi et al., 2012). Three different TiO₂ samples
855 were investigated, including Degussa P25 TiO₂, Aldrich anatase, and Aldrich rutile. H₂O₂
856 decays did not occur in the absence of TiO₂. In addition, production of HO₂ radicals was only
857 observed in the presence of H₂O₂, and the presence of O₂ did not have a significant effect.
858 Therefore, Yi et al. (2012) suggested that the production of HO₂ radicals is due to the
859 photodecomposition of H₂O₂ on TiO₂ surfaces. Decays of H₂O₂ and formation of HO₂ are
860 found to vary with TiO₂ samples (Yi et al., 2012). Photo-degradation of H₂O₂ is fast for P25
861 TiO₂ samples and much slower for anatase and rutile; furthermore, significant production of
862 HO₂ radicals in the gas phase was observed for anatase and rutile but not for P25 TiO₂.
863 However, no uptake coefficients were reported by Yi et al. (2012).

864 Zhou et al. (2012) first explored the temperature dependence of heterogeneous
865 reactivity of mineral dust towards H₂O₂, using a Knudsen cell reactor coupled to a quadrupole
866 mass spectrometer. The uptake kinetics show negative temperature dependence, with $\gamma_0(\text{H}_2\text{O}_2)$
867 (BET surface area based) decreasing from $(12.6 \pm 2.52) \times 10^{-5}$ at 253 K to $(6.08 \pm 1.22) \times 10^{-5}$ at
868 313 K for SiO₂ and from $(7.11 \pm 1.42) \times 10^{-5}$ at 253 K to $(3.00 \pm 0.60) \times 10^{-5}$ at 313 K for CaCO₃



869 (Zhou et al., 2012). Complete surface deactivation was observed for both dust samples after
870 long exposure to H₂O₂ (Zhou et al., 2012). In a following study, the effects of temperature on
871 the uptake of H₂O₂ by ATD and two Chinese dust samples were also investigated (Zhou et al.,
872 2016). $\gamma_0(\text{H}_2\text{O}_2)$, based on the BET surface area, was observed to decrease with temperature,
873 from $(2.71 \pm 0.54) \times 10^{-4}$ at 253 K to $(1.47 \pm 0.29) \times 10^{-4}$ at 313 K for ATD, and from
874 $(3.56 \pm 0.71) \times 10^{-4}$ at 253 K to $(2.19 \pm 0.44) \times 10^{-4}$ at 313 K for Inner Mongolia desert dust, and
875 from $(7.34 \pm 1.47) \times 10^{-5}$ at 268 K to $(4.46 \pm 0.889) \times 10^{-4}$ at 313 K for Xinjiang sierozem (Zhou et
876 al., 2016). In addition, loss of heterogeneous reactivity towards H₂O₂ was observed for all the
877 three dust samples (Zhou et al., 2016).



878 **Table 5:** Summary of previous laboratory studies on heterogeneous reactions of mineral dust with H₂O₂

Dust	Reference	T (K)	Concentration (molecule cm ⁻³)	Uptake coefficient	Techniques
TiO ₂	Pradhan et al., 2010a	295±2	~4.1×10 ¹²	(1.53±0.11)×10 ⁻³ at 15% RH, (6.47±0.74)×10 ⁻⁴ at 40% RH, and (5.04±0.58)×10 ⁻⁴ at 70% RH	AFT-CIMS
	Romanias et al., 2012a	275-320	(0.17-120)×10 ¹²	Under dark conditions at 275 K, γ ₀ was determined to be (4.1±1.2)×10 ⁻³ at 0% RH, (5.1±1.5)×10 ⁻⁴ at 20% RH, (3.4±1.0)×10 ⁻⁴ at 40% RH, (2.7±0.8)×10 ⁻⁴ at 60% RH, and (2.3±0.7)×10 ⁻⁴ at 80% RH. Surface deactivation was observed under dark conditions, and UV illumination could enhance the steady state uptake of H ₂ O ₂ .	CRFT-MS
	Yi et al., 2012	not stated	(3±1)×10 ¹³	No uptake coefficients were not reported.	CRDS
SiO ₂	Zhao et al., 2011	298±1	(3.2-34.5)×10 ¹³	γ(H ₂ O ₂) decreased from (1.55±0.14)×10 ⁻⁸ at 2% RH to (0.81±0.11)×10 ⁻⁸ at 21% RH, and further increase in RH (up to 76%) did not affect uptake kinetics.	T-FTIR, HPLC
	Wang et al., 2011	298	(1-25)×10 ¹¹	γ ₀ : (5.22±0.90)×10 ⁻⁵	KC-MS
	Zhou et al., 2012	253-313	(0.37-3.7)×10 ¹²	Under dry conditions, γ ₀ decreased from (12.6±2.52)×10 ⁻⁵ at 253 K to (6.08±1.22)×10 ⁻⁵ at 313 K.	KC-MS
Al ₂ O ₃	Zhao et al., 2011	298±1	(3.2-34.5)×10 ¹³	γ(H ₂ O ₂) decreased from (1.21±0.04)×10 ⁻⁷ at 2% RH to (0.84±0.07)×10 ⁻⁷ at 21% RH, and the effect of RH was not significant for RH in the range of 21-76%.	T-FTIR, HPLC
	Wang et al., 2011	298	(1-25)×10 ¹¹	γ ₀ : (1.00±0.11)×10 ⁻⁴ ; γ ₈₀ : 1.1×10 ⁻⁵	KC-MS
	Romanias et al., 2013	268-320	(0.16-12.6)×10 ¹²	At 280 K, γ ₀ was determined to be (1.1±0.3)×10 ⁻³ at 0% RH, (1.2±0.3)×10 ⁻⁴ at 10% RH, (3.5±1.0)×10 ⁻⁵ at 40% RH, and (2.1±0.6)×10 ⁻⁵ at 70% RH, showing a negative dependence on RH. No significant effect was observed for UV illumination.	CRFT-MS



Fe ₃ O ₃	Wang et al., 2011	298	(1-25)×10 ¹¹	γ ₀ : (9.70±1.95)×10 ⁻⁴ ; γ _{ss} : 5.5×10 ⁻⁵	KC-MS
	Romanias et al., 2013	268-320	(0.16-12.6)×10 ¹²	At 280 K, γ ₀ was determined to be (1.1±0.3)×10 ⁻³ at 0% RH, (1.7±0.5)×10 ⁻⁴ at 10% RH, (6.7±2.0)×10 ⁻⁵ at 40% RH, and (4.5±1.4)×10 ⁻⁵ at 70% RH, showing a negative dependence on RH. No significant effect was observed for UV illumination.	CRFT-MS
CaCO ₃	Zhou et al., 2012	253-313	(0.37-3.7)×10 ¹²	Under dry conditions, γ ₀ decreased from (7.11±1.42)×10 ⁻⁵ at 253 K to (3.00±0.60)×10 ⁻⁵ at 313 K.	KC-MS
	Zhao et al., 2013	298±1	1.3×10 ¹⁴	The uptake of H ₂ O ₂ on fresh CaCO ₃ particles decreased drastically with RH. Pretreatment with SO ₂ always enhances its reactivity towards H ₂ O ₂ , whereas exposure to HNO ₃ could either enhance or suppress H ₂ O ₂ uptake, depending on RH. Numerical values for uptake coefficients were reported.	T-FTIR, HPLC
ATD	El Zein et al., 2014	268-320	(0.18-5.1)×10 ¹²	Under dark conditions at 275 K, γ ₀ was determined to be (4.8±1.4)×10 ⁻⁴ at 0% RH, (5.8±1.8)×10 ⁻⁵ at 20% RH, (3.9±1.2)×10 ⁻⁵ at 40% RH, and (3.0±0.9)×10 ⁻⁵ at 60% RH. Surface deactivation was observed under dark conditions, and UV illumination could enhance the steady state uptake of H ₂ O ₂ .	CRFT-MS
	Zhou et al., 2016	253-313	(0.26-1.2)×10 ¹²	Under dry conditions, γ ₀ decreased with temperature, from (2.71±0.54)×10 ⁻⁴ at 253 K to (1.47±0.29)×10 ⁻⁴ at 313 K.	KC-MS
Saharan dust	Pradhan et al., 2012b	295±2	~4.2×10 ¹²	γ(H ₂ O ₂) increased from (6.20±0.22)×10 ⁻⁴ at 15% RH to (9.42±0.41)×10 ⁻⁴ at 70% RH.	AFT-CIMS
	Pradhan et al., 2012b	295±2	~4.2×10 ¹²	γ(H ₂ O ₂) increased from (3.33±0.26)×10 ⁻⁴ at 15% RH to (6.03±0.42)×10 ⁻⁴ at 70% RH.	AFT-CIMS
Chinese dust	Zhou et al., 2016	253-313	(0.26-1.2)×10 ¹²	Under dry conditions, γ ₀ decreased with temperature, from (3.56±0.71)×10 ⁻⁴ at 253 K to (2.19±0.44)×10 ⁻⁴ at 313 K for Inner Mongolia desert dust and	KC-MS



			from $(7.34 \pm 1.47) \times 10^{-4}$ at 268 K to $(4.46 \pm 0.89) \times 10^{-4}$ at 313 K for Xinjiang sierozen.	
MgO	Wang et al., 2011	298	$(1.25) \times 10^{11}$	$\gamma_0: (1.66 \pm 0.23) \times 10^{-4}; \gamma_{\text{st}}: 1.6 \times 10^{-3}$ KC-MS



880 A coated rod flow tube was coupled to a quadrupole mass spectrometer to investigate
881 heterogeneous reactions of H₂O₂ with a variety of mineral dust particles as a function of initial
882 H₂O₂ concentrations, irradiance intensity, RH, and temperature (Romanias et al., 2012b;
883 Romanias et al., 2013; El Zein et al., 2014). Under dark conditions, quick surface deactivation
884 was observed for TiO₂. When [H₂O₂]₀ was <1×10¹² molecule cm⁻³, γ₀ was found to be
885 independent of [H₂O₂]₀; however, when [H₂O₂]₀ was above this threshold, a negative
886 dependence of γ₀ on [H₂O₂]₀ occurred. At 275 K, γ₀ (based on BET surface area) depended on
887 RH (up to 82%), given by (Romanias et al., 2012b):

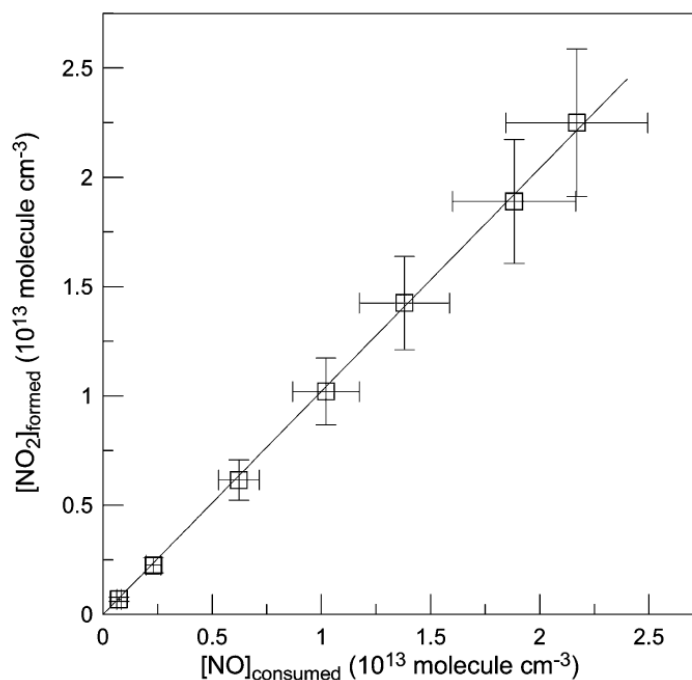
$$888 \quad \gamma_0(\text{dark}) = 4.1 \times 10^{-3} / (1 + RH^{0.65}) \quad (9)$$

889 The uncertainty was estimated to be ±30%.

890 UV illumination could lead to photocatalytic decomposition of H₂O₂ on TiO₂ surface.
891 The steady state uptake coefficient, γ_{ss}(UV), increasing linearly with illumination intensity, was
892 found to be independent of RH and depended inversely on [H₂O₂]₀ (Romanias et al., 2012b).
893 When [H₂O₂]₀ is ~5×10¹¹ molecule cm⁻³ and J(NO₂) for UV illumination is 0.012 s⁻¹, the
894 dependence of γ_{ss}(UV) on temperature (275-320 K) at 0.3% RH can be described by (Romanias
895 et al., 2012b):

$$896 \quad \gamma_{ss}(UV) = (7.2 \pm 1.9) \times 10^{-4} \times \exp[(460 \pm 80)/T] \quad (10)$$

897 It has also been found that NO added into the gas flow was converted to NO₂ during
898 heterogeneous reaction of H₂O₂ with TiO₂. As shown in Figure 7, the ratio of consumed NO to
899 formed NO₂ is close to 1. This indirect evidence suggests that HO₂ radicals (which could
900 convert NO to NO₂) were found in the gas phase due to photocatalytic reaction of H₂O₂ with
901 TiO₂ particles (Romanias et al., 2012b).



902

903 **Figure 7.** Consumed NO versus formed NO₂ in the heterogeneous reaction of H₂O₂ with TiO₂
904 particles under illumination. Reprinted with permission from Romanias et al. (2012a).
905 Copyright 2012 American Chemical Society.

906

907 Gradual surface deactivation was also observed for uptake of H₂O₂ by ATD particles.
908 γ_0 , independent of [H₂O₂]₀ in the range of (0.18-5.1)×10¹² molecule cm⁻³ and irradiation for
909 $J(\text{NO}_2)$ up to 0.012 s⁻¹, was observed to decrease with RH and temperature (El Zein et al., 2014).
910 At 275 K, the dependence of γ_0 on RH (up to 69%) can be described by (El Zein et al., 2014):

911
$$\gamma_0 = 4.8 \times 10^{-4} / (1 + RH^{0.66}) \quad (11)$$

912 At 0.35% RH, the effect of temperature on γ_0 is given by (El Zein et al., 2014):

913
$$\gamma_0 = 3.2 \times 10^{-4} / [1 + 2.5 \times 10^{10} \times \exp(-\frac{7360}{T})] \quad (12)$$

914 It has also been found that γ_{ss} , independent of RH and T , decreased with [H₂O₂]₀ under dark
915 and irradiated conditions, given by (El Zein et al., 2014):



916
$$\gamma_{ss}(\text{dark}) = 3.8 \times 10^{-5} \times ([\text{H}_2\text{O}_2]_0)^{-0.6} \quad (13)$$

917 UV irradiation could enhance heterogeneous reactivity of ATD towards H₂O₂. For example,
918 when $J(\text{NO}_2)$ was equal to 0.012 s⁻¹, $\gamma_{ss}(\text{dark})$ and $\gamma_{ss}(\text{UV})$ were determined to be
919 $(0.95 \pm 0.30) \times 10^{-5}$ and $(1.85 \pm 0.55) \times 10^{-5}$, respectively (El Zein et al., 2014).

920 Romanias et al. (2013) examined heterogeneous interactions of H₂O₂ with $\gamma\text{-Al}_2\text{O}_3$ and
921 Fe₂O₃, and found that both surfaces were gradually deactivated after exposure to H₂O₂. γ_0 ,
922 independent of $[\text{H}_2\text{O}_2]_0$ in the range of $(0.15\text{-}16.6) \times 10^{12}$ molecule cm⁻³, was found to vary with
923 RH and temperature (Romanias et al., 2013). At 280 K, the dependence of γ_0 on RH (up to
924 73%) can be given by

925
$$\gamma_0(\text{Al}_2\text{O}_3) = 1.10 \times 10^{-3} / (1 + \text{RH}^{0.93}) \quad (14)$$

926
$$\gamma_0(\text{Fe}_2\text{O}_3) = 1.05 \times 10^{-3} / (1 + \text{RH}^{0.73}) \quad (15)$$

927 At 0.3% RH, the dependence of γ_0 on temperature (T) in the range of 268-320 K can be
928 described by:

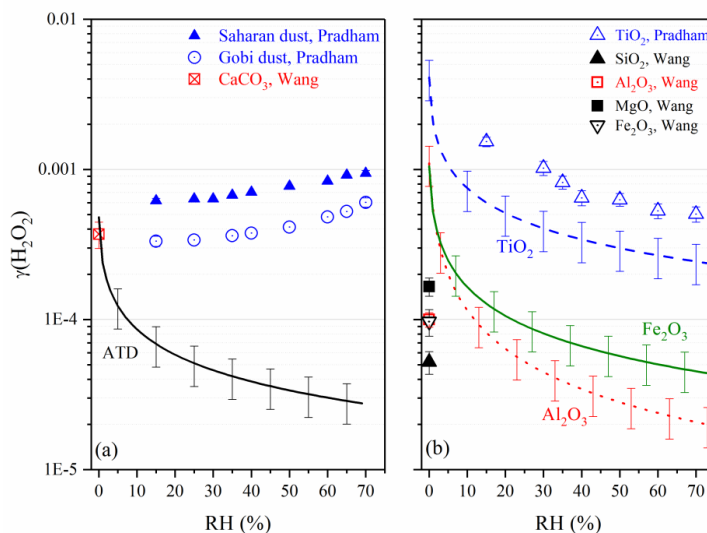
929
$$\gamma_0(\text{Al}_2\text{O}_3) = 8.7 \times 10^{-4} / [1 + 5.0 \times 10^{13} \times \exp(-9700/T)] \quad (16)$$

930
$$\gamma_0(\text{Fe}_2\text{O}_3) = 9.3 \times 10^{-4} / [1 + 3.6 \times 10^{14} \times \exp(-10300/T)] \quad (17)$$

931 In contrast to TiO₂ and ATD, no significant effects of UV irradiation with $J(\text{NO}_2)$ up to
932 0.012 s⁻¹ were observed for $\gamma\text{-Al}_2\text{O}_3$ and Fe₂O₃ (Romanias et al., 2013).

933 3.2.1 Discussion of previous laboratory studies

934 The dependence of $\gamma(\text{H}_2\text{O}_2)$ on RH, measured at room temperature, is plotted in Figure
935 8 for different dust particles. Uptake coefficients reported by Zhao et al. (2011b) are several
936 orders of magnitude smaller than those reported by other studies, and therefore they are not
937 included in Figure 8. For studies using dust particles supported on substrates, $\gamma_0(\text{H}_2\text{O}_2)$ are
938 plotted.



939

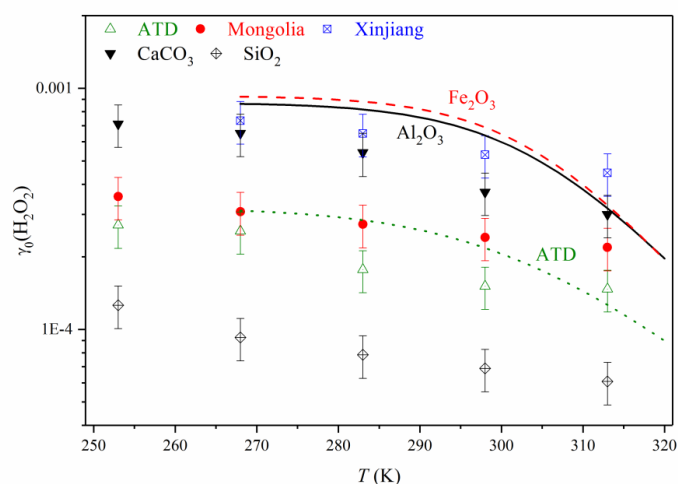
940 **Figure 8.** RH dependence of $\gamma(\text{H}_2\text{O}_2)$ for mineral dust particles as reported by previous studies
941 (Pradhan et al., 2010a; Pradhan et al., 2010b; Wang et al., 2011; Romanias et al., 2012b;
942 Romanias et al., 2013; El Zein et al., 2014).

943

944 Figure 8 suggests that different minerals show various heterogeneous reactivity towards
945 H_2O_2 , and the effects of RH also appear to be different. Two previous studies have investigated
946 heterogeneous uptake of H_2O_2 by TiO_2 at different RH under dark conditions, one using an
947 aerosol flow tube (Pradhan et al., 2010a) and the other using coated rod flow tube (Romanias
948 et al., 2012b). For TiO_2 , $\gamma(\text{H}_2\text{O}_2)$ reported by Romanias et al. (2012a) are around 40-50% of
949 those determined by Pradhan et al. (2010a) over 10-75% RH. The agreement is quite good
950 considering the fact that two very different techniques were used. Wang et al. (2011) and
951 Romanias (2013) examined heterogeneous reactions of H_2O_2 with Fe_2O_3 and Al_2O_3 . Their
952 reported $\gamma_0(\text{H}_2\text{O}_2)$ differ significantly, though BET surface area was used by both studies to
953 calculate uptake coefficients. This may be largely explained by the variation of interrogation
954 depth of H_2O_2 molecules under investigation in different studies, as discussed in Section 2.2.1.



955 Experiments in which aerosol samples are used can largely overcome the difficulty in
956 estimating surface area available for heterogeneous uptake. Up to now only two studies
957 (Pradhan et al., 2010a; Pradhan et al., 2010b) used aerosol flow tubes, and more aerosol flow
958 tube studies will help better constrain $\gamma(\text{H}_2\text{O}_2)$ onto mineral dust particles.



959

960 **Figure 9.** Temperature dependence of $\gamma_0(\text{H}_2\text{O}_2)$ for mineral dust particles under dark conditions
961 as reported by previous studies. Upward triangles: ATD (Zhou et al., 2016); circles: Inner
962 Mongolia desert dust (Zhou et al., 2016); squares: Xinjiang sierozeum (Zhou et al., 2016);
963 downward triangles: CaCO_3 (Zhou et al., 2012); diamonds: SiO_2 (Zhou et al., 2012); olive
964 circle: ATD (El Zein et al., 2014); solid black curve: Al_2O_3 (Romanias et al., 2013); dashed red
965 curve: Fe_2O_3 (Romanias et al., 2013).

966

967 The effects of temperature on heterogeneous reactions of H_2O_2 with mineral dust have
968 also been explored. As shown in Figure 9, $\gamma_0(\text{H}_2\text{O}_2)$ decrease with increasing temperature. Zhou
969 et al. (2012, 2016) suggest that $\gamma_0(\text{H}_2\text{O}_2)$ are reduced by a factor of ~ 2 for all the five minerals
970 they investigated when temperature increases from 253 K to 313 K. Romanias et al. (2013) and
971 El Zein et al. (2014) reported larger temperature impacts, with $\gamma_0(\text{H}_2\text{O}_2)$ reduced by a factor of



972 ~4 when temperature increases from 268 to 320 K. These studies show that the temperature
973 effect is significant and should be taken into account when assessing the importance of
974 heterogeneous uptake of H₂O₂ by mineral dust in the troposphere. It should also be pointed out
975 that the effect of temperature on heterogeneous reactions of H₂O₂ with airborne mineral dust
976 particles has never been investigated.

977 In addition, it has been suggested that uptake of H₂O₂ by mineral dust can affect
978 heterogeneous oxidation of other trace gases (Zhao et al., 2011b; Zhao et al., 2013; Huang et
979 al., 2015a). For examples, heterogeneous uptake of H₂O₂ could convert sulfite formed by the
980 adsorption of SO₂ on CaCO₃ particles to sulfate, and this conversion is enhanced by adsorbed
981 water (Zhao et al., 2013). Similarly, Huang et al. (2015a) found that the presence of H₂O₂ could
982 enhance the uptake of SO₂ on Asian mineral dust, Tengger desert dust, and ATD, and the
983 enhancement factors, varying with dust mineralogy and RH, can be as large as a factor of ~6.
984 Heterogeneous oxidation of methacrolein on kaolinite, α -Al₂O₃, α -Fe₂O₃, and TiO₂ (but not on
985 CaCO₃) is largely accelerated by the presence of H₂O₂, which also changes the oxidation
986 products (Zhao et al., 2011b).

987 3.2.2 Atmospheric implication

988 For reasons we have discussed in Section 2.2.1, $\gamma(\text{H}_2\text{O}_2)$ reported by studies using
989 aerosol samples (Pradhan et al., 2010a; Pradhan et al., 2010b) are preferred. Since Saharan dust
990 is the most abundant mineral dust particles in the troposphere, in our work we use $\gamma(\text{H}_2\text{O}_2)$
991 reported by Pradhan et al. (2010b) for Saharan dust to assess the atmospheric importance of
992 heterogeneous uptake of H₂O₂. $\gamma(\text{H}_2\text{O}_2)$ onto Saharan dust depends on RH, increasing from
993 6.2×10^{-4} at 15% to 9.4×10^{-4} at 70% RH. For simplicity, a $\gamma(\text{H}_2\text{O}_2)$ value of 1×10^{-3} , very close
994 to that at 70%, is used here to calculate $\tau_{\text{het}}(\text{H}_2\text{O}_2)$. When dust mass concentrations are 10, 100,
995 and 1000 $\mu\text{g m}^{-3}$, $\tau_{\text{het}}(\text{H}_2\text{O}_2)$ are calculated to be 120, 12, and 1.2 h, using Eq. (6). Typical
996 $\tau(\text{H}_2\text{O}_2)$ are estimated to be 33-56 h with respect to photolysis and 16-160 h with respect to



1997 reaction with OH radicals. Therefore, heterogeneous uptake by mineral dust particles can be a
1998 significant sink for H₂O₂ when dust mass concentration is as low as 10 µg m⁻³.

1999 Several modelling studies have also discussed and evaluated the contribution of
1000 heterogeneous uptake by mineral dust to the removal of H₂O₂ in the troposphere. Pradhan et al.
1001 (2010b) determined $\gamma(\text{H}_2\text{O}_2)$ for Saharan dust as a function of RH experimentally and then
1002 included this reaction in a box model based on the MCM. It has been found that heterogeneous
1003 uptake by mineral dust could reduce simulated H₂O₂ concentrations by up to ~40%, and its
1004 impacts on total peroxy organic radicals, OH, O₃, and NO_x are small but non-negligible
1005 (Pradhan et al., 2010b). In another box model study, $\gamma(\text{H}_2\text{O}_2)$ onto Saharan dust was varied in
1006 order to reproduce H₂O₂ concentrations measured in July/August 2002 at Tenerife (de Reus et
1007 al., 2005). It is found that using $\gamma(\text{H}_2\text{O}_2)$ of 5×10^{-4} , which agrees very well with these measured
1008 by Pradhan et al. (2010b), could reach the best agreement between measured and simulated
1009 H₂O₂ concentrations (de Reus et al., 2005).

1010 In addition to the uncertainties in $\gamma(\text{H}_2\text{O}_2)$ related to the effects of mineralogy, RH, and
1011 temperature, products formed in heterogeneous reactions of H₂O₂ with mineral dust are not
1012 entirely clear. Three pathways have been proposed, including i) simple partitioning of H₂O₂
1013 onto dust particles (Zhao et al., 2011b; Zhao et al., 2013), ii) surface decomposition of H₂O₂ to
1014 H₂O and O₂, and iii) heterogeneous conversion of H₂O₂ to HO₂ radicals (Romanias et al., 2012b;
1015 Yi et al., 2012). Branching ratios seem to depend on mineralogy, RH, and probably also UV
1016 illumination (Zhao et al., 2011b; Yi et al., 2012; Zhao et al., 2013); however, our knowledge
1017 in this aspect is very limited. Since these three different pathways may have very different
1018 impacts on tropospheric oxidation capacity, product distribution in heterogeneous reactions of
1019 H₂O₂ with mineral dust deserves further investigation.



1020 **3.3 O₃**

1021 Heterogeneous reactions of O₃ with Al₂O₃, CaCO₃, and Saharan dust were explored
1022 using a fluidized bed reactor more than two decades ago, and substantial O₃ decays were
1023 observed after interactions with dust power in the reactor (Alebić-Juretić et al., 1992). This
1024 study did not report uptake coefficients and thus is not included in Table 4. Uptake coefficients
1025 in the range of (1-100)×10⁻¹¹ were reported for Al₂O₃ (Hanning-Lee et al., 1996). Since their
1026 experiments were carried out with O₃ concentrations in the range of (5-200)×10¹⁵ molecule
1027 cm⁻³ which are several orders of magnitude higher than typical O₃ levels in the troposphere,
1028 this work is also not included in Table 4.

1029 A Knudsen cell reactor was used by Grassian and co-workers (Michel et al., 2002;
1030 Michel et al., 2003; Usher et al., 2003b) to study heterogeneous reactions of O₃ with fresh and
1031 aged mineral dust particles. Measurements were carried out in the linear mass dependent
1032 regime (see Section 2.2.1 for more explanations of the linear mass dependent regime), and thus
1033 the BET surface areas of dust samples were used to calculate uptake coefficients. In the first
1034 study (Michel et al., 2002), $\gamma_0(\text{O}_3)$ was determined to be $(1.8\pm 0.7)\times 10^{-4}$ for $\alpha\text{-Fe}_2\text{O}_3$, $(8\pm 5)\times 10^{-5}$
1035 for $\alpha\text{-Al}_2\text{O}_3$, $(5\pm 3)\times 10^{-5}$ for SiO₂, $(2.7\pm 0.9)\times 10^{-5}$ for China loess, $(6\pm 3)\times 10^{-5}$ for ground
1036 Saharan dust, and $(4\pm 2)\times 10^{-6}$ for sieved Saharan dust at 296 K when [O₃]₀ was 1.9×10^{11}
1037 molecule cm⁻³. In a following study, Michel et al. (2003) systematically investigated
1038 heterogeneous reactions of O₃ with several mineral dust particles, and progressive surface
1039 deactivation was observed for all the dust samples. At 295±1 K and [O₃]₀ of $(1.9\pm 0.6)\times 10^{11}$
1040 molecule cm⁻³, $\gamma_0(\text{O}_3)$ were reported to be $(2.0\pm 0.3)\times 10^{-4}$ for $\alpha\text{-Fe}_2\text{O}_3$, $(1.2\pm 0.4)\times 10^{-4}$ for 25
1041 μm $\alpha\text{-Al}_2\text{O}_3$, $(6.3\pm 0.9)\times 10^{-5}$ for SiO₂, $(3\pm 1)\times 10^{-5}$ for kaolinite, $(2.7\pm 0.8)\times 10^{-5}$ for China loess,
1042 $(6\pm 2)\times 10^{-5}$ for ground Saharan dust, and $(2.7\pm 0.9)\times 10^{-6}$ for ground Saharan dust, respectively.
1043 $\gamma_0(\text{O}_3)$ was also measured for 1 μm $\alpha\text{-Al}_2\text{O}_3$, and with the experimental uncertainties it shows
1044 no difference with that for 25 μm $\alpha\text{-Al}_2\text{O}_3$. The steady-state uptake coefficients, γ_{ss} , were



1045 determined to be 2.2×10^{-5} for $\alpha\text{-Fe}_2\text{O}_3$, 7.6×10^{-6} for $\alpha\text{-Al}_2\text{O}_3$, and 6×10^{-6} for ground Saharan
1046 dust. The effect of initial O_3 concentration in the range of $(1-10) \times 10^{11}$ molecule cm^{-3} on $\gamma_0(\text{O}_3)$
1047 is insignificant for either $\alpha\text{-Al}_2\text{O}_3$ or $\alpha\text{-Fe}_2\text{O}_3$. In addition, $\gamma_0(\text{O}_3)$ was found to have a very weak
1048 dependence on temperature (250-330 K) for $\alpha\text{-Al}_2\text{O}_3$, with an activation energy of 7 ± 4 kJ mol^{-1}
1049 (Michel et al., 2003).

1050 Heterogeneous processing of mineral dust particles by other trace gases could affect O_3
1051 uptake. It has been observed that $\gamma_0(\text{O}_3)$ was reduced by $\sim 70\%$ after pretreatment of $\alpha\text{-Al}_2\text{O}_3$
1052 with HNO_3 and increased by 33% after pretreatment with SO_2 (Usher et al., 2003b). Similarly,
1053 functionalization of SiO_2 with a C8 alkene would increase its heterogeneous reactivity towards
1054 O_3 by 40% whereas its heterogeneous reactivity was reduced by about 40% if functionalized
1055 by a C8 alkane (Usher et al., 2003b). The presence of O_3 can also promote heterogeneous
1056 oxidation of other trace gases on mineral dust surface (Ullerstam et al., 2002; Hanisch and
1057 Crowley, 2003b; Li et al., 2006; Chen et al., 2008; Wu et al., 2011), including NO, SO_2 ,
1058 methacrolein, methyl vinyl ketone, and etc.

1059



1060 **Table 6:** Summary of previous laboratory studies on heterogeneous reactions of mineral dust with O₃

Dust	Reference	T (K)	Concentration (molecule cm ⁻³)	Uptake coefficient	Techniques
Al ₂ O ₃	Michel et al., 2002	296	1.9×10 ¹¹	γ_0 : (8±5)×10 ⁻⁵	KC-MS
	Michel et al., 2003	250-330	(1-10)×10 ¹¹	At 296 K, γ_0 was determined to be (1.2±0.4)×10 ⁻⁴ and γ_{ss} was determined to be 7.6×10 ⁻⁶ . A very weak temperature dependence was observed.	KC-MS
	Usher et al., 2003b	295±1	1.9×10 ¹¹	Compared to fresh particles, γ_0 were reduced by 72% to (3.4±0.6)×10 ⁻⁵ when the surface coverage of HNO ₃ was (6±3)×10 ⁻¹⁴ molecule cm ⁻² and increased by 33% to (1.6±0.2)×10 ⁻⁴ when the surface coverage of SO ₂ was (1.5±0.3)×10 ⁻¹⁴ molecule cm ⁻² .	KC-MS
	Sullivan et al., 2004	room temperature	(1-10)×10 ¹³	γ (O ₃) decreased from ~1×10 ⁻⁵ to ~1×10 ⁻⁶ when initial O ₃ concentration increased from 1×10 ¹³ to 1×10 ¹⁴ molecule cm ⁻³ .	static reactor
	Mogili et al., 2006a	room temperature	1×10 ¹⁵	γ (O ₃) decreased from (3.5±0.9)×10 ⁻⁸ at <1% RH to (4.5±1.1)×10 ⁻⁹ at 19% RH.	EC
	Chen et al., 2011a	room temperature	~1.9×10 ¹⁵	Irradiation from a solar simulation could enhance O ₃ uptake by α -Al ₂ O ₃ , but no uptake coefficient was reported.	EC
	Chen et al., 2011b	room temperature	(2-3)×10 ¹⁵	Uptake of O ₃ by α -Al ₂ O ₃ was insignificant under both dark and irradiated conditions.	EC



Saharan dust	Michel et al., 2002	296	1.9×10^{11}	γ_0 was determined to be $(6 \pm 3) \times 10^{-5}$ for ground Saharan dust and $(4 \pm 2) \times 10^{-6}$ for sieved Saharan dust.	KC-MS
	Hanisch and Crowley, 2003	296	$(0.54-84) \times 10^{11}$	$\gamma_0 = 3.5 \times 10^{-4}$ and $\gamma_{ss} = 4.8 \times 10^{-5}$ when $[O_3]_0 = 5.4 \times 10^{10}$ molecule cm^{-3} ; $\gamma_0 = 5.8 \times 10^{-5}$ and $\gamma_{ss} = 1.3 \times 10^{-5}$ when $[O_3]_0 = 2.8 \times 10^{11}$ molecule cm^{-3} ; $\gamma_0 = 5.5 \times 10^{-6}$ and $\gamma_{ss} = 2.2 \times 10^{-6}$ when $[O_3]_0 = 8.4 \times 10^{12}$ molecule cm^{-3} .	KC-MS
	Michel et al., 2003	295±1	$(1.9 \pm 0.6) \times 10^{11}$	For ground Saharan dust, $\gamma_0: (6 \pm 2) \times 10^{-5}$ and $\gamma_{ss}: 6 \times 10^{-6}$. For sieved Saharan dust, $\gamma_0: (2.7 \pm 0.9) \times 10^{-6}$.	KC-MS
	Chang et al., 2005	room temperature	$(0.2-10) \times 10^{13}$	$\gamma(O_3)$ decreased from 6×10^{-6} to $\sim 2 \times 10^{-7}$ when $[O_3]$ increased from 2×10^{12} to 1×10^{14} molecule cm^{-3} .	static reactor
	Karagulian and Rossi, 2006	298±2	$(3.5-10) \times 10^{12}$	$\gamma_0 = (9.3 \pm 2.6) \times 10^{-2}$ and $\gamma_{ss} = (6.7 \pm 1.3) \times 10^{-3}$ when $[O_3]_0 = 3.5 \times 10^{12}$ molecule cm^{-3} ; $\gamma_0 = (3.7 \pm 1.8) \times 10^{-3}$ and $\gamma_{ss} = (3.3 \pm 2.5) \times 10^{-3}$ when $[O_3]_0 = 1.0 \times 10^{13}$ molecule cm^{-3} . Reported uptake coefficients were based on the projected surface area.	KC-MS
Fe₂O₃	Michel et al., 2002	296	1.9×10^{11}	$\gamma_0: (1.8 \pm 0.7) \times 10^{-4}$	KC-MS
	Michel et al., 2003	295±1	$(1-10) \times 10^{11}$	$\gamma_0: (2.0 \pm 0.3) \times 10^{-4}$; $\gamma_{ss}: 2.2 \times 10^{-5}$	KC-MS
	Mogili et al., 2006a	room temperature	$(1.8-8.5) \times 10^{14}$	When $[O_3]_0$ was 7.9×10^{14} molecule cm^{-3} , $\gamma(O_3)$ decreased from $(1.0 \pm 0.3) \times 10^{-7}$ at <1% RH to $(1.2 \pm 0.3) \times 10^{-8}$ at 23% RH and to $(2.5 \pm 0.6) \times 10^{-9}$ at 58% RH. When $[O_3]_0$ was 2.1×10^{14} molecule cm^{-3} ,	EC



					$\gamma(\text{O}_3)$ decreased from $(5.0 \pm 1.2) \times 10^{-8}$ at <1% RH to $(2.0 \pm 0.5) \times 10^{-8}$ at 21% RH and to $(9.0 \pm 2.3) \times 10^{-9}$ at 43% RH.	
Chen et al., 2011a	room temperature	$\sim 1.9 \times 10^{15}$			Irradiation from a solar simulation could enhance the O_3 uptake by $\alpha\text{-Fe}_2\text{O}_3$, but no uptake coefficient was reported.	EC
Chen et al., 2011b	room temperature	$(2\text{-}3) \times 10^{15}$			Under dark conditions, $\gamma(\text{O}_3)$ decreased from $(4.1 \pm 0.2) \times 10^{-7}$ at <2% RH to $(2.7 \pm 0.1) \times 10^{-7}$ at 21% RH. When irradiated, $\gamma(\text{O}_3)$ decreased from $(6.6 \pm 0.3) \times 10^{-7}$ at <2% RH to $(5.5 \pm 0.3) \times 10^{-7}$ at 12% RH and to $(1.1 \pm 0.1) \times 10^{-7}$ at 25% RH.	EC
SiO ₂						
Michel et al., 2002	296	1.9×10^{11}			$\gamma_0: (5 \pm 3) \times 10^{-5}$	KC-MS
Michel et al., 2003	295 ± 1	$(1.9 \pm 0.6) \times 10^{11}$			$\gamma_0: (6.3 \pm 0.9) \times 10^{-5}$	KC-MS
Usher et al., 2003b	295 ± 1	1.9×10^{11}			Compared to fresh particles, γ_0 was increased by 40% to $(7 \pm 2) \times 10^{-5}$ when the surface coverage of a C8 alkene was $(2 \pm 1) \times 10^{14}$ molecule cm ⁻² and reduced by 40% to $(3 \pm 1) \times 10^{-5}$ when the surface coverage of a C8 alkane was $(2 \pm 1) \times 10^{14}$ molecule cm ⁻² .	KC-MS
Nicolas et al., 2009	298	$(1.3\text{-}7.3) \times 10^{12}$			$\gamma(\text{O}_3)$ was found to be $< 1 \times 10^{-8}$, showing negative dependence on $[\text{O}_3]_0$ and RH. No difference in $\gamma(\text{O}_3)$ under dark and illuminated conditions was reported.	CWFT
China loess						
Michel et al., 2002	296	1.9×10^{11}			$\gamma_0: (2.7 \pm 0.9) \times 10^{-5}$	KC-MS
Michel et al., 2003	295 ± 1	$(1.9 \pm 0.6) \times 10^{11}$			$\gamma_0: (2.7 \pm 0.8) \times 10^{-5}$	KC-MS



kaolinite	Michel et al., 2003 295±1	$(1.9±0.6)×10^{11}$	$\gamma_0: (3±1)×10^{-5}$	KC-MS
	Karagulian and Rossi, 2006	$(2.4±0.7)×10^{12}$	Projected surface area based: $\gamma_0 = (6.3±0.2)×10^{-2}$ and $\gamma_{ss} = (1.0±0.2)×10^{-2}$; pore diffusion corrected $\gamma_{ss}: (2.7±0.3)×10^{-6}$.	KC-MS
CaCO ₃	Karagulian and Rossi, 2006	$(5.3±0.7)×10^{12}$	Projected surface area based: $\gamma_0 = (1.2±0.3)×10^{-2}$ and $\gamma_{ss} = (3.6±0.2)×10^{-3}$; pore diffusion corrected $\gamma_{ss}: (7.8±0.7)×10^{-7}$.	KC-MS
TiO ₂	Nicolas et al., 2009 298	$(1.3-7.3)×10^{12}$	$\gamma(O_3)$ on TiO ₂ /SiO ₂ decreased with $[O_3]_0$ and RH under both dark and illuminated conditions. Under illuminated conditions it increased with TiO ₂ mass fraction in TiO ₂ /SiO ₂ and depended almost linearly on irradiance intensity. At 24% RH and $[O_3]_0$ of 51 ppbv, $\gamma(O_3)$ on 1 wt% TiO ₂ /SiO ₂ was reported to be $(2.8±0.4)×10^{-9}$ under dark conditions and $(4.7±0.7)×10^{-8}$ under a near UV irradiance of $3.2×10^{-8}$ mW cm ⁻² .	CWFT
	Chen et al., 2011b room temperature	$(2-3)×10^{15}$	Uptake of O ₃ was negligible under dark conditions. Under the irradiation of a solar simulator, $\gamma(O_3)$ was determined to be $(2.0±0.1)×10^{-7}$ at <2% RH, $(2.2±0.1)×10^{-7}$ at 12% RH, $(2.4±0.1)×10^{-7}$ at 22% RH, and $(1.9±0.1)×10^{-7}$ at 39% RH, respectively.	EC
ATD	Karagulian and Rossi, 2006	$(3.3-8.0)×10^{12}$	$\gamma_0 = (1.3±0.6)×10^{-2}$ and $\gamma_{ss} = (2.2±1.2)×10^{-3}$ when $[O_3]_0 = 3.3×10^{12}$ molecule cm ⁻³ ; $\gamma_0 = (1.3±0.7)×10^{-2}$ and $\gamma_{ss} = (2.5±1.2)×10^{-3}$ when $[O_3]_0 = 8×10^{12}$ molecule cm ⁻³ . Reported uptake coefficients were based on the projected surface area.	KC-MS



limestone Karagulian and Rossi, 2006 298 ± 2 $(3-20) \times 10^{12}$ $\gamma_0 = (1.3 \pm 0.2) \times 10^{-2}$ and $\gamma_{ss} = (1.6 \pm 0.5) \times 10^{-3}$ when $[O_3]_0 = 3 \times 10^{12}$ molecule cm^{-3} ; $\gamma_0 = (2.1 \pm 0.3) \times 10^{-3}$ and $\gamma_{ss} = (2.4 \pm 0.7) \times 10^{-4}$ when $[O_3]_0 = 2 \times 10^{13}$ molecule cm^{-3} . Reported uptake coefficients were based on the projected surface area. KC-MS



1062 Another two groups also utilized Knudsen cell reactors to investigate O₃ uptake by
1063 mineral dust (Hanisch and Crowley, 2003a; Karagulian and Rossi, 2006). The uptake of O₃ by
1064 Saharan dust was investigated over a broad range of [O₃]₀ by Hanisch and Crowley (2003), and
1065 $\gamma_0(\text{O}_3)$ and $\gamma_{\text{ss}}(\text{O}_3)$ were determined to be 3.5×10^{-4} and 4.8×10^{-5} when [O₃]₀ was $(5.4 \pm 0.8) \times 10^{10}$
1066 molecule cm⁻³, 5.8×10^{-5} and 1.3×10^{-5} when [O₃]₀ was 2.8×10^{11} molecule cm⁻³, and 5.5×10^{-6}
1067 and 2.2×10^{-4} when [O₃]₀ was $(8.4 \pm 3.4) \times 10^{12}$ molecule cm⁻³, showing a negative dependence
1068 on [O₃]₀. It should be noted that the KML model (Keyser et al., 1991; Keyser et al., 1993) was
1069 applied by Hanisch and Crowley (2003) to derive the uptake coefficients. Furthermore, they
1070 found that O₃ was converted to O₂ after reaction with Saharan dust and physisorption was
1071 negligible (Hanisch and Crowley, 2003a).

1072 Karagulian and Rossi et al. (2006) investigated heterogeneous interactions of O₃ with
1073 kaolinite, CaCO₃, natural limestone, Saharan dust, and ATD. Based on the projected surface
1074 areas of dust samples, their reported γ_0 are in the range of $(2.3 \pm 0.4) \times 10^{-2}$ to $(9.3 \pm 2.6) \times 10^{-2}$ and
1075 γ_{ss} are in the range of $(3.5 \pm 1.6) \times 10^{-5}$ to $(1.0 \pm 0.2) \times 10^{-2}$. These values, summarized in Table 4
1076 together with corresponding [O₃]₀, are not repeated here. Pore diffusion corrected γ_{ss} were
1077 reported to be $(2.7 \pm 0.3) \times 10^{-6}$ for kaolinite when [O₃]₀ was 2.4×10^{12} molecule cm⁻³ and
1078 $(7.8 \pm 0.7) \times 10^{-7}$ for CaCO₃ when [O₃]₀ was 5.3×10^{12} molecule cm⁻³, more than three orders of
1079 magnitude smaller than those based on the projected surface area (Karagulian and Rossi, 2006).

1080 The uptake of O₃ on $\alpha\text{-Al}_2\text{O}_3$ (Sullivan et al., 2004) and Saharan dust (Chang et al.,
1081 2005) was investigated using a static reactor, in which a dust-coated Pyrex tube was exposed
1082 to O₃ at room temperature. In the first few tens of seconds after exposure to dust particles, O₃
1083 decays followed an exponential manner, and the average decay rates were used to derive uptake
1084 coefficients. $\gamma(\text{O}_3)$, based on the BET surface area, was found to decrease with increasing initial
1085 [O₃]. For $\alpha\text{-Al}_2\text{O}_3$, $\gamma(\text{O}_3)$ decreased from $\sim 1 \times 10^{-5}$ to $\sim 1 \times 10^{-6}$ when [O₃] increased from 1×10^{13}
1086 to 1×10^{14} molecule cm⁻³ (Sullivan et al., 2004). For Saharan dust, $\gamma(\text{O}_3)$ decreased from 2×10^{-7}

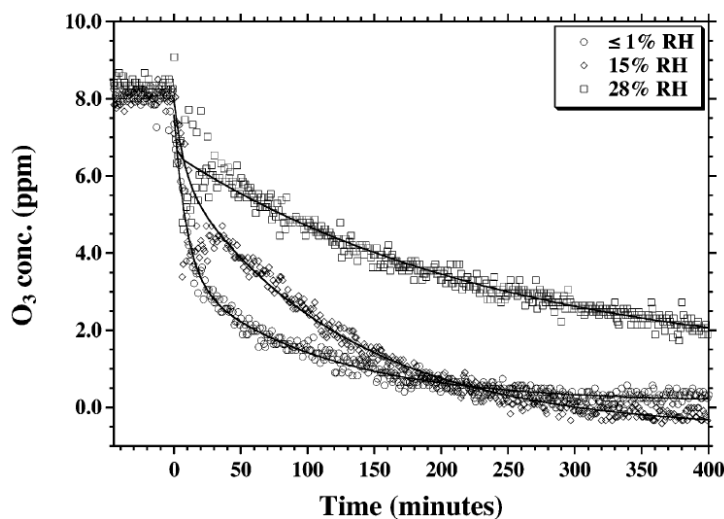


1087 to 2×10^{-6} for Saharan dust when $[O_3]$ increased from 2×10^{12} to 1×10^{14} molecule cm^{-3} , and the
1088 dependence of $\gamma(O_3)$ on $[O_3]$ can be described by Eq. (18) (Chang et al., 2005):

1089
$$\gamma(O_3) = 7.5 \times 10^5 \times [O_3]^{-0.90} \quad (18)$$

1090 where $[O_3]$ is the O_3 concentration in molecule cm^{-3} . No significant effect of RH (0-75%) on
1091 uptake kinetics was observed for $\alpha\text{-Al}_2\text{O}_3$ and Saharan dust (Sullivan et al., 2004; Chang et al.,
1092 2005).

1093 An environmental chamber in which O_3 was exposed to suspended particles was
1094 deployed to investigate heterogeneous reactions of airborne mineral dust with O_3 under dark
1095 and illuminated conditions (Mogili et al., 2006a; Chen et al., 2011a; Chen et al., 2011b). O_3
1096 concentrations in the chamber, detected using FTIR or UV/Vis absorption spectroscopy, were
1097 found to decay exponentially with reaction time. As shown in Figure 10, uptake of O_3 by α -
1098 Fe_2O_3 was significantly suppressed at increasing RH, and a negative effect of RH was also
1099 observed for uptake of O_3 by $\alpha\text{-Al}_2\text{O}_3$ (Mogili et al., 2006a). In addition, increasing $[O_3]_0$
1100 resulted in reduction in $\gamma(O_3)$ for both minerals. Heterogeneous reactivity towards O_3 under
1101 similar conditions is higher for $\alpha\text{-Fe}_2\text{O}_3$ when compared to $\alpha\text{-Al}_2\text{O}_3$ (Mogili et al., 2006a). For
1102 $\alpha\text{-Fe}_2\text{O}_3$, when $[O_3]_0$ was 7.9×10^{14} molecule cm^{-3} , $\gamma(O_3)$ decreased from $(1.0 \pm 0.3) \times 10^{-7}$ at <1%
1103 RH to $(1.2 \pm 0.3) \times 10^{-8}$ at 23% RH and to $(2.5 \pm 0.6) \times 10^{-9}$ at 58% RH; when $[O_3]_0$ was 2.1×10^{14}
1104 molecule cm^{-3} , $\gamma(O_3)$ was reduced from $(5.0 \pm 1.2) \times 10^{-8}$ at <1% RH to $(2.0 \pm 0.5) \times 10^{-8}$ at 21%
1105 RH and to $(9.0 \pm 2.3) \times 10^{-9}$ at 43% RH. Meanwhile, $\gamma(O_3)$ was observed to decrease from
1106 $(3.5 \pm 0.9) \times 10^{-8}$ at <1% RH to $(4.5 \pm 1.1) \times 10^{-9}$ at 19% RH for $\alpha\text{-Al}_2\text{O}_3$ when $[O_3]_0$ was 1×10^{15}
1107 molecule cm^{-3} .

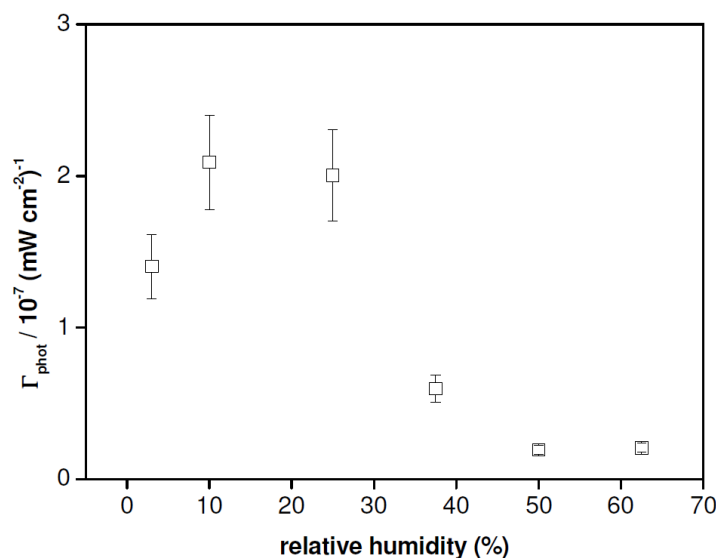


1108

1109 **Figure 10.** Measured O_3 decays in an aerosol chamber due to interaction with airborne $\alpha\text{-Fe}_2\text{O}_3$
1110 particles (starting at 0 min). The solid curves represent exponential fits to the measured O_3
1111 concentrations as a function of reaction time. Reprinted with permission from Mogili et al.
1112 (2006b). Copyright 2006 American Chemical Society.

1113

1114 A solar simulator was coupled to the environmental chamber by Chen et al. (2011a),
1115 and irradiation from the solar simulator was found to enhance heterogeneous uptake of O_3 by
1116 $\alpha\text{-Fe}_2\text{O}_3$ and $\alpha\text{-Al}_2\text{O}_3$; however, no uptake coefficient was reported. In a following study, Chen
1117 et al. (2011b) found that heterogeneous uptake of O_3 by $\alpha\text{-Al}_2\text{O}_3$ was insignificant under both
1118 dark and irradiated conditions. In contrast, while the uptake of O_3 by TiO_2 was negligible under
1119 dark conditions, when irradiated $\gamma(\text{O}_3)$ was determined to be $(2.0 \pm 0.1) \times 10^{-7}$ at <2% RH,
1120 $(2.2 \pm 0.1) \times 10^{-7}$ at 12% RH, $(2.4 \pm 0.1) \times 10^{-7}$ at 22% RH, and $(1.9 \pm 0.1) \times 10^{-7}$ at 39% RH,
1121 respectively (Chen et al., 2011b). Photo-enhanced O_3 uptake was also observed for $\alpha\text{-Fe}_2\text{O}_3$
1122 (Chen et al., 2011b). Under dark conditions $\gamma(\text{O}_3)$ decreased from $(4.1 \pm 0.2) \times 10^{-7}$ at <2% RH
1123 to $(2.7 \pm 0.1) \times 10^{-7}$ at 21% RH, while when irradiated $\gamma(\text{O}_3)$ was reported to be $(6.6 \pm 0.3) \times 10^{-7}$ at
1124 <2% RH, $(5.5 \pm 0.3) \times 10^{-7}$ at 12% RH, and $(1.1 \pm 0.1) \times 10^{-7}$ at 25% RH, respectively.



1125

1126 **Figure 11.** Effects of RH on the irradiance-normalized O₃ uptake coefficients. The TiO₂/SiO₂
1127 films which contained 1 wt% TiO₂ were exposed to 37 ppbv O₃ at 298 K under irradiance of
1128 2.7×10^{14} photons cm⁻² s⁻¹. Reprinted with permission from Nicolas et al. (2009). Copyright
1129 2009 American Chemical Society.

1130

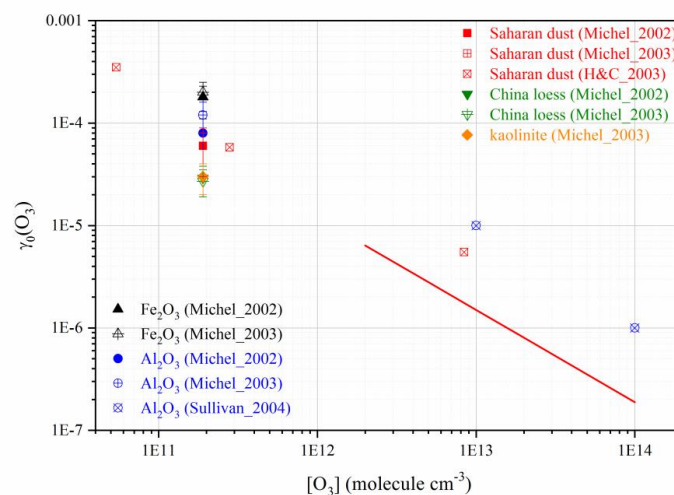
1131 Photo-enhanced catalytic decomposition of O₃ on mineral dust was in fact first reported
1132 by a coated wall flow tube study at 298 K (Nicolas et al., 2009). Under their experimental
1133 conditions ([O₃]₀: 50-290 ppbv; RH: 3-60%), the BET surface area based $\gamma_{\text{ss}}(\text{O}_3)$, was found to
1134 be $< 1 \times 10^{-8}$ for SiO₂ and TiO₂/SiO₂ mixture with TiO₂ mass fraction up to 5% under dark
1135 conditions. Near UV irradiation could largely increase the uptake of O₃ by TiO₂/SiO₂ mixture,
1136 and the effect increased with the TiO₂ mass fraction (the effect is insignificant for pure SiO₂)
1137 and almost depended linearly on the intensity of UV irradiance (Nicolas et al., 2009). When
1138 RH was 24% and [O₃]₀ was 51 ppbv, $\gamma(\text{O}_3)$ for TiO₂/SiO₂ mixture with a TiO₂ mass fraction of
1139 1% was measured to be $(2.8 \pm 0.4) \times 10^{-9}$ under dark conditions and $(4.7 \pm 0.7) \times 10^{-8}$ under near
1140 UV irradiation of 3.0×10^{-8} mW cm⁻². RH was found to play a profound role in heterogeneous



1141 photochemical reaction of O_3 with TiO_2/SiO_2 . Figure 11 shows that the irradiance-normalized
1142 uptake coefficient, defined as the uptake coefficient divided by the irradiance intensity,
1143 increased with RH for RH <20% and then decreased significantly with RH when RH was
1144 further increased. This phenomenon was also observed by Chen et al. (2011b), who found that
1145 under illuminated conditions $\gamma(O_3)$ first increased and then decreased with RH for TiO_2 aerosol
1146 particles.

1147 3.3.1 Discussion

1148 All the initial $\gamma(O_3)$ reported by previous studies for different minerals are summarized
1149 in Figure 12 as a function of $[O_3]$. Karagulian and Rossi (2006) reported projected area based
1150 $\gamma_0(O_3)$, which are several orders of magnitude larger than values reported by other work. This
1151 is because O_3 uptake by mineral dust is relatively slow and some underlying dust layers, if not
1152 all, must be accessible by O_3 molecules. Therefore, results reported by Karagulian and Rossi
1153 (2006) are not included in Figure 12. Sullivan et al. (2004) and Chang et al. (2005) measured
1154 O_3 decay rates in the first tens of seconds due to interaction with dust particles deposited onto
1155 the inner wall of a Pyrex tube to derive $\gamma(O_3)$. Their reported $\gamma(O_3)$ are in fact the average uptake
1156 coefficients in the first tens of seconds, and can be classified as either $\gamma_0(O_3)$ and $\gamma_{ss}(O_3)$.
1157 Therefore, $\gamma(O_3)$ reported by Sullivan et al. (2004) and Chang et al. (2005) are included in
1158 Figure 12 which summarizes $\gamma_0(O_3)$ and also in Figure 13 which summarizes $\gamma_{ss}(O_3)$.

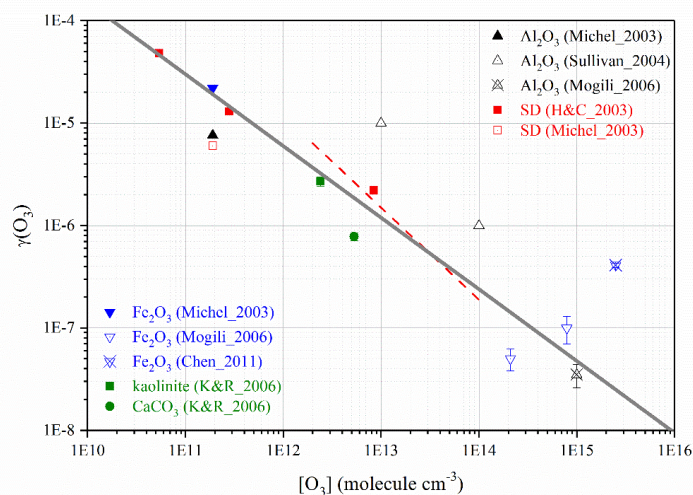


1159

1160 **Figure 12.** Dependence of $\gamma_0(\text{O}_3)$ on initial O_3 concentrations under dry conditions for different
1161 mineral dust particles as reported by previous studies: Michel_2002 (Michel et al., 2002),
1162 Michel_2003 (Michel et al., 2003), H&C_2003 (Hanisch and Crowley, 2003a), Sullivan_2004
1163 (Sullivan et al., 2004). The red curve represents the dependence of $\gamma(\text{O}_3)$ on $[\text{O}_3]$ for Saharan
1164 dust reported by Chang et al. (2005).

1165

1166 It should be noted that all the studies included in Figure 12 used dust powder samples
1167 supported on substrates. Significant variation in reported $\gamma_0(\text{O}_3)$ is evident from Figure 12. For
1168 examples, $\gamma_0(\text{O}_3)$ determined at $[\text{O}_3]$ of $\sim 2 \times 10^{11}$ molecule cm^{-3} are differed by a factor of ~ 10 .
1169 The observed difference in $\gamma_0(\text{O}_3)$ may be caused by 1) variability in heterogeneous reactivity
1170 of different minerals and 2) that different experimental methods can lead to different results.
1171 For example, it has been suggested that pretreatment of mineral dust particles (e.g., heating,
1172 grinding, and evacuation) could modify their initial heterogeneous reactivity towards O_3
1173 (Hanisch and Crowley, 2003a; Michel et al., 2003). Furthermore, as discussed in Section 2.2,
1174 time resolution in different studies is also different, making interpretation of γ_0 difficult.



1175

1176 **Figure 13.** Dependence of $\gamma_{ss}(\text{O}_3)$ on initial O_3 concentrations under dry conditions for different
1177 mineral dust particles: Michel_2003 (Michel et al., 2003), H&C_2003 (Hanisch and Crowley,
1178 2003a), Sullivan_2004 (Sullivan et al., 2004), Mogili_2006 (Mogili et al., 2006a), K&R_2006
1179 (Karagulian and Rossi, 2006), and Chen_2011 (Chen et al., 2011b). The red dashed curve
1180 represents the dependence of $\gamma(\text{O}_3)$ on $[\text{O}_3]$ for Saharan dust reported by Chang et al. (2005),
1181 and the grey solid curve represents the dependence of $\gamma(\text{O}_3)$ on $[\text{O}_3]$ for mineral dust particles
1182 recommended by the IUPAC Task Group on Atmospheric Chemical Kinetic Data Evaluation.
1183 Reprinted (with modification) with permission from the IUPAC Task Group on Atmospheric
1184 Chemical Kinetic Data Evaluation (<http://iupac.pole-ether.fr>).

1185

1186 In contrast, $\gamma_{ss}(\text{O}_3)$ reported by previous studies under dry conditions show fairly good
1187 agreement (as displayed in Figure 13), considering the fact that very different experimental
1188 techniques have been used (for example, aerosol samples were used by Mogili et al. (2006b)
1189 and Chen et al. (2011b) while all the other studies used dust powder samples supported on
1190 substrates). In addition, a rather strong dependence of $\gamma_{ss}(\text{O}_3)$ on initial O_3 concentration can be
1191 observed. Eq. (19) has been recommended by the IUPAC task group on Atmospheric Chemical



1192 Kinetic Data Evaluation to parameterize the dependence of $\gamma_{ss}(O_3)$ on $[O_3]$ (Crowley et al.,
1193 2010a):

$$1194 \quad \gamma(O_3) = 1500 \times [O_3]^{-0.7} \quad (19)$$

1195 where $[O_3]$ is O_3 concentration in molecule cm^{-3} . It is quite surprising that $\gamma_{ss}(O_3)$ under dry
1196 conditions are very similar for all the minerals investigated. It can also be observed from
1197 Figure 13 that $\gamma_{ss}(O_3)$ for $\alpha\text{-Al}_2O_3$ reported by Sullivan et al. (2004) and for $\alpha\text{-Fe}_2O_3$ reported
1198 by Chen et al. (2011b) may be significantly larger than those recommended by Crowley et al.
1199 (2010), and the reason is not very clear yet. It should be pointed out that the work by Sullivan
1200 et al. (2005), though published, was not included in the original figure prepared by the IUPAC
1201 Task Group. In addition, the work by Chen et al. (2011b) was published after the IUACP report
1202 was released online.

1203 Only three previous studies have explored effects of RH on heterogeneous reactions of
1204 O_3 with mineral dust, and different results have been reported. While a strong negative effect
1205 of RH on O_3 uptake kinetics was observed for $\alpha\text{-Al}_2O_3$ and $\alpha\text{-Fe}_2O_3$ by Mogili et al. (2006b),
1206 the other two studies (Sullivan et al., 2004; Chang et al., 2005) suggested that the influence of
1207 RH on heterogeneous uptake of O_3 by $\alpha\text{-Al}_2O_3$ and Saharan dust was insignificant. Further
1208 experimental and theoretical work is required to better understand the effect of RH on O_3
1209 uptake by mineral dust. As discussed below, surface adsorbed water may play different roles
1210 in heterogeneous reaction of minerals with O_3 .

1211 A few other studies (Li et al., 1998; Li and Oyama, 1998; Roscoe and Abbatt, 2005;
1212 Lampimaki et al., 2013) used different surface techniques to monitor mineral dust surfaces
1213 during exposure to O_3 . These studies did not report uptake coefficients and hence are not
1214 included in Table 4. Nevertheless, they have provided valuable insights into reaction
1215 mechanisms at the molecular level and are worthy of further discussion. A new Raman peak at
1216 884 cm^{-1} was observed after exposure MnO_2 to O_3 , and it is attributed to peroxide species (i.e.



1217 SS-O₂) by combining Raman spectroscopy, ¹⁸O isotope substitution measurements, and ab
1218 initio calculation (Li et al., 1998). Consequently, the following reaction mechanism has been
1219 proposed for heterogeneous reaction of O₃ with metal oxides (Li et al., 1998):



1222 where SS represents reactive surface sites towards O₃. The intensity of the SS-O₂ peak was
1223 found to decrease gradually with time after O₃ exposure was terminated, suggesting that SS-
1224 O₂ would slowly decompose to O₂ (Li et al., 1998):



1226 A following study by the same group (Li and Oyama, 1998) suggested that the steady-state and
1227 transient kinetics of heterogeneous decomposition of O₃ on MnO₂ could be well described by
1228 the aforementioned reaction mechanism (R18a, R18b, and R18c). Reaction R18a is expected
1229 to be of the Eley-Rideal type, because desorption of O₃ from mineral surfaces has never been
1230 observed (Hanisch and Crowley, 2003a; Michel et al., 2003; Karagulian and Rossi, 2006) and
1231 thus the Langmuir-Hinshelwood mechanism is unlikely. It is also suggested that reaction R18a
1232 is much faster than the other two steps and the reactivation step (R18c) is slowest (Li et al.,
1233 1998; Li and Oyama, 1998).

1234 The reaction mechanism proposed by Li et al. was supported by several following
1235 studies. For examples, gradual surface passivation was observed for a variety of minerals
1236 (Hanisch and Crowley, 2003a; Michel et al., 2003), suggesting that the number of reactive
1237 surface sites towards O₃ is limited, as implied by reactions R18a and R18b. On the other hand,
1238 two previous studies (Hanisch and Crowley, 2003a; Sullivan et al., 2004) observed that surface
1239 reactivation would slowly occur after O₃ exposure was stopped, and Michel et al. (2003) found
1240 that heterogeneous uptake of O₃ by minerals is of catalytic nature to some extent. These studies
1241 (Hanisch and Crowley, 2003a; Michel et al., 2003; Sullivan et al., 2004) clearly demonstrate



1242 that a slow surface reactivation step exists, consistent with the reaction mechanism (more
1243 precisely, reaction R18c) proposed by Li and coworkers (Li et al., 1998; Li and Oyama, 1998).
1244 Using DRIFTS, Roscoe and Abbatt (2005) monitored the change of alumina during its
1245 heterogeneous interaction with O₃ and water vapor. A new IR peak at 1380 cm⁻¹, attributed to
1246 SS-O, appeared after alumina was exposed to O₃. Because alumina is opaque below 1100 cm⁻¹,
1247 the SS-O₂ peak, expected to appear at around 884 cm⁻¹ (Li et al., 1998), could not be detected
1248 by IR. When alumina was simultaneously exposed O₃ and water vapor, the intensity of the
1249 SS-O peak was substantially decreased, compared to the case when exposure to O₃ alone. This
1250 suggests that water molecules can be adsorbed strongly to sites which would otherwise react
1251 with O₃, thus suppressing the formation of SS-O on the surface (Roscoe and Abbatt, 2005). In
1252 this aspect, increasing RH will reduce heterogeneous reactivity of alumina towards O₃. It was
1253 further found that if O₃-reacted alumina was exposed to water vapor, the intensity of the SS-O
1254 IR peak would gradually decrease while the amount of surface adsorbed water would increase.
1255 This indicates that SS-O would react with adsorbed water to regenerate reactive surface sites
1256 (i.e. SS as shown in reaction R18a), implying that the presence of water vapor may also
1257 promote O₃ uptake by alumina. As we discussed before, previous studies which examined the
1258 effects of RH on heterogeneous reactions of O₃ with minerals (Sullivan et al., 2004; Chang et
1259 al., 2005; Mogili et al., 2006a) do not agree with each other. This inconsistency may be (at least
1260 partly) be caused by complex roles which adsorbed water plays in heterogeneous uptake of O₃
1261 by mineral dust. Further work is required to elucidate the effect of RH, especially considering
1262 that heterogeneous reaction of O₃ with minerals is of interest not only for atmospheric
1263 chemistry but also for indoor air quality and industrial application (Dhandapani and Oyama,
1264 1997).



1265 **3.3.2 Atmospheric implications**

1266 Using the dependence of $\gamma(\text{O}_3)$ on $[\text{O}_3]$ recommended by Crowley et al. (2010) and
1267 assuming an typical O_3 concentration of 1.5×10^{12} molecule cm^{-3} (~60 ppbv) in the troposphere,
1268 $\gamma(\text{O}_3)$ is calculated to be 4.5×10^{-6} . Consequently, lifetimes of O_3 with respect to heterogeneous
1269 reaction with mineral dust, $\tau_{\text{het}}(\text{O}_3)$, are estimated to be about 1280, 128, 13 days for dust mass
1270 concentrations of 10, 100, and 1000 $\mu\text{g m}^{-3}$, respectively. As discussed in Section 2.1.2, in
1271 polluted and forested areas where alkenes are abundant, O_3 lifetimes are around several hours;
1272 in these regions, O_3 removal due to direct heterogeneous uptake by mineral dust is unlikely to
1273 be significant. On the other hand, O_3 lifetimes in remote free troposphere are in the range of
1274 several days to a few weeks; therefore, direct removal of O_3 by heterogeneous reaction with
1275 mineral dust could play a minor but non-negligible role for some regions in the remote free
1276 troposphere heavily impact by mineral dust.

1277 **3.4 HCHO**

1278 The photocatalytic oxidation of HCHO on P25 TiO_2 surface was investigated as a
1279 function of HCHO concentration and RH (Obee and Brown, 1995). It has been shown that at a
1280 given HCHO concentration, oxidation rates of HCHO first increased and then decreased with
1281 RH. Noguchi et al. (1998) found that under dark conditions, P25 TiO_2 particles showed higher
1282 HCHO adsorption capacity (after normalized to surface area) than activated carbon. Under UV
1283 illumination, TiO_2 thin films could convert HCHO completely to CO_2 and H_2O , with formic
1284 acid (HCOOH) being an intermediate product; furthermore, the dependence of photo-
1285 degradation rates on $[\text{HCHO}]_0$ could be described by the Langmuir-Hinshelwood model
1286 (Noguchi et al., 1998). In another study (Liu et al., 2005), it has also been suggested that
1287 kinetics of photocatalytic oxidation of HCHO on TiO_2 surface could be described by the
1288 Langmuir-Hinshelwood model, and CO was identified as one of the products.



1289 Ao et al. (2004) explored effects of NO, SO₂, and VOCs (including benzene, toluene,
1290 ethylbenzene, and o-xylene) on the photo-degradation of HCHO on P25 TiO₂ particles. Formic
1291 acid was identified as a major reaction intermediate, and HCHO degradation rates and HCOOH
1292 yields both decreased with increasing RH (Ao et al., 2004). In addition, NO could accelerate
1293 HCHO oxidation rates and HCOOH yields, whereas co-presence of SO₂ and VOCs used in this
1294 study was found to inhibit photo-oxidation of HCHO (Ao et al., 2004). DRIFTS was used by
1295 Sun et al. (2010) to investigate adsorption and photo-oxidation of HCHO on TiO₂. It has been
1296 shown that adsorbed HCHO molecules can be rapidly converted to formate on the surface under
1297 UV irradiation, and the presence of water vapor could significantly accelerate oxidation of
1298 HCHO on TiO₂ (Sun et al., 2010).

1299 All the aforementioned studies (Obee and Brown, 1995; Noguchi et al., 1998; Ao et al.,
1300 2004; Liu et al., 2005; Sun et al., 2010) clearly showed that UV illumination could largely
1301 enhance heterogeneous uptake of HCHO by TiO₂ particles, and HCOOH/HCOO⁻, CO₂, CO,
1302 and H₂O were identified as reaction intermediates and/or products. Though these studies
1303 provide useful insights into mechanisms of heterogeneous reaction of HCHO with TiO₂ surface,
1304 they are not listed in Table 5 because no uptake coefficients have been reported. Heterogeneous
1305 reaction of HCHO (10-40 ppbv) with soil samples was investigated using a coated wall flow
1306 tube (Li et al., 2016). At 0% RH, the initial uptake coefficient was determined to be
1307 $(1.1 \pm 0.05) \times 10^{-4}$, gradually decreasing to $(5.5 \pm 0.4) \times 10^{-5}$ within 8 h. Increasing RH would
1308 suppress the uptake of HCHO, and around two thirds of HCHO molecules uptaken by the soil
1309 was reversible (Li et al., 2016). The soil sample used by Li et al. were collected from a
1310 cultivated field site (Mainz, Germany) and may not resemble the composition and mineralogy
1311 of mineral dust aerosol; therefore, this study is not included in Table 7.



1312 **Table 7:** Summary of previous laboratory studies on heterogeneous reactions of mineral dust with HCHO

Dust	Reference	T (K)	Concentration (molecule cm ⁻³)	Uptake coefficient	Techniques
TiO ₂	Xu et al., 2010	163-673	(1-20)×10 ¹³	At 295±2 K, γ_0 (based on the BET surface area) were determined to be in the range of 0.5×10^{-8} to 5×10^{-8} , increasing linearly with HCHO concentration (1×10^{13} to 2×10^{14} molecule cm ⁻³). UV irradiation and increasing temperature could both accelerate this reaction.	DRIFTS, IC
	Sassine et al., 2010	278-303	(9-82)×10 ¹⁰	γ_{ss} were determined to range from $(3.00 \pm 0.45) \times 10^{-9}$ to $(2.26 \pm 0.34) \times 10^{-6}$, depending on UV irradiation, HCHO concentration, RH, and temperature.	CWFT
Al ₂ O ₃	Carlos-Cuellar et al., 2003	295	room temperature	γ_0 : $(7.7 \pm 0.3) \times 10^{-5}$	KC-MS
	Xu et al., 2006	273-333	(1-10)×10 ¹³	At 296 K, γ_0 was determined to be $(9.4 \pm 1.7) \times 10^{-9}$ based on the BET surface area and $(2.3 \pm 0.5) \times 10^{-5}$ based on the geometrical area for α -Al ₂ O ₃ . UV irradiation and increasing temperature could both accelerate this reaction.	DRIFTS, IC
SiO ₂	Xu et al., 2011	84-573	(1.3-3.6)×10 ¹³	At 295±2 K, γ_0 was determined to be $(3.6 \pm 0.8) \times 10^{-4}$ based on the geometrical area and $(1.4 \pm 0.3) \times 10^{-8}$ based on the BET surface area for γ -Al ₂ O ₃ . UV irradiation and increasing temperature could both accelerate this reaction.	DRIFTS, IC
	Carlos-Cuellar et al., 2003	295	room temperature	γ_0 : $(2.6 \pm 0.9) \times 10^{-7}$	KC-MS
Fe ₂ O ₃	Sassine et al., 2010	278-303	(9-82)×10 ¹⁰	γ_{ss} under dark conditions: $\sim 3 \times 10^{-9}$	CWFT
	Carlos-Cuellar et al., 2003	295	room temperature	γ_0 : $(1.1 \pm 0.5) \times 10^{-5}$	KC-MS



1314 Carlos-Cuellar et al. (2003) first determined uptake coefficients of HCHO on several
1315 mineral dust particles at room temperature, using a Knudsen cell reactor. Gradual surface
1316 deactivation was observed for all three types of particles, and initial uptake coefficients (γ_0),
1317 based on the BET surface area, were reported to be $(1.1 \pm 0.5) \times 10^{-4}$ for α -Fe₂O₃, $(7.7 \pm 0.3) \times 10^{-5}$
1318 for α -Al₂O₃, and $(2.6 \pm 0.9) \times 10^{-7}$ for SiO₂, respectively (Carlos-Cuellar et al., 2003).

1319 Using DRIFTS and ion chromatography, Xu and co-workers systematically investigated
1320 heterogeneous reactions of HCHO with α -Al₂O₃ (Xu et al., 2006), γ -Al₂O₃ (Xu et al., 2011),
1321 and TiO₂ particles (Xu et al., 2010) as a function of temperature, UV irradiation, and HCHO
1322 concentration. It has been found that HCHO was first converted to dioxymethylene which was
1323 then oxidized to formate on the surface, and UV irradiation and increasing temperature both
1324 could enhance heterogeneous reactivity of all three types of particles towards HCHO (Xu et al.,
1325 2006; Xu et al., 2010; Xu et al., 2011). $\gamma_0(\text{HCHO})$ on α -Al₂O₃ at 293 K was determined to be
1326 $(9.4 \pm 1.7) \times 10^{-9}$ based on the BET surface area of the sample and $(2.3 \pm 0.5) \times 10^{-5}$ based on the
1327 geometrical area of the sample holder (Xu et al., 2006). At room temperature (295 ± 2 K) and
1328 under dark conditions, $\gamma_0(\text{HCHO})$, based on the BET surface area, were determined to be in the
1329 range of 0.5×10^{-8} to 5×10^{-8} for TiO₂ (Xu et al., 2010), increasing linearly with HCHO
1330 concentration (1×10^{13} to 2×10^{14} molecule cm⁻³). Under the same condition, $\gamma_0(\text{HCHO})$ was
1331 determined to be $(3.6 \pm 0.8) \times 10^{-4}$ based on the geometrical area and $(1.4 \pm 0.31) \times 10^{-8}$ based on
1332 the BET surface area for γ -Al₂O₃ (Xu et al., 2011). The effect of RH was further studied for γ -
1333 Al₂O₃ at 295 ± 2 K, and the dependence of BET surface area based $\gamma_0(\text{HCHO})$ on RH is given
1334 by (Xu et al., 2011):

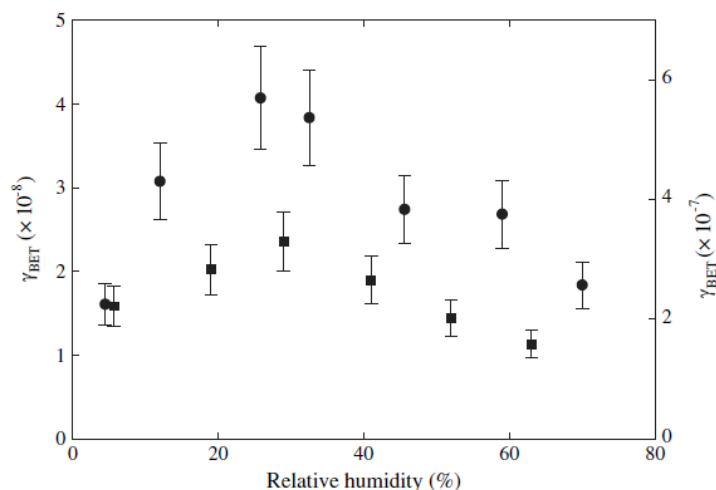
$$1335 \quad \ln[\gamma_0(\text{BET})] = -17.5 - 0.0127 \times \text{RH} \quad (20)$$

1336 where RH is in the unit of %.

1337 A coated wall flow tube was deployed to investigate heterogeneous reactions of HCHO
1338 with TiO₂ and SiO₂ particles, and the effects of UV irradiation, temperature (278-303 K), RH



1339 (6-70 %), and HCHO concentration (3.5-32.5 ppbv) were systematically examined (Sassine et
1340 al., 2010). Under dark conditions, the uptake of HCHO onto SiO₂ and TiO₂ was very slow,
1341 with BET surface area based γ_{ss} being $(3.00\pm 0.45)\times 10^{-9}$. Nevertheless, its uptake on TiO₂ and
1342 TiO₂/SiO₂ mixture was largely enhanced by near-UV irradiation (340-420 nm) (Sassine et al.,
1343 2010). For pure TiO₂ under the condition of 293 K, 30% RH and 2 ppbv HCHO, γ_{ss} depended
1344 linearly on irradiation intensity (1.9×10^{15} to 2.7×10^{15} photons cm⁻² s⁻¹). The uptake kinetics can
1345 be described by the Langmuir-Hinshelwood model: under the condition of 293 K, 6% RH, and
1346 2.7×10^{15} photons cm⁻² s⁻¹, γ_{ss} decreased from $(6.0\pm 0.9)\times 10^{-7}$ to $(2.0\pm 0.3)\times 10^{-7}$ for TiO₂ when
1347 [HCHO] increased from 3.5 to 32.5 ppbv (Sassine et al., 2010).



1348
1349 **Figure 14.** Effects of RH on heterogeneous uptake of HCHO by pure TiO₂ (circles, right y-
1350 axis) and TiO₂/SiO₂ mixture (squares, left y-axis) which contains 5% wt TiO₂. Experimental
1351 conditions: 293 K, 11 ppbv HCHO, 2.7×10^{15} photons cm⁻² s⁻¹ illumination. Reprinted with
1352 permission from Sassine et al. (2010). Copyright Elsevier 2010.

1353

1354 In addition, the effects of RH and temperature were also explored. As shown in Figure
1355 14, γ_{ss} was found to first increase with RH for TiO₂ (and TiO₂/SiO₂ mixture as well), reaching



1356 a maximum at ~30%, and then decrease with RH. Under conditions of 30% RH, 11 ppbv
1357 HCHO, and 2.7×10^{15} photons $\text{cm}^{-2} \text{s}^{-1}$, γ_{ss} increased from $(1.8 \pm 0.3) \times 10^{-7}$ at 298 K to
1358 $(3.2 \pm 0.5) \times 10^{-7}$ at 303 K (Sassine et al., 2010).

1359 **3.4.1 Discussion and atmospheric implication**

1360 Two previous studies determined BET surface area based $\gamma_0(\text{HCHO})$ for $\alpha\text{-Al}_2\text{O}_3$
1361 particles under dry conditions at room temperature, and $\gamma_0(\text{HCHO})$ reported by Carlos-Cuellar
1362 et al. (2003) is >3 orders of magnitude larger than that reported by Xu et al. (2006). It is not
1363 very clear yet why such a large difference was found between these two studies. Two studies
1364 (Sassine et al., 2010; Xu et al., 2010) measured $\gamma(\text{HCHO})$ for TiO_2 particles; however, it is
1365 difficult to make comparison because one study reported γ_0 (Xu et al., 2010) and the other one
1366 reported γ_{ss} (Sassine et al., 2010).

1367 What we can conclude from previous studies as summarized in Table 7 is that our
1368 understanding of atmospheric heterogeneous reaction of HCHO with mineral dust is very
1369 limited. For example, all the previous studies only examined its reactions with oxides, while
1370 clay minerals and authentic dust samples have never been investigated. Second, as discussed
1371 above, large discrepancies are found for uptake coefficients reported by previous studies.
1372 Furthermore, roles of RH in heterogeneous uptake of HCHO by mineral dust are not fully
1373 understood. Last but not least, though several studies have observed that UV illumination could
1374 largely enhance heterogeneous reaction of HCHO with mineral particles, it is non-trivial to
1375 know that compared to dark conditions, to which extent this reaction is accelerated under
1376 irradiation conditions relevant to the troposphere. Therefore, it is difficult to assess the
1377 significance of heterogeneous uptake by mineral dust aerosol particles as a sink for HCHO in
1378 a reliable manner.

1379 An uptake coefficient of $(9.7 \pm 1.4) \times 10^{-6}$ was used by Sassine et al. (2010) to evaluate
1380 the significance of heterogeneous reaction of HCHO with pure TiO_2 particles as a sink for



1381 HCHO. This value was linearly extrapolated from their experimental measurements (2 ppbv
1382 HCHO, 293 K, and 30% RH) to realistic solar conditions in the troposphere (1.21×10^{16} photons
1383 $\text{cm}^{-2} \text{s}^{-1}$). The value used by Sassine et al. (2010) is also adopted here to preliminarily assess
1384 the impact of heterogeneous reaction of HCHO with mineral dust. For simplicity in our work
1385 $\gamma(\text{HCHO})$ is set to 1×10^{-5} which is only 3% larger than that used by Sassine et al. (2010).
1386 Consequently, $\tau_{\text{het}}(\text{HCHO})$ are calculated to be about 456, 46, and 4.6 days for mineral dust
1387 mass concentrations of 10, 100, and 1000 $\mu\text{g m}^{-3}$, respectively. For comparison, as we have
1388 discussed in Section 2.1, typical lifetimes of HCHO are a few hours in the troposphere, with
1389 photolysis and reaction with OH radicals being the two major removal processes. It is quite
1390 clear that $\tau_{\text{het}}(\text{HCHO})$ are much larger than typical lifetimes of HCHO, and thus heterogeneous
1391 reaction with mineral dust is unlikely to be significant for the removal of HCHO in the
1392 troposphere.

1393 3.5 HONO

1394 Bedjanian and coworkers utilized a coated rod flow tube coupled to a mass spectrometer
1395 to investigate heterogeneous reaction of HONO with TiO_2 , $\gamma\text{-Al}_2\text{O}_3$, Fe_2O_3 , and ATD particles
1396 under dark and illuminated conditions (El Zein and Bedjanian, 2012; Romanias et al., 2012a;
1397 El Zein et al., 2013a; El Zein et al., 2013b). All these measurements were carried out with dust
1398 mass in the linear mass dependent regime, and thus BET surface area was used to calculate
1399 uptake coefficients. We note that several previous studies have explored heterogeneous
1400 interactions of HONO with Pyrex (Kaiser and Wu, 1977; Ten Brink and Spoolstra, 1998),
1401 borosilicate glass (Syomin and Finlayson-Pitts, 2003), and TiO_2 -doped commercial paints
1402 (Laufs et al., 2010). However, these studies are not further discussed here because they are not
1403 of direct atmospheric relevance. Uptake of HONO by soil samples was investigated using a
1404 coated-wall flow tube (Donaldson et al., 2014), and uptake coefficients were found to decrease
1405 with RH, from $(2.5 \pm 0.4) \times 10^{-4}$ at 0% RH to $(1.1 \pm 0.4) \times 10^{-5}$ at 80% RH. Soil used by Donaldson



1406 et al. were collected from an agricultural field in Indiana and its mineralogical composition
1407 may be quite different from mineral dust aerosol; as a result, this study is not included in Table
1408 8.



1409 **Table 8:** Summary of previous laboratory studies on heterogeneous reactions of mineral dust with HONO

Dust	Reference	T (K)	Concentration (molecule cm ⁻³)	Uptake coefficient	Techniques
TiO ₂	El Zein and Bedjarian, 2012	275-320	(0.3-3.3)×10 ¹²	γ ₀ was determined to be ~4.2×10 ⁻⁶ at 10% RH and 300 K, showing negative dependence on RH (up to 12.6%) and T (275-320 K).	CRFT-MS
	El Zein et al., 2013a	275-320	(0.5-5)×10 ¹²	Under illuminated condition, γ ₀ increased to ~3.5×10 ⁻⁴ at 10% RH and 280 K, showing negative dependence on RH (up to 60%) and T (275-320 K). Though illumination enhanced HONO uptake compared to dark conditions, further increase in illumination intensity for J(NO ₂) in the range of 0.002-0.012 s ⁻¹ did not affect γ ₀ .	CRFT-MS
Al ₂ O ₃	Romanias et al., 2012b	275-320	(0.6-3.5)×10 ¹²	At 10% RH, γ ₀ was determined to be ~1.2×10 ⁻⁶ and ~6.2×10 ⁻⁶ under dark and illuminated conditions, respectively. γ ₀ was found to increase linearly with J(NO ₂) in the range of 0.002-0.012 s ⁻¹ . In addition, γ ₀ decreased with RH, and no dependence on temperature was observed.	CRFT-MS
Fe ₂ O ₃	El Zein et al., 2013b	275-320	(0.6-15.0)×10 ¹²	No significant effect of UV illumination, with J(NO ₂) up to 0.012 s ⁻¹ , was observed. γ ₀ was determined to be ~4.1×10 ⁻⁷ at 10% RH and 300 K, showing negative dependence on RH (up to 14.4 %) and no dependence on T (275-320 K).	CRFT-MS
ATD	El Zein et al., 2013b	275-320	(0.6-15.0)×10 ¹²	No significant effect of UV illumination, with J(NO ₂) up to 0.012 s ⁻¹ , was observed. γ ₀ was determined to be ~9.3×10 ⁻⁷ at 10% RH and 275 K, showing negative dependence on RH (up to 84.1 %) and no dependence on T (275-320 K).	CRFT-MS



1411 El Zein and Bedjanian (2012) measured heterogeneous uptake of HONO by TiO₂
1412 particles under dark conditions. Upon exposure to HONO, heterogeneous reactivity of TiO₂
1413 was progressively reduced, and the steady-state uptake coefficients were at least one order of
1414 magnitude smaller than the corresponding initial uptake coefficients, γ_0 (El Zein and Bedjanian,
1415 2012). γ_0 , independent of initial HONO concentrations in the range of $(0.3-3.3)\times 10^{12}$ molecule
1416 cm⁻³, showed strong dependence on RH and a slightly negative dependence on temperature.
1417 The effects of temperature (275-320 K) at 0.001% RH and of RH at 300 K on γ_0 are given by
1418 (El Zein and Bedjanian, 2012):

$$1419 \quad \gamma_0 = (1.4 \pm 0.5) \times 10^{-5} \times \exp[(1405 \pm 110)/T] \quad (21)$$

$$1420 \quad \gamma_0 = 1.8 \times 10^{-5} \times RH^{-0.63} \quad (22)$$

1421 HONO uptaken by TiO₂ undergoes chemical conversion on the surface, and molecularly
1422 adsorbed HONO is insignificant (El Zein and Bedjanian, 2012). This was confirmed by gas
1423 phase production analysis, showing that the total yield of NO and NO₂ is equal to 1 within the
1424 experimental uncertainties. The yields of NO and NO₂ were determined to be 0.42 ± 0.07 and
1425 0.60 ± 0.09 , respectively, independent of RH, temperature, and the initial HONO concentration
1426 (El Zein and Bedjanian, 2012).

1427 In a following study, El Zein et al. (2013a) examined the effect of illumination on the
1428 uptake of HONO by TiO₂, and found that under illuminated conditions HONO uptake rates
1429 also decreased with reaction time. Compared to dark conditions, HONO uptake was enhanced,
1430 though no difference in the γ_0 was observed by varying UV illumination from 0.002 to 0.012 s⁻¹
1431 (El Zein et al., 2013a). Under illuminated conditions, γ_0 is independent of initial HONO
1432 concentration but depends inversely on temperature and RH. The effects of temperature (275-
1433 320 K) at 0.002% RH and of RH (0.001-60%) at 280 K can be described by (El Zein et al.,
1434 2013a):

$$1435 \quad \gamma_0 = (3.0 \pm 1.5) \times 10^{-5} \times \exp[(1390 \pm 150)/T] \quad (23)$$



1436
$$\gamma_0 = 6.9 \times 10^{-4} \times RH^{-0.3} \quad (24)$$

1437 Similar to dark conditions, all the HONO molecules removed from the gas phase have been
1438 converted NO and NO₂. Yields of NO and NO₂ were determined to be 0.48±0.07 and 0.52±0.08,
1439 respectively (El Zein et al., 2013a), independent of RH, temperature, and initial HONO
1440 concentration.

1441 The uptake of HONO by γ -Al₂O₃, Fe₂O₃, and ATD particles was also investigated under
1442 dark and illuminated conditions as a function of temperature and RH. Progressive surface
1443 deactivation was observed in all the experiments. For uptake onto γ -Al₂O₃, under both dark
1444 and irradiated conditions γ_0 (HONO) were found to be independent of initial HONO
1445 concentration (0.3×10¹² to 3.3×10¹² molecule cm⁻³) and temperature (275-320 K), though RH
1446 has a profound influence. Under dark conditions, γ_0 is given by (Romanias et al., 2012a):

1447
$$\gamma_0 = 4.8 \times 10^{-6} \times RH^{-0.61} \quad (25)$$

1448 for RH in the range of 0.00014% to 10.5%. UV illumination linearly enhances initial HONO
1449 uptake, with γ_0 under illumination with $J(\text{NO}_2)$ equal to 0.012 s⁻¹ given by (Romanias et al.,
1450 2012a):

1451
$$\gamma_0 = 1.7 \times 10^{-5} \times RH^{-0.44} \quad (26)$$

1452 for RH in the range of 0.0003% to 35.4%. NO and NO₂ yields were determined to be 0.40±0.06
1453 and 0.60±0.09 for all the experimental conditions.

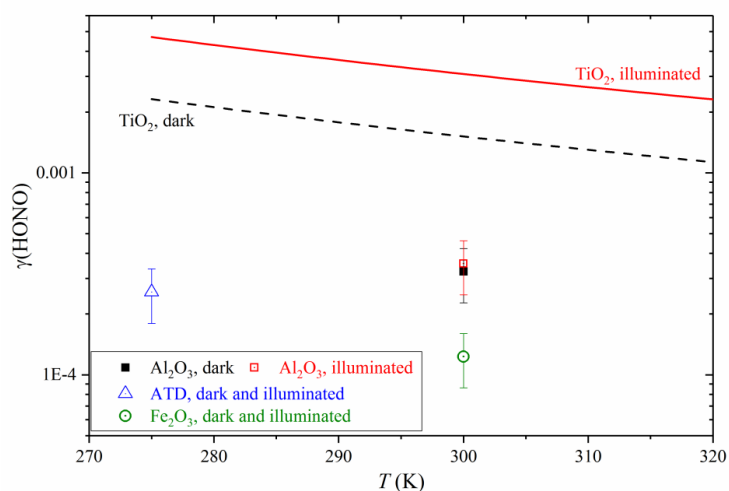
1454 No significant effects of UV irradiation with $J(\text{NO}_2)$ up to 0.012 s⁻¹ were observed for
1455 heterogeneous reaction of HONO with Fe₂O₃ and ATD particles (El Zein et al., 2013b).
1456 γ_0 (HONO) were found to be independent of initial HONO concentration (0.6×10¹² to 15.0×10¹²
1457 molecule cm⁻³) and temperature (275-320 K), while RH has a significant impact, given by (El
1458 Zein et al., 2013b):

1459
$$\gamma_0 = 1.7 \times 10^{-6} \times RH^{-0.62} \quad (27)$$

1460 for Fe₂O₃ and RH in the range of 0.0003% to 14.4%, and



1461 $\gamma_0 = 3.8 \times 10^{-6} \times RH^{-0.61}$ (28)
1462 for ATD and RH in the range of 0.00039% to 84.1%. NO and NO₂ yields, independent of
1463 experimental conditions, were reported to be 0.40±0.06 and 0.60±0.09, respectively (El Zein
1464 et al., 2013b).



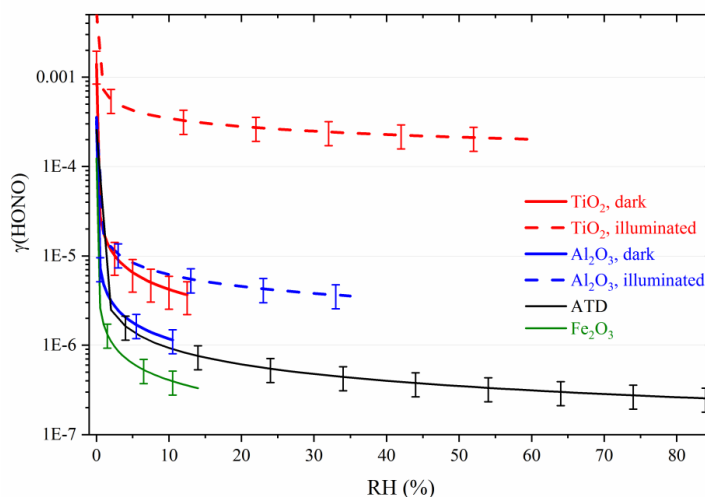
1465
1466 **Figure 15.** Temperature dependence of $\gamma_0(\text{HONO})$ for TiO₂ (El Zein and Bedjanian, 2012; El
1467 Zein et al., 2013a), Al₂O₃ (Romanias et al., 2012a), ATD (El Zein et al., 2013b) and Fe₂O₃ (El
1468 Zein et al., 2013b) under dark and illuminated conditions. Data at 0.001% RH were presented
1469 except for illuminated TiO₂ at 0.002% RH. Please note that no significant temperature (275-
1470 320 K) effect was found for Al₂O₃, ATD, and Fe₂O₃. In addition, no difference in uptake
1471 kinetics was observed between dark and illuminated conditions for ATD and Fe₂O₃.

1472

1473 The dependence of $\gamma_0(\text{HONO})$ on temperature is displayed in Figure 15 for different
1474 mineral dust under dark and illuminated conditions. No significant effect of temperature was
1475 observed for uptake onto Al₂O₃, Fe₂O₃, and ATD. When temperature increases from 275 K to
1476 320 K, $\gamma_0(\text{HONO})$ is reduced by a factor of about 2 under both dark and illuminated conditions
1477 for TiO₂. It is interesting to note that UV illumination has different impacts on HONO uptake



1478 for different minerals. HONO uptake onto Al_2O_3 is enhanced by UV radiation, and the extent
1479 of enhancement shows linear dependence on illumination intensity for $J(\text{NO}_2)$ in the range of
1480 $0.002\text{--}0.012\text{ s}^{-1}$ (Romanias et al., 2012a). In contrast, photo-enhancement was found to be
1481 insignificant for ATD and Fe_2O_3 with $J(\text{NO}_2)$ up to 0.012 s^{-1} (El Zein et al., 2013b). Significant
1482 enhancement in $\gamma_0(\text{HONO})$ was observed for illuminated TiO_2 with $J(\text{NO}_2)$ of 0.002 s^{-1} when
1483 compared to dark conditions, especially at evaluated RH as shown in Figure 16; however,
1484 further increase in illumination intensity with $J(\text{NO}_2)$ up to 0.012 s^{-1} did not lead to further
1485 increase in $\gamma_0(\text{HONO})$ (El Zein et al., 2013a). In addition, we note that NO and NO_2 yields were
1486 found to be ~ 0.40 and 0.60 for all the four types of minerals investigated, independent of
1487 experimental conditions.



1488

1489 **Figure 16.** RH dependence of $\gamma_0(\text{HONO})$ for TiO_2 (El Zein and Bedjanian, 2012; El Zein et al.,
1490 2013a), Al_2O_3 (Romanias et al., 2012a), ATD (El Zein et al., 2013b) and Fe_2O_3 (El Zein et al.,
1491 2013b) under dark and illuminated conditions at around room temperature.

1492

1493 Figure 16 shows effects of RH on $\gamma_0(\text{HONO})$ at around room temperature for TiO_2 ,
1494 Al_2O_3 , ATD, and Fe_2O_3 . Most of measurements were only carried out at low RH ($<15\%$), and



1495 thus their atmospheric relevance is rather limited. Experiments using ATD and illuminated
1496 TiO₂ particles were conducted at RH over a wide range, and a negative dependence of
1497 $\gamma_0(\text{HONO})$ on RH was observed. When RH increases from 10% to 60%, $\gamma_0(\text{HONO})$ is reduced
1498 by ~66% and ~42% for ATD and illuminated TiO₂, respectively.

1499 **3.5.1 Discussion and atmospheric implication**

1500 All the four studies, as shown in Figures 15 and 16, were carried out by the same group.
1501 Furthermore, heterogeneous interactions of HONO with authentic dust and clay minerals which
1502 are the major components for tropospheric dust, have not been explored yet. Future studies can
1503 provide more scientific insights to reaction mechanisms and better quantify uptake kinetics.

1504 In this work we use $\gamma_0(\text{HONO})$ for ATD, the only authentic dust sample investigated,
1505 to preliminarily assess the significance of heterogeneous uptake by mineral dust as a HONO
1506 sink. As shown in Figure 16, $\gamma_0(\text{HONO})$ decreases from 9.3×10^{-7} at 10% to 2.6×10^{-7} at 80%. A
1507 $\gamma(\text{HONO})$ value of 1×10^{-6} is adopted here to calculate $\tau_{\text{het}}(\text{HONO})$ with respect to
1508 heterogeneous reaction with mineral dust. This may represent an upper limit for its atmospheric
1509 significance, because i) at typical RH found in the troposphere, $\gamma_0(\text{HONO})$ should be $< 1 \times 10^{-6}$
1510 according to the work by El Zein et al. (2013b); ii) surface deactivation was observed, and thus
1511 the average $\gamma(\text{HONO})$ should be smaller than $\gamma_0(\text{HONO})$ (El Zein et al., 2013b). Using Eq. (6),
1512 $\tau_{\text{het}}(\text{HONO})$ is calculated to be ~57 days for dust mass concentration of $1000 \mu\text{g m}^{-3}$ which can
1513 only occur during dust storms. For comparison, typical HONO lifetimes in the troposphere are
1514 estimated to be 10-20 min, with the major sink being photolysis (in Section 2.1). Therefore,
1515 heterogeneous uptake by mineral dust is a negligible sink for HONO in the troposphere.

1516 **3.6 N₂O₅ and NO₃ radicals**

1517 N₂O₅ and NO₃ in the troposphere are in the dynamic equilibrium, as introduced in
1518 Section 2.1.3. Therefore, their heterogeneous reactions with mineral dust are discussed together
1519 in this section.



1520 **3.6.1 N₂O₅**

1521 Heterogeneous reaction of N₂O₅ with mineral dust particles was investigated for the
1522 first time by Seisel et al. (2005), using DRIFTS and a Knudsen cell reactor coupled to quadruple
1523 mass spectrometry. The initial uptake coefficient of N₂O₅ on Saharan dust was determined to
1524 be 0.080±0.003 at 298 K, and slowly decreased to a steady-state value of 0.013±0.003 (Seisel
1525 et al., 2005). Formation of nitrate on dust particles was observed, and N₂O₅ uptake was
1526 suggested to proceed with two mechanisms, i.e. heterogeneous hydrolysis and its reaction with
1527 surface OH groups (Seisel et al., 2005). A Knudsen cell reactor was also used by Karagulian
1528 et al. (2006) to investigate heterogeneous uptake of N₂O₅ by several different types of mineral
1529 dust. Both the initial and steady-state uptake coefficient were found to decrease with increasing
1530 initial N₂O₅ concentrations. When N₂O₅ concentration was (4.0±1.0)×10¹¹ molecule cm⁻³, γ_0
1531 and γ_{ss} were determined to be 0.30±0.08 and 0.20±0.05 for Saharan dust, 0.12±0.04 and
1532 0.021±0.006 for CaCO₃, 0.20±0.06 and 0.11±0.03 for ATD, 0.16±0.04 and 0.021±0.006 for
1533 kaolinite, and 0.43±0.13 and 0.043±0.013 for natural limestone, respectively. When N₂O₅
1534 concentration increased to (3.8±0.5)×10¹² molecule cm⁻³, γ_0 and γ_{ss} were determined to be
1535 0.090±0.026 and 0.059±0.016 for Saharan dust, 0.033±0.010 and 0.0062±0.0018 for CaCO₃,
1536 0.064±0.019 and 0.016±0.004 for ATD, 0.14±0.04 and 0.022±0.006 for kaolinite, and
1537 0.011±0.003 and 0.0022±0.0006 for natural limestone, respectively (Karagulian et al., 2006).
1538 Formation of HNO₃ in the gas phase was detected, with production yield varying with dust
1539 mineralogy. The postulated reason is that partitioning of formed HNO₃ between gas and
1540 particle phases may vary for different dust samples (Karagulian et al., 2006).

1541 Wagner et al. (2008) utilized a Knudsen cell reactor to study heterogeneous uptake of
1542 N₂O₅ by Saharan dust, ATD, and CaCO₃ particles at 296±2 K. Interestingly, surface
1543 deactivation was only observed for CaCO₃ under their experimental conditions. Therefore, γ_0
1544 and γ_{ss} are equal for the other two types of dust, being 0.037±0.012 for Saharan dust and



1545 0.022±0.008 for ATD, respectively (Wagner et al., 2008). The initial uptake coefficient was
1546 reported to be 0.05±0.02 for CaCO₃; pre-heating could reduce its heterogeneous reactivity
1547 towards N₂O₅ (Wagner et al., 2008), very likely due to the loss of surface adsorbed water and
1548 surface OH groups. It should be noted that all the uptake coefficients measured by using
1549 Knudsen cell reactors are based on the projected area of dust samples (Seisel et al., 2005;
1550 Karagulian et al., 2006; Wagner et al., 2008).

1551 Heterogeneous reactions of N₂O₅ with airborne mineral dust particles were also
1552 investigated by several previous studies, with the first one being carried out by Mogili et al.
1553 (2006b). In this study, in-situ FTIR measurements was carried out to determine N₂O₅ loss due
1554 to reactions with dust particles in an environmental chamber at 290 K. The uptake coefficients
1555 of N₂O₅, based on the BET area of dust particles, increase with RH for SiO₂, from
1556 (4.4±0.4)×10⁻⁵ at <1% RH, to (9.3±0.1)×10⁻⁵ at 11% RH, (1.2±0.2)×10⁻⁴ at 19% RH, and
1557 (1.8±0.4)×10⁻⁴ at 43% RH (Mogili et al., 2006b). In addition, γ(N₂O₅) at <1% RH were
1558 determined to be for (1.9±0.2)×10⁻⁴ for CaCO₃, (9.8±0.1)×10⁻⁴ for kaolinite, (4.0±0.4)×10⁻⁴ for
1559 α-Fe₂O₃, and (1.9±0.2)×10⁻⁴ for montmorillonite, respectively (Mogili et al., 2006b).



1560

Table 9: Summary of previous laboratory studies on heterogeneous reactions of mineral dust with N_2O_5

Dust	Reference	T (K)	Concentration (molecule cm^{-3})	Uptake coefficient	Techniques
Saharan dust	Seisel et al., 2005	298	$(0.03\text{--}5)\times 10^{12}$	$\gamma_0: 0.080\pm 0.003$ and $\gamma_{ss}: 0.013\pm 0.003$	KC, DRIFTS
	Karagulian et al., 2006	298±2	$(0.4\text{--}3.8)\times 10^{12}$	When $[\text{N}_2\text{O}_5]$ was $(4.0\pm 1.0)\times 10^{11}$ molecule cm^{-3} , $\gamma_0 = 0.30\pm 0.08$ and $\gamma_{ss} = 0.20\pm 0.05$; when $[\text{N}_2\text{O}_5]$ was $(3.8\pm 0.5)\times 10^{12}$ molecule cm^{-3} , $\gamma_0 = 0.090\pm 0.026$ and $\gamma_{ss} = 0.059\pm 0.016$.	KC
	Wagner et al., 2008	296±2	KC: $(3.0\text{--}11.0)\times 10^9$; AFT: $(5\text{--}20)\times 10^{12}$	KC measurements: $\gamma_0 = \gamma_{ss} = 0.037\pm 0.012$; AFT measurements: 0.026 ± 0.004 at 0% RH, 0.016 ± 0.004 at 29% RH, and 0.010 ± 0.004 at 58% RH.	KC-MS, AFT-CLD
	Tang et al., 2012	297±1	$(0.5\text{--}30)\times 10^{12}$	0.02 ± 0.01 , independent of RH (0-67%)	AFT- CRDS
ATD	Karagulian et al., 2006	298±2	$(0.4\text{--}3.8)\times 10^{12}$	When $[\text{N}_2\text{O}_5]$ was $(4.0\pm 1.0)\times 10^{11}$ molecule cm^{-3} , $\gamma_0 = 0.20\pm 0.06$ and $\gamma_{ss} = 0.11\pm 0.03$; when $[\text{N}_2\text{O}_5]$ was $(3.8\pm 0.5)\times 10^{12}$ molecule cm^{-3} , $\gamma_0 = 0.064\pm 0.019$ and $\gamma_{ss} = 0.016\pm 0.004$.	KC-MS
	Wagner et al., 2008	296±2	$(3.3\text{--}10.4)\times 10^9$	$\gamma_0 = \gamma_{ss} = 0.022\pm 0.008$	KC-MS
	Wagner et al., 2009	296±2	$(10\text{--}44)\times 10^{12}$	0.0098 ± 0.0010 at 0% RH and 0.0073 ± 0.0007 at 29% RH	AFT-CLD
	Tang et al., 2014c	297±1	$(11\text{--}22)\times 10^{12}$	$(7.7\pm 1.0)\times 10^{-3}$ at 0% RH, $(6.0\pm 2.0)\times 10^{-3}$ at 17% RH, $(7.4\pm 0.7)\times 10^{-3}$ at 33% RH, $(4.9\pm 1.3)\times 10^{-3}$ at 50% RH, and $(5.0\pm 0.3)\times 10^{-3}$ at 67% RH.	AFT- CRDS
CaCO ₃	Karagulian et al., 2006	298±2	$(0.4\text{--}3.8)\times 10^{12}$	When $[\text{N}_2\text{O}_5]$ was $(4.0\pm 1.0)\times 10^{11}$ molecule cm^{-3} , $\gamma_0 = 0.12\pm 0.04$ and $\gamma_{ss} = 0.021\pm 0.006$; when $[\text{N}_2\text{O}_5]$ was $(3.8\pm 0.5)\times 10^{12}$ molecule cm^{-3} , $\gamma_0 = 0.033\pm 0.010$ and $\gamma_{ss} = 0.0062\pm 0.0018$.	KC
	Mogili et al., 2006b	290	$(2\text{--}3)\times 10^{15}$	$(1.9\pm 0.2)\times 10^{-4}$ at <1% RH	EC



	Wagner et al., 2008	296±2	$(1.7\text{--}4.5)\times 10^9$	$\gamma_0 = 0.05\pm 0.02$	KC-MS
	Wagner et al., 2009	296±2	$(1\text{--}40)\times 10^{12}$	0.0048±0.0007 at 0% RH, 0.0053±0.0010 at 29% RH, 0.0113±0.0016 at 58% RH, and 0.0194±0.0022 at 71% RH.	AFT-CLD
SiO ₂	Mogili et al., 2006b	290	$(2\text{--}3)\times 10^{15}$	$(4.4\pm 0.4)\times 10^{-5}$ at <1% RH, $(9.3\pm 0.1)\times 10^{-5}$ at 11% RH, $(1.2\pm 0.2)\times 10^{-4}$ at 19% RH, and $(1.8\pm 0.4)\times 10^{-4}$ at 43% RH.	EC
	Wagner et al., 2009	296±2	$(0.5\text{--}30)\times 10^{12}$	0.0086±0.0006 at 0% RH and 0.0045±0.0005 at 29%	AFT-CLD
	Tang et al., 2014a	296±2	$(10\text{--}50)\times 10^{12}$	$(7.2\pm 0.6)\times 10^{-3}$ at (7±2)% RH, $(5.6\pm 0.6)\times 10^{-3}$ at (26±2)% RH, and $(5.3\pm 0.8)\times 10^{-3}$ at (40±3)% RH.	AFT-CLD
kaolinite	Karagulian et al., 2006	298±2	$(0.4\text{--}3.8)\times 10^{12}$	When $[\text{N}_2\text{O}_5]$ was $(4.0\pm 1.0)\times 10^{11}$ molecule cm ⁻³ , $\gamma_0 = 0.16\pm 0.04$ and $\gamma_{ss} = 0.021\pm 0.006$; when $[\text{N}_2\text{O}_5]$ was $(3.8\pm 0.5)\times 10^{12}$ molecule cm ⁻³ , $\gamma_0 = 0.14\pm 0.04$ and $\gamma_{ss} = 0.022\pm 0.006$.	KC
	Mogili et al., 2006b	290	$(2\text{--}3)\times 10^{15}$	$(9.8\pm 0.1)\times 10^{-4}$ at <1% RH	EC
natural limestone	Karagulian et al., 2006	298±2	$(0.4\text{--}3.8)\times 10^{12}$	When $[\text{N}_2\text{O}_5]$ was $(4.0\pm 1.0)\times 10^{11}$ molecule cm ⁻³ , $\gamma_0 = 0.43\pm 0.13$ and $\gamma_{ss} = 0.043\pm 0.013$; when $[\text{N}_2\text{O}_5]$ was $(3.8\pm 0.5)\times 10^{12}$ molecule cm ⁻³ , $\gamma_0 = 0.011\pm 0.003$ and $\gamma_{ss} = 0.0022\pm 0.0006$.	KC
montmorillonite	Mogili et al., 2006b	290	$(2\text{--}3)\times 10^{15}$	$(1.8\pm 0.2)\times 10^{-4}$ at <1% RH	EC
illite	Tang et al., 2014c	297±1	$(8\text{--}24)\times 10^{12}$	0.091±0.039 at 0% RH and 0.093±0.008 at 17% RH, 0.072±0.021 at 33% RH, 0.049±0.006 at 50% RH, and 0.039±0.012 at 67% RH.	AFT-CRDS
TiO ₂	Tang et al., 2014d	296±2	$(10\text{--}50)\times 10^{12}$	$(1.83\pm 0.32)\times 10^{-3}$ at (5±1)% RH, $(2.01\pm 0.27)\times 10^{-3}$ at (12±2)% RH, $(1.02\pm 0.20)\times 10^{-3}$ at (23±2)% RH, $(1.29\pm 0.26)\times 10^{-3}$ at (33±2)% RH, $(2.28\pm 0.51)\times 10^{-3}$ at (45±3)% RH, and $(4.47\pm 2.04)\times 10^{-3}$ at (30±3)% RH.	AFT-CLD
Fe ₂ O ₃	Mogili et al., 2006b	290	$(2\text{--}3)\times 10^{15}$	$(4.0\pm 0.4)\times 10^{-4}$ at <1% RH	EC



1563 An atmospheric pressure aerosol flow tube was deployed by Wagner et al. (2008, 2009)
1564 to investigate heterogeneous reactions of N_2O_5 with Saharan dust, ATD, calcite, and SiO_2
1565 aerosol particles at 296 ± 2 K, and N_2O_5 decays in the flow tube were detected by using a
1566 modified chemiluminescence method. Slightly negative dependence of $\gamma(\text{N}_2\text{O}_5)$ on RH was
1567 observed for Saharan dust, ATD, and SiO_2 aerosol particles. $\gamma(\text{N}_2\text{O}_5)$ was determined to be
1568 0.026 ± 0.004 at 0% RH, 0.016 ± 0.004 at 29% RH, and 0.010 ± 0.004 at 58% RH for Saharan dust
1569 (Wagner et al., 2008), 0.0086 ± 0.0006 at 0% RH and 0.0045 ± 0.0005 at 29% for SiO_2 (Wagner
1570 et al., 2009), and 0.0098 ± 0.0010 at 0% RH and 0.0073 ± 0.0007 at 29% RH for ATD (Wagner
1571 et al., 2009), respectively. In contrast, $\gamma(\text{N}_2\text{O}_5)$ increases with RH for CaCO_3 , from
1572 0.0048 ± 0.0007 at 0% RH to 0.0194 ± 0.0022 at 71% RH (Wagner et al., 2009). It should be
1573 pointed out that in the original paper (Wagner et al., 2008) the uptake coefficients for Saharan
1574 dust were based on the aerosol surface area concentrations after the shape factor correction was
1575 applied. In order to keep consistence with other studies, $\gamma(\text{N}_2\text{O}_5)$ reported by Wagner et al.
1576 (2008) have been recalculated in this review without taking into account the shape factor of
1577 Saharan dust.

1578 Tang and co-workers systematically investigated the dependence of $\gamma(\text{N}_2\text{O}_5)$ on RH and
1579 dust mineralogy, using aerosol flow tubes with N_2O_5 measured by a modified
1580 chemiluminescence method (Tang et al., 2012; Tang et al., 2014c) or cavity ring-down
1581 spectroscopy (Tang et al., 2014a; Tang et al., 2014e). Within experimental uncertainties,
1582 $\gamma(\text{N}_2\text{O}_5)$ was determined to be 0.02 ± 0.01 for Saharan dust (Tang et al., 2012), independent of
1583 RH (0-67%) and initial N_2O_5 concentration (5×10^{11} to 3×10^{13} molecule cm^{-3}). Products
1584 analysis suggests that N_2O_5 is converted to particulate nitrate after heterogeneous reaction with
1585 Saharan dust, and that the formation of NO_2 in the gas phase is negligible (Tang et al., 2012).
1586 It has also been shown that if pretreated with high levels of gaseous HNO_3 , heterogeneous
1587 reactivity of Saharan dust towards N_2O_5 would be substantially reduced (Tang et al., 2012). A

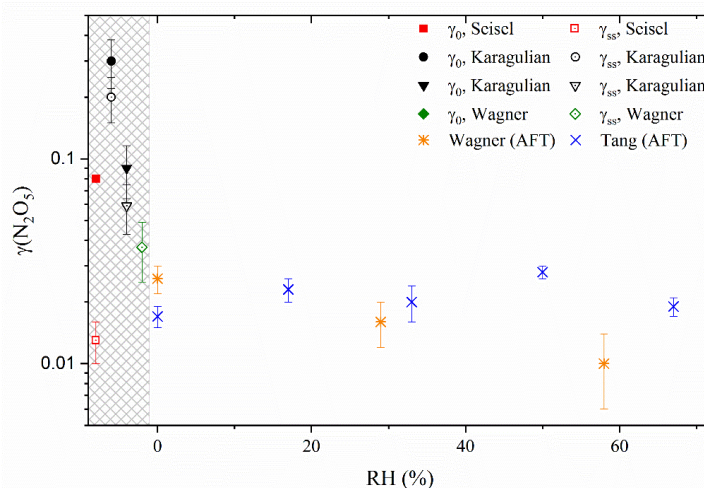


1588 strong negative effect of RH on $\gamma(\text{N}_2\text{O}_5)$ was found for uptake onto illite, with $\gamma(\text{N}_2\text{O}_5)$
1589 decreasing from 0.091 ± 0.039 at 0% RH to 0.039 ± 0.012 at 67% RH. The negative effect of RH
1590 is much smaller for ATD, with $\gamma(\text{N}_2\text{O}_5)$ determined to be 0.0077 ± 0.0010 at 0% RH and
1591 0.0050 ± 0.0003 at 67% RH (Tang et al., 2014c). $\gamma(\text{N}_2\text{O}_5)$ on SiO_2 particles decreases from
1592 0.0072 ± 0.0006 at $(7\pm 2)\%$ RH to 0.0053 ± 0.0008 at $(40\pm 2)\%$ RH (Tang et al., 2014a), also
1593 showing a weak negative RH dependence. RH exhibits complex effects on heterogeneous
1594 reaction of N_2O_5 with TiO_2 particles, and the reported $\gamma(\text{N}_2\text{O}_5)$ first decreases with RH from
1595 $(1.83\pm 0.32)\times 10^{-3}$ at $(5\pm 1)\%$ RH to $(1.02\pm 0.20)\times 10^{-3}$ at $(23\pm 2)\%$ RH, and then increases with
1596 RH to $(4.47\pm 2.04)\times 10^{-3}$ at $(60\pm 3)\%$ RH (Tang et al., 2014d). Analysis of optically levitated
1597 single micrometer sized SiO_2 particles using Raman spectroscopy during their reaction with
1598 N_2O_5 (Tang et al., 2014a) suggests that HNO_3 formed in this reaction can partition between gas
1599 and particle phases, with partitioning largely governed by RH.

1600 Figure 17 summarizes $\gamma(\text{N}_2\text{O}_5)$ onto Saharan dust reported by previous work. $\gamma(\text{N}_2\text{O}_5)$
1601 reported by the three studies using Knudsen cell reactors (Seisel et al., 2005; Karagulian et al.,
1602 2006; Wagner et al., 2008) show large variation, with $\gamma_{\text{ss}}(\text{N}_2\text{O}_5)$ ranging from 0.013 ± 0.003 to
1603 0.20 ± 0.05 . This comparison demonstrates that sample preparation methods could largely
1604 influence reported uptake coefficients using particles supported on a substrate, even though
1605 they all used Knudsen cell reactor (as discussed in Section 2.2.1). In addition, significant
1606 surface saturation was observed by Seisel et al. (2005) and Karagulian et al. (2006), but not by
1607 Wagner et al. (2008). For the same reason, $\gamma(\text{N}_2\text{O}_5)$ reported by two Knudsen studies
1608 (Karagulian et al., 2006; Wagner et al., 2008) exhibit significant discrepancy for Arizona Test
1609 Dust (and reasonably good agreement is found for CaCO_3). Instead, the two aerosol flow tube
1610 studies (Wagner et al., 2008; Tang et al., 2012) show good agreement in $\gamma(\text{N}_2\text{O}_5)$ onto Saharan
1611 dust considering experimental uncertainties, though RH was found to have a slightly negative
1612 effect by Wagner et al. (2008) while no significant effect of RH was observed by Tang et al.



1613 (2012). Since cavity ring-down spectroscopy used by Tang et al. (2012) to detect N_2O_5 is more
1614 sensitive and selective than the chemiluminescence method used by Wagner et al. (2008), in
1615 this work we choose to use the uptake coefficient (0.02 ± 0.01) reported by Tang et al. (2012),
1616 as recommended by the IUPAC task group, to assess $\tau_{\text{het}}(\text{N}_2\text{O}_5)$ in the troposphere.



1617

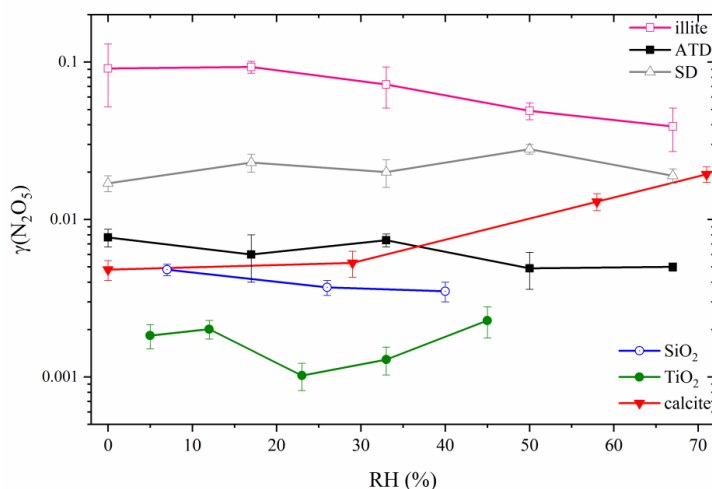
1618 **Figure 17.** Uptake coefficients of N_2O_5 for Saharan dust, as reported by previous studies.
1619 Knudsen cell studies were all carried out under vacuum conditions (i.e. 0% RH), and for better
1620 readability these results are plotted in the region of $\text{RH} < 0\%$ (shaded region). Karagulian et
1621 al. (2006) reported γ_0 and γ_{ss} at two different N_2O_5 concentrations (circles: $\sim 4 \times 10^{11}$ molecule
1622 cm^{-3} ; triangles: $\sim 4 \times 10^{12}$ molecule cm^{-3}); γ_0 and γ_{ss} reported by Wagner et al. (2008) using a
1623 Knudsen cell reactor are equal and thus overlapped with each other in Figure 17.

1624

1625 It is somehow unexpected that $\gamma(\text{N}_2\text{O}_5)$ onto SiO_2 reported by the first two studies
1626 (Mogili et al., 2006b; Wagner et al., 2009), both using aerosol samples, differ by about two
1627 orders of magnitude. A third study (Tang et al., 2014a), using an aerosol flow tube, concluded
1628 that this discrepancy is largely due to the fact that SiO_2 particles are likely to be porous. Mogili
1629 et al. (2006b) and Wagner et al. (2009) used BET surface area and the Stokes diameter to



1630 calculate the aerosol surface area, respectively. If BET surface area is used, $\gamma(\text{N}_2\text{O}_5)$ reported
1631 by Tang et al. (2014a) show good agreement with those determined by Mogili et al. (2006b);
1632 if mobility diameters are used to derive aerosol surface area, they agree well with those reported
1633 by Wagner et al. (2009). Nevertheless, some discrepancies still remain: Wagner et al. (2009)
1634 and Tang et al. (2014a) suggested a small negative dependence of $\gamma(\text{N}_2\text{O}_5)$ on RH, and Mogili
1635 et al. (2006b) found that $\gamma(\text{N}_2\text{O}_5)$ significantly increase with RH. In addition, $\gamma(\text{N}_2\text{O}_5)$ onto
1636 CaCO_3 aerosol particles at <1% RH, as reported by Mogili et al. (2006b) and Wagner et al.
1637 (2009), differ by a factor of >20. It is not yet clear if the difference in calculating surface area
1638 (BET surface area versus Stokes diameter based surface area) could explain such a large
1639 difference, and further work is required to resolve this issue.



1640
1641 **Figure 18.** Uptake coefficients of N_2O_5 for Saharan dust (Tang et al., 2012), ATD (Tang et al.,
1642 2014c), illite (Tang et al., 2014c), CaCO_3 (Wagner et al., 2009), SiO_2 (Tang et al., 2014a), and
1643 TiO_2 (Tang et al., 2014e), as reported by aerosol flow tube studies.

1644

1645 Aerosol flow tubes have been deployed to investigate heterogeneous interactions of
1646 N_2O_5 with different types of mineral dust, with reported $\gamma(\text{N}_2\text{O}_5)$ summarized in Figure 18.



1647 Two distinctive features can be identified. First, different minerals exhibit very different
1648 heterogeneous reactivity towards N_2O_5 . $\gamma(\text{N}_2\text{O}_5)$ at <10% RH increase from $(1.83 \pm 0.32) \times 10^{-3}$
1649 for TiO_2 to 0.091 ± 0.039 for illite, spanning over almost two orders of magnitude. Second, RH
1650 (and thus surface adsorbed water) plays important and various roles in uptake kinetics. For
1651 example, increasing RH significantly suppresses N_2O_5 uptake onto illite but largely enhances
1652 its uptake onto CaCO_3 , while it does not show a significant effect for Saharan dust. In this paper
1653 $\gamma(\text{N}_2\text{O}_5)$ onto Saharan dust is used to assess the significance of heterogeneous reaction of N_2O_5
1654 with mineral dust. Mineralogy of Asian dust is different from Saharan dust, and thus their
1655 heterogeneous reactivity (and probably the effect of RH) towards N_2O_5 can be different.
1656 Considering that Asian dust is transported over East Asia with high levels of NO_x and O_3
1657 (Zhang et al., 2007; Geng et al., 2008; Shao et al., 2009; Ding et al., 2013; Itahashi et al., 2014)
1658 and thus also N_2O_5 (Brown et al., 2016; Tham et al., 2016; Wang et al., 2016), heterogeneous
1659 reaction of N_2O_5 with Asian dust deserves further investigation.

1660 Using $\gamma(\text{N}_2\text{O}_5)$ of 0.02, $\tau_{\text{het}}(\text{N}_2\text{O}_5)$ are estimated to be ~10 h, ~1 h, and ~6 min for dust
1661 loading of 10, 100, and $1000 \mu\text{m}^{-3}$, respectively. N_2O_5 lifetimes in the troposphere is typically
1662 in the range of several minutes to several hours, as shown in Table 1. Therefore, heterogeneous
1663 uptake by mineral dust could contribute significantly to and in some regions even dominate
1664 tropospheric N_2O_5 removal. Since uptake of N_2O_5 leads to the formation of nitrate, it can also
1665 substantially modify chemical composition and physicochemical properties of mineral dust.

1666 A global modelling study (Dentener and Crutzen, 1993) suggested that including
1667 heterogeneous reaction of N_2O_5 with tropospheric aerosol particles with $\gamma(\text{N}_2\text{O}_5)$ equal to 0.1
1668 could reduce modelled yearly average global NO_x burden by 50%. It is found by other global
1669 and regional modelling studies (Evans and Jacob, 2005; Chang et al., 2016) that modelled NO_x
1670 and O_3 concentrations agree better with observations if $\gamma(\text{N}_2\text{O}_5)$ parameterization based on new
1671 laboratory results is adopted. In the study by Evans and Jacob (2005), $\gamma(\text{N}_2\text{O}_5)$ was set to be



1672 0.01 for mineral dust, independent of RH. A recent modelling study (Macintyre and Evans,
1673 2010) suggests that simulated NO_x, O₃, and OH concentrations are very sensitive to the choice
1674 of $\gamma(\text{N}_2\text{O}_5)$ in the range of 0.001-0.02, which significantly overlaps with the range of laboratory
1675 measured $\gamma(\text{N}_2\text{O}_5)$ for mineral dust particles. Therefore, in order to better assess the impacts of
1676 heterogeneous reaction of N₂O₅ with mineral dust on tropospheric oxidation capacity, $\gamma(\text{N}_2\text{O}_5)$
1677 and its dependence on mineralogy and RH should be better understood.

1678 Mineralogy and composition of mineral dust aerosol particles in the ambient air are
1679 always more complex than those for dust samples used in laboratory studies. Measurements of
1680 NO₃, N₂O₅, and other trace gases and aerosols in the troposphere enable steady-state NO₃ and
1681 N₂O₅ lifetimes to be determined and $\gamma(\text{N}_2\text{O}_5)$ onto ambient aerosol particles to be derived
1682 (Brown et al., 2006; Brown et al., 2009; Morgan et al., 2015; Phillips et al., 2016). It will be
1683 very beneficial to investigate N₂O₅ uptake (and other reactive trace gases as well) by ambient
1684 mineral dust aerosol. Recently such experimental apparatus, based on the aerosol flow tube
1685 technique, has been developed and deployed to directly measure $\gamma(\text{N}_2\text{O}_5)$ onto ambient aerosol
1686 particles (Bertram et al., 2009a; Bertram et al., 2009b). To our knowledge these measurements
1687 have never been carried out in dust-impacted regions yet, though they will undoubtedly
1688 improve our understanding of heterogeneous reaction of N₂O₅ with mineral dust in the
1689 troposphere.



1690 **Table 10:** Summary of previous laboratory studies on heterogeneous reactions of mineral dust with NO₃ radicals

Dust	Reference	T (K)	Concentration (molecule cm ⁻³)	Uptake coefficient	Techniques
Saharan dust	Karagulian and Rossi, 2005	298±2	(0.7-4.0)×10 ¹⁰	$\gamma_0 = 0.23 \pm 0.20$ and $\gamma_{ss} = 0.12 \pm 0.08$ when $[\text{NO}_3]_0 = (7.0 \pm 1.0) \times 10^{11} \text{ cm}^{-3}$; $\gamma_0 = 0.16 \pm 0.05$ and $\gamma_{ss} = 0.065 \pm 0.012$ when $[\text{NO}_3]_0 = (4.0 \pm 1.0) \times 10^{12} \text{ cm}^{-3}$.	KC
	Tang et al., 2010	296±2	(0.4-1.6)×10 ¹⁰	$\gamma(\text{NO}_3)/\gamma(\text{N}_2\text{O}_5)$ was reported to be 0.9±0.4, independent of RH (up to 70%).	CRDS
CaCO ₃	Karagulian and Rossi, 2005	298±2	(0.4-3.8)×10 ¹²	$\gamma_0 = 0.13 \pm 0.10$ and $\gamma_{ss} = 0.067 \pm 0.040$ when $[\text{NO}_3]_0 = (7.0 \pm 1.0) \times 10^{11} \text{ cm}^{-3}$; $\gamma_0 = 0.14 \pm 0.05$ and $\gamma_{ss} = 0.014 \pm 0.004$ when $[\text{NO}_3]_0 = (4.0 \pm 1.0) \times 10^{12} \text{ cm}^{-3}$.	KC
kaolinite	Karagulian and Rossi, 2005	298±2	(0.4-3.8)×10 ¹²	$\gamma_0 = 0.11 \pm 0.08$ and $\gamma_{ss} = 0.14 \pm 0.02$ when $[\text{NO}_3]_0 = (7.0 \pm 1.0) \times 10^{11} \text{ cm}^{-3}$; $\gamma_0 = 0.12 \pm 0.04$ and $\gamma_{ss} = 0.065 \pm 0.012$ when $[\text{NO}_3]_0 = (4.0 \pm 1.0) \times 10^{12} \text{ cm}^{-3}$.	KC
limestone	Karagulian and Rossi, 2005	298±2	(0.4-3.8)×10 ¹²	$\gamma_0 = 0.12 \pm 0.08$ and $\gamma_{ss} = 0.034 \pm 0.016$ when $[\text{NO}_3]_0 = (7.0 \pm 1.0) \times 10^{11} \text{ cm}^{-3}$; $\gamma_0 = 0.20 \pm 0.07$ and $\gamma_{ss} = 0.022 \pm 0.005$ when $[\text{NO}_3]_0 = (4.0 \pm 1.0) \times 10^{12} \text{ cm}^{-3}$.	KC
ATD	Karagulian and Rossi, 2005	298±2	(0.4-3.8)×10 ¹²	$\gamma_0 = 0.2 \pm 0.1$ and $\gamma_{ss} = 0.10 \pm 0.016$ when $[\text{NO}_3]_0 = (7.0 \pm 1.0) \times 10^{11} \text{ cm}^{-3}$; $\gamma_0 = 0.14 \pm 0.04$ and $\gamma_{ss} = 0.025 \pm 0.007$ when $[\text{NO}_3]_0 = (4.0 \pm 1.0) \times 10^{12} \text{ cm}^{-3}$.	KC



1692 **3.6.2 NO₃ radicals**

1693 To our knowledge only two previous studies have explored heterogeneous uptake of
1694 NO₃ radicals by mineral dust particles. Heterogeneous reaction of NO₃ radicals with mineral
1695 dust was investigated for the first time at 298±2 K, using a Knudsen cell reactor (Karagulian
1696 and Rossi, 2005). Products observed in the gas phase include N₂O₅ (formed in the Eley-Rideal
1697 reaction of NO₃ with NO₂ on the dust surface) and HNO₃ (formed in the heterogeneous reaction
1698 of N₂O₅ and subsequently released into the gas phase) (Karagulian and Rossi, 2005). Surface
1699 deactivation occurred for all types of dust particles investigated. Dependence of uptake kinetics
1700 on the initial NO₃ concentration was observed (Karagulian and Rossi, 2005). When [NO₃]₀ was
1701 (7.0±1.0)×10¹¹ cm⁻³, the initial and steady-state uptake coefficients (γ_0 and γ_{ss}) were determined
1702 to be 0.13±0.10 and 0.067±0.040 for CaCO₃, 0.12±0.08 and 0.034±0.016 for natural limestone,
1703 0.11±0.08 and 0.14±0.02 for kaolinite, 0.23±0.20 and 0.12±0.08 for Saharan dust, and 0.2±0.1
1704 and 0.10±0.06 for ATD, respectively. When [NO₃]₀ was (4.0±1.0)×10¹² cm⁻³, γ_0 and γ_{ss} were
1705 determined to be 0.14±0.05 and 0.014±0.004 for CaCO₃, 0.20±0.07 and 0.022±0.005 for
1706 natural limestone, 0.12±0.04 and 0.050±0.014 for kaolinite, 0.16±0.05 and 0.065±0.012 for
1707 Saharan dust, and 0.14±0.04 and 0.025±0.007 for ATD, respectively.

1708 In the second study (Tang et al., 2010), a novel relative rate method was developed to
1709 investigate heterogeneous uptake of NO₃ and N₂O₅ by mineral dust. Changes in NO₃ and N₂O₅
1710 concentrations due to reactions with dust particles (loaded on filters) were simultaneously
1711 detected by cavity ring-down spectroscopy. Experiments were carried out at room temperature
1712 (296±2 K) and at different RH up to 70%. $\gamma(\text{NO}_3)/\gamma(\text{N}_2\text{O}_5)$ was reported to be 0.9±0.4 for
1713 Saharan dust particles, independent of RH within the experimental uncertainties (Tang et al.,
1714 2010). In addition, even though very low levels of NO₃ and N₂O₅ (a few hundred pptv) were
1715 used, surface deactivation was still observed for both species (Tang et al., 2010).



1716 With the reported $\gamma(\text{NO}_3)/\gamma(\text{N}_2\text{O}_5)$ ratio of 0.9 (Tang et al., 2010), $\gamma(\text{NO}_3)$ of 0.018 is
1717 thus adopted to evaluate $\tau_{\text{het}}(\text{NO}_3)$ due to its heterogeneous uptake by mineral dust, based on
1718 the $\gamma(\text{N}_2\text{O}_5)$ value of 0.02 (Section 3.6.1). Using Eq. (6), mineral dust mass concentrations of
1719 10, 100, and 1000 $\mu\text{m m}^{-3}$ result in $\tau_{\text{het}}(\text{NO}_3)$ of ~9 h, ~52 min, and ~5 min, respectively. Field
1720 measurements, as summarized in Table 1, suggest that tropospheric NO_3 lifetimes are typically
1721 several minutes. Therefore, uptake by mineral dust is unlikely to be a significant sink for NO_3
1722 in the troposphere, except for regions which are close to dust sources and thus heavily impacted
1723 by dust storms. Similar conclusions were drawn by Tang et al. (2010a) who used an uptake
1724 coefficient of 0.009 which is a factor of 2 smaller than the value used here. 3D GEOS-Chem
1725 model simulations suggest that modelled O_3 appears to be insensitive to the choice of $\gamma(\text{NO}_3)$
1726 in the range of 0.0001 to 0.1 (Mao et al., 2013b). To conclude, heterogeneous reaction with
1727 mineral dust is not an important sink for tropospheric NO_3 radicals unless in regions with heavy
1728 dust loadings.

1729 **4. Summary and outlook**

1730 It has been widely recognized that heterogeneous reactions with mineral dust particles
1731 can significantly affect tropospheric oxidation capacity directly and indirectly. These reactions
1732 can also change the composition of dust particles, thereby modifying their physicochemical
1733 properties important for direct and indirect radiative forcing. In the past two decades there have
1734 been a large number of laboratory (as well as field and modelling) studies which have examined
1735 these reactions. In this paper we provide a comprehensive and timely review of laboratory
1736 studies of heterogeneous reactions of mineral dust aerosol with OH, NO_3 , and O_3 as well as
1737 several other reactive species (including HO_2 , H_2O_2 , HCHO, HONO, and N_2O_5) which are
1738 directly related to OH, NO_3 , and O_3 . Lifetimes of these species with respect to heterogeneous
1739 uptake by mineral dust are compared to their lifetimes due to other major loss processes in the
1740 troposphere in order to provide a quick assessment of atmospheric significance of



1741 heterogeneous reactions as sinks for these species. In addition, representative field and
1742 modelling work is also discussed to further illustrate the roles these heterogeneous reactions
1743 play in tropospheric oxidation capacity. As shown in Section 3, these studies have significantly
1744 improved our understanding of the effects of these reactions on tropospheric oxidation capacity.
1745 Nevertheless, there are still a number of open questions which cannot be answered by
1746 laboratory work alone but only by close collaboration among laboratory, field, and modelling
1747 studies. Several major challenges, and strategies we proposed to address these challenges, are
1748 outlined below.

1749 1) Mineral dust in the troposphere are in fact mineralogically complex and its
1750 mineralogy vary with dust sources and also residence time in the troposphere (Claquin et al.,
1751 1999; Ta et al., 2003; Zhang et al., 2003; Nickovic et al., 2012; Journet et al., 2014; Scanza et
1752 al., 2015). Different minerals can exhibit large variabilities in heterogeneous reactivity towards
1753 trace gases, as shown by Tables 4-10. However, Tables 4-10 also reveal that simple oxides
1754 (e.g., SiO_2 and Al_2O_3) and CaCO_3 have been much more widely investigated compared to
1755 authentic dust samples (probably except ATD) and clay minerals which are the major
1756 components of mineral dust aerosol particles (Claquin et al., 1999). The relative importance of
1757 clay minerals will be increased after long-range transport due to their smaller sizes compared
1758 to SiO_2 and CaCO_3 . Therefore, more attention should be paid in future work to heterogeneous
1759 reactions of clay minerals and authentic dust samples.

1760 2) In the last several years, important roles that RH (and thus surface adsorbed water)
1761 plays in heterogeneous reactions of mineral dust have been widely recognized by many studies
1762 and discussed in a recent review paper (Rubasinghege and Grassian, 2013). Tables 4-10 show
1763 that most of previous studies have been conducted at $\text{RH} < 80\%$, and heterogeneous reactivity
1764 at higher RH largely remain unknown. In addition, effects of RH on heterogeneous reactions
1765 of mineral dust with a few important reactive trace gases, such as HO_2 radicals (Bedjanian et



1766 al., 2013b; Matthews et al., 2014) and O₃ (Sullivan et al., 2004; Chang et al., 2005; Mogili et
1767 al., 2006a), are still under debate. It has been known that heterogeneous processing can modify
1768 chemical composition and hygroscopicity of mineral dust particles (Tang et al., 2016a), and at
1769 evaluated RH aged dust particles may consist of a solid core and an aqueous shell (Krueger et
1770 al., 2003b; Laskin et al., 2005a; Liu et al., 2008b; Shi et al., 2008; Li and Shao, 2009; Ma et
1771 al., 2012). Under such circumstances, reactions are no longer limited to particle surface but
1772 instead involve gas, liquid, and solid phases and their interfaces, and hence mutual influence
1773 among chemical reactivity, composition, and physiochemical properties has to be taken into
1774 account (Tang et al., 2016a).

1775 3) Temperature in the troposphere varies from <200 K to >300 K. However, most of
1776 laboratory studies of heterogeneous reactions of mineral dust were carried out at room
1777 temperature (around 296 K). Once lifted into the atmosphere, mineral dust aerosol is mainly
1778 transported in the free troposphere in which temperature is much lower than that at the ground
1779 level. Some work has started to examine the influence of temperature on heterogeneous uptake
1780 by mineral dust (Michel et al., 2003; Xu et al., 2006; Xu et al., 2010; Wu et al., 2011; Xu et al.,
1781 2011; Romanias et al., 2012b; Romanias et al., 2012a; Zhou et al., 2012; Bedjanian et al., 2013b;
1782 El Zein et al., 2013a; El Zein et al., 2013b; Romanias et al., 2013; Wu et al., 2013b; El Zein et
1783 al., 2014; Hou et al., 2016; Zhou et al., 2016). It has been found temperature may have
1784 significant effects on some reactions. However, to the best of our knowledge, no study has
1785 explored the influence of temperature on heterogeneous reactions of airborne mineral dust
1786 particles.

1787 4) Laboratory studies may not entirely mimic actual heterogeneous reactions in the
1788 troposphere due to several reasons. First of all, laboratory studies are typically carried out with
1789 time scales of <1 min to several hours, compared to lifetimes of a few days for mineral dust in
1790 the troposphere. Secondly, it is not uncommon that concentrations of reactive trace gases used



1791 in laboratory work are several orders of magnitude larger than those in the troposphere. These
1792 two aspects can make it non-trivial to extrapolate laboratory results to the real atmosphere. In
1793 addition, dust samples used in laboratory studies, even when authentic dust samples are used,
1794 do not exactly mimic the complexity of ambient dust particles in composition and mineralogy.
1795 Very recently a new type of experiments, sometimes called “laboratory work in the field”, can
1796 at least partly provide solutions to this challenge. For example, an aerosol flow tube has been
1797 deployed to explore heterogeneous uptake of N_2O_5 by ambient aerosol particles at a few
1798 locations (Bertram et al., 2009a; Bertram et al., 2009b; Ryder et al., 2014), revealing the roles
1799 of RH and particle composition in heterogeneous reactivity of ambient aerosol particles. To
1800 our knowledge, this technique has not been used to investigate heterogeneous uptake of N_2O_5
1801 by ambient mineral dust aerosol. This technique can also be extended to examine
1802 heterogeneous reactions of ambient aerosol particles with other reactive trace gases, especially
1803 those whose heterogeneous reactions are anticipated to be efficient (e.g., HO_2 and H_2O_2).

1804 5) Decrease in heterogeneous reactivity due to surface passivation has been observed
1805 by many studies using dust powders supported by substrates. On the other hand, increase in
1806 heterogeneous reactivity, due to conversion of solid particles to aqueous droplets with solid
1807 cores (caused by formation of hygroscopic materials), has also been reported. In addition, it
1808 has been widely recognized that the co-presence of two or more reactive trace gases may
1809 change the rates of heterogeneous reactions of each individual gases (Li et al., 2006; Raff et
1810 al., 2009; Liu et al., 2012; Rubasinghege and Grassian, 2012; Wu et al., 2013a; Zhao et al.,
1811 2015; Yang et al., 2016a), typically termed as synergistic effects. Parameterization of these
1812 complex processes is very difficult, and lack of sophisticated bulk parameterizations impedes
1813 us from a quantitative assessment of their atmospheric significance via modelling studies.
1814 Kinetic models have been developed to integrate physical and chemical processes in and
1815 between different phases (Pöschl et al., 2007; Shiraiwa et al., 2012; Berkemeier et al., 2013),



1816 and these models have been successfully used to investigate multiphase chemistry of aqueous
1817 aerosol particles and cloud droplets (Shiraiwa et al., 2011; Arangio et al., 2015; Pöschl and
1818 Shiraiwa, 2015). Future efforts devoted to development and application of comprehensive
1819 kinetic models to study heterogeneous and multiphase reactions of mineral dust particles would
1820 largely improve our understanding in the field.

1821 6) It has been found that UV and visible radiation can substantially enhance the
1822 heterogeneous reactivity of mineral dust towards several trace gases, including but not limited
1823 to H₂O₂, O₃, and HCHO, and in some cases even reactivate mineral surfaces which have been
1824 passivated (Cwiertny et al., 2008; Chen et al., 2012; George et al., 2015). In addition, photolysis
1825 of materials (such as nitrate) formed on mineral surface can also be sources for some trace
1826 gases (Nanayakkara et al., 2013; Gankanda and Grassian, 2014; Nanayakkara et al., 2014).
1827 Although the effects of photo-radiation in heterogeneous reactions with mineral dust have been
1828 recognized for more than one decade, it largely remains unclear to which extent these reactions
1829 are photo-enhanced under ambient solar radiation and thus quantitative evaluation of impacts
1830 of heterogeneous photochemistry on tropospheric oxidation capacity is lacking.

1831 7) There still exists a considerably large gap between laboratory work and modelling
1832 studies used to explain field measurements and predict future changes. One reason is that the
1833 communication and collaboration between laboratory and modelling communities, though
1834 enhanced in the past few decades, are still not enough and should be further encouraged and
1835 stimulated in future. Furthermore, many laboratory studies have been designed from the
1836 perspective of classical chemical kinetics such that although experimental results are beautiful,
1837 they are difficult to be parameterized and then included in models. As mentioned,
1838 heterogeneous reactivity is highly dependent on temperature, RH, co-presence of other trace
1839 gases and mutual influences among these factors. Given that most models are capable of
1840 resolving/assimilating meteorological variables and trace gas concentrations at high temporal



1841 resolution, multivariate analysis and integrated numerical expressions are encouraged to be
1842 conducted in laboratory studies so as to better characterize heterogeneous chemistry and its
1843 climate and environmental effects in numerical models. Therefore, it is suggested that when a
1844 laboratory study is designed, it should be kept in mind how experimental results can be used
1845 by modelling studies. On the other hand, modelling work is encouraged to include new
1846 laboratory results in numerical simulations and to identify missing reactions and key
1847 parameters which deserve further laboratory investigation. Field campaigns which are
1848 specifically designed to assess the impacts of mineral dust aerosol on tropospheric oxidation
1849 capacity have been proved to be very beneficial (de Reus et al., 2000; Galy-Lacaux et al., 2001;
1850 Seinfeld et al., 2004; Tang et al., 2004; de Reus et al., 2005; Umann et al., 2005; Arimoto et
1851 al., 2006; Song et al., 2007), and more campaigns of this types should be organized. Overall,
1852 as urged by a few recent articles (Kolb et al., 2010; Abbatt et al., 2014), the three-legged stool
1853 approach (laboratory studies, field observations, and modelling studies) adopted by
1854 atmospheric chemistry research for a long time should be emphasized, and mutual
1855 communication and active collaboration among these three “legs” should be further enhanced.

1856 **Acknowledgement**

1857 The preparation of this manuscript was inspired by the first International Workshop on
1858 Heterogeneous Atmospheric Chemistry (August 2015, Beijing, China) endorsed by the
1859 International Global Atmospheric Chemistry (IGAC) Project, and Mingjin Tang and Tong Zhu
1860 would like to thank all the participants for their valuable presentations and discussion. Financial
1861 support provided by Chinese National Science Foundation (41675140 and 21522701), Chinese
1862 Academy of Sciences international collaborative project (132744KYSB20160036), and State
1863 Key Laboratory of Organic Geochemistry (SKLOGA201603A) is acknowledged. Mingjin
1864 Tang is also sponsored by Chinese Academy of Sciences Pioneer Hundred Talents Program.

1865 **Reference**

- 1866 Abbatt, J., George, C., Melamed, M., Monks, P., Pandis, S., and Rudich, Y.: New Directions:
1867 Fundamentals of atmospheric chemistry: Keeping a three-legged stool balanced, Atmos.
1868 Environ., 84, 390-391, 2014.
- 1869 Abbatt, J. P. D., Lee, A. K. Y., and Thornton, J. A.: Quantifying trace gas uptake to
1870 tropospheric aerosol: recent advances and remaining challenges, Chem. Soc. Rev., 41, 6555-
1871 6581, 2012.
- 1872 Akimoto, H.: Heterogeneous Reactions in the Atmosphere and Uptake Coefficients, in:
1873 Atmospheric Reaction Chemistry, Springer Japan, Tokyo, 239-284, 2016.
- 1874 Aldener, M., Brown, S. S., Stark, H., Williams, E. J., Lerner, B. M., Kuster, W. C., Goldan,
1875 P. D., Quinn, P. K., Bates, T. S., Fehsenfeld, F. C., and Ravishankara, A. R.: Reactivity and
1876 loss mechanisms of NO₃ and N₂O₅ in a polluted marine environment: Results from in situ
1877 measurements during New England Air Quality Study 2002, J. Geophys. Res.-Atmos., 111,
1878 D23S73, DOI: 10.1029/2006JD007252, 2006.
- 1879 Alebić-Juretić, A., Cvitaš, T., and Klasinc, L.: Ozone Destruction on Powders, Ber.
1880 Bunsenges. Phys. Chem., 96, 493-495, 1992.
- 1881 Alfaro, S. C., Gomes, L., Rajot, J. L., Lafon, S., Gaudichet, A., Chatenet, B., Maille, M.,
1882 Cautenet, G., Lasserre, F., Cachier, H., and Zhang, X. Y.: Chemical and optical
1883 characterization of aerosols measured in spring 2002 at the ACE-Asia supersite, Zhenbeitai,
1884 China, J. Geophys. Res.-Atmos., 108, 2003.
- 1885 Aliche, B., Geyer, A., Hofzumahaus, A., Holland, F., Konrad, S., Patz, H. W., Schafer, J.,
1886 Stutz, J., Volz-Thomas, A., and Platt, U.: OH formation by HONO photolysis during the
1887 BERLIOZ experiment, J. Geophys. Res.-Atmos., 108, 8247, doi: 8210.1029/2001jd000579,
1888 2003.
- 1889 Ammann, M., and Pöschl, U.: Kinetic model framework for aerosol and cloud surface
1890 chemistry and gas-particle interactions - Part 2: Exemplary practical applications and
1891 numerical simulations, Atmos. Chem. Phys., 7, 6025-6045, 2007.
- 1892 Ammann, M., Cox, R. A., Crowley, J. N., Jenkin, M. E., Mellouki, A., Rossi, M. J., Troe, J.,
1893 and Wallington, T. J.: Evaluated kinetic and photochemical data for atmospheric chemistry:
1894 Volume VI - heterogeneous reactions with liquid substrates, Atmos. Chem. Phys., 12, 8045-
1895 8228, 2013.
- 1896 Ammar, R., Monge, M. E., George, C., and D'Anna, B.: Photoenhanced NO₂ Loss on
1897 Simulated Urban Grime, ChemPhysChem, 11, 3956-3961, 2010.
- 1898 Ao, C. H., Lee, S. C., Yu, J. Z., and Xu, J. H.: Photodegradation of formaldehyde by
1899 photocatalyst TiO₂: effects on the presences of NO, SO₂ and VOCs, Appl. Catal., B:
1900 Environ., 54, 41-50, 2004.
- 1901 Arangio, A. M., Slade, J. H., Berkemeier, T., Pöschl, U., Knopf, D. A., and Shiraiwa, M.:
1902 Multiphase Chemical Kinetics of OH Radical Uptake by Molecular Organic Markers of
1903 Biomass Burning Aerosols: Humidity and Temperature Dependence, Surface Reaction, and
1904 Bulk Diffusion, J. Phys. Chem. A, 119, 4533-4544, 2015.
- 1905 Arimoto, R., Kim, Y. J., Kim, Y. P., Quinn, P. K., Bates, T. S., Anderson, T. L., Gong, S.,
1906 Uno, I., Chin, M., Huebert, B. J., Clarke, A. D., Shinozuka, Y., Weber, R. J., Anderson, J. R.,
1907 Guazzotti, S. A., Sullivan, R. C., Sodeman, D. A., Prather, K. A., and Sokolik, I. N.:
1908 Characterization of Asian Dust during ACE-Asia, Glob. Planet. Change, 52, 23-56, 2006.
- 1909 Atkinson, R., Baulch, D. L., Cox, R. A., Crowley, J. N., Hampson, R. F., Hynes, R. G.,
1910 Jenkin, M. E., Rossi, M. J., and Troe, J.: Evaluated kinetic and photochemical data for
1911 atmospheric chemistry: Volume I - gas phase reactions of Ox, HOx, NOx and SOx species,
1912 Atmos. Chem. Phys., 4, 1461-1738, 2004.



- 1913 Atkinson, R., Baulch, D. L., Cox, R. A., Crowley, J. N., Hampson, R. F., Hynes, R. G.,
1914 Jenkin, M. E., Rossi, M. J., and Troe, J.: Evaluated kinetic and photochemical data for
1915 atmospheric chemistry: Volume II - gas phase reactions of organic species, *Atmos. Chem.*
1916 *Phys.*, 6, 3625-4055, 2006.
- 1917 Baergen, A. M., and Donaldson, D. J.: Formation of reactive nitrogen oxides from urban
1918 grime photochemistry, *Atmos. Chem. Phys.*, 16, 6355-6363, 2016.
- 1919 Balkanski, Y., Schulz, M., Claquin, T., and Guibert, S.: Reevaluation of Mineral Aerosol
1920 Radiative Forcings Suggests a Better Agreement with Satellite and AERONET Data, *Atmos.*
1921 *Chem. Phys.*, 7, 81-95, 2007.
- 1922 Bauer, S. E., Balkanski, Y., Schulz, M., Hauglustaine, D. A., and Dentener, F.: Global
1923 modeling of heterogeneous chemistry on mineral aerosol surfaces: Influence on tropospheric
1924 ozone chemistry and comparison to observations, *J. Geophys. Res.-Atmos.*, 109, D02304,
1925 doi: 10.1029/2003JD003868, 2004.
- 1926 Bedjanian, Y., Romanias, M. N., and El Zein, A.: Interaction of OH Radicals with Arizona
1927 Test Dust: Uptake and Products, *J. Phys. Chem. A*, 117, 393-400, 2013a.
- 1928 Bedjanian, Y., Romanias, M. N., and El Zein, A.: Uptake of HO₂ Radicals on Arizona Test
1929 Dust, *Atmos. Chem. Phys.*, 12, 6461-6471, 2013b.
- 1930 Berkemeier, T., Huisman, A. J., Ammann, M., Shiraiwa, M., Koop, T., and Pöschl, U.:
1931 Kinetic regimes and limiting cases of gas uptake and heterogeneous reactions in atmospheric
1932 aerosols and clouds: a general classification scheme, *Atmos. Chem. Phys.*, 13, 6663-6686,
1933 2013.
- 1934 Bertram, A. K., Ivanov, A. V., Hunter, M., Molina, L. T., and Molina, M. J.: The Reaction
1935 Probability of OH on Organic Surfaces of Tropospheric Interest, *J. Phys. Chem. A*, 105,
1936 9415-9421, 2001.
- 1937 Bertram, T. H., Thornton, J. A., and Riedel, T. P.: An experimental technique for the direct
1938 measurement of N₂O₅ reactivity on ambient particles, *Atmos. Meas. Tech.*, 2, 231-242,
1939 2009a.
- 1940 Bertram, T. H., Thornton, J. A., Riedel, T. P., Middlebrook, A. M., Bahreini, R., Bates, T. S.,
1941 Quinn, P. K., and Coffman, D. J.: Direct observations of N₂O₅ reactivity on ambient aerosol
1942 particles, *Geophys. Res. Lett.*, 36, L19803, 10.1029/2009gl040248, 2009b.
- 1943 Bian, H. S., and Zender, C. S.: Mineral dust and global tropospheric chemistry: Relative roles
1944 of photolysis and heterogeneous uptake, *J. Geophys. Res.-Atmos.*, 108, 2003.
- 1945 Bogart, K. H. A., Cushing, J. P., and Fisher, E. R.: Effects of Plasma Processing Parameters
1946 on the Surface Reactivity of OH(X2II) in Tetraethoxysilane/O₂ Plasmas during Deposition of
1947 SiO₂, *J. Phys. Chem. B*, 101, 10016-10023, 1997.
- 1948 Boyd, P. W., and Ellwood, M. J.: The biogeochemical cycle of iron in the ocean, *Nature*
1949 *Geosci.*, 3, 675-682, 2010.
- 1950 Brauers, T., Hausmann, M., Bister, A., Kraus, A., and Dorn, H.-P.: OH radicals in the
1951 boundary layer of the Atlantic Ocean: 1. Measurements by long-path laser absorption
1952 spectroscopy, *J. Geophys. Res.-Atmos.*, 106, 7399-7414, 2001.
- 1953 Brown, S. S., Ryerson, T. B., Wollny, A. G., Brock, C. A., Peltier, R., Sullivan, A. P., Weber,
1954 R. J., Dube, W. P., Trainer, M., Meagher, J. F., Fehsenfeld, F. C., and Ravishankara, A. R.:
1955 Variability in nocturnal nitrogen oxide processing and its role in regional air quality, *Science*,
1956 311, 67-70, 2006.
- 1957 Brown, S. S., Dube, W. P., Fuchs, H., Ryerson, T. B., Wollny, A. G., Brock, C. A., Bahreini,
1958 R., Middlebrook, A. M., Neuman, J. A., Atlas, E., Roberts, J. M., Osthoff, H. D., Trainer, M.,
1959 Fehsenfeld, F. C., and Ravishankara, A. R.: Reactive uptake coefficients for N₂O₅
1960 determined from aircraft measurements during the Second Texas Air Quality Study:
1961 Comparison to current model parameterizations, *J. Geophys. Res.-Atmos.*, 114, D00F10,
1962 DOI: 10.1029/2008JD011679, 2009.



- 1963 Brown, S. S., and Stutz, J.: Nighttime radical observations and chemistry, *Chem. Soc. Rev.*,
1964 41, 6405-6447, 2012.
- 1965 Brown, S. S., Dube, W. P., Tham, Y. J., Zha, Q. Z., Xue, L. K., Poon, S., Wang, Z., Blake, D.
1966 R., Tsui, W., Parrish, D. D., and Wang, T.: Nighttime chemistry at a high altitude site above
1967 Hong Kong, *J. Geophys. Res.-Atmos.*, 121, 2457-2475, 2016.
- 1968 Burkholder, J. B., Sander, S. P., Abbatt, J. P. D., Barker, J. R., Huie, R. E., Kolb, C. E.,
1969 Kurylo, M. J., Orkin, V. L., Wilmouth, D. M., and Wine, P. H.: Chemical Kinetics and
1970 Photochemical Data for Use in Atmospheric Studies, Evaluation No. 18, JPL Publication 15-
1971 10, Jet Propulsion Lab., Pasadena, CA, 2015.
- 1972 Carlos-Cuellar, S., Li, P., Christensen, A. P., Krueger, B. J., Burrichter, C., and Grassian, V.
1973 H.: Heterogeneous Uptake Kinetics of Volatile Organic Compounds on Oxide Surfaces Using
1974 a Knudsen Cell Reactor: Adsorption of Acetic Acid, Formaldehyde, and Methanol on α -
1975 Fe_2O_3 , α - Al_2O_3 , and SiO_2 , *J. Phys. Chem. A*, 107, 4250-4261, 2003.
- 1976 Chang, R. Y. W., Sullivan, R. C., and Abbatt, J. P. D.: Initial uptake of ozone on Saharan
1977 dust at atmospheric relative humidities, *Geophys. Res. Lett.*, 32, L14815, doi:
1978 14810.11029/12005GL023317, 2005.
- 1979 Chang, W. L., Brown, S. S., Stutz, J., Middlebrook, A. M., Bahreini, R., Wagner, N. L.,
1980 Dubé, W. P., Pollack, I. B., Ryerson, T. B., and Riemer, N.: Evaluating N_2O_5 heterogeneous
1981 hydrolysis parameterizations for CalNex 2010, *J. Geophys. Res.-Atmos.*, 121, 5051-5070,
1982 2016.
- 1983 Chatani, S., Shimo, N., Matsunaga, S., Kajii, Y., Kato, S., Nakashima, Y., Miyazaki, K.,
1984 Ishii, K., and Ueno, H.: Sensitivity analyses of OH missing sinks over Tokyo metropolitan
1985 area in the summer of 2007, *Atmos. Chem. Phys.*, 9, 8975-8986, 2009.
- 1986 Chen, H. H., Navea, J. G., Young, M. A., and Grassian, V. H.: Heterogeneous
1987 Photochemistry of Trace Atmospheric Gases with Components of Mineral Dust Aerosol, *J.*
1988 *Phys. Chem. A*, 115, 490-499, 2011a.
- 1989 Chen, H. H., Stanier, C. O., Young, M. A., and Grassian, V. H.: A Kinetic Study of Ozone
1990 Decomposition on Illuminated Oxide Surfaces, *J. Phys. Chem. A*, 115, 11979-11987, 2011b.
- 1991 Chen, H. H., Nanayakkara, C. E., and Grassian, V. H.: Titanium Dioxide Photocatalysis in
1992 Atmospheric Chemistry, *Chem. Rev.*, 112, 5919-5948, 2012.
- 1993 Chen, Z. M., Jie, C. Y., Li, S., Wang, H. L., Wang, C. X., Xu, J. R., and Hua, W.:
1994 Heterogeneous reactions of methacrolein and methyl vinyl ketone: Kinetics and mechanisms
1995 of uptake and ozonolysis on silicon dioxide, *J. Geophys. Res.-Atmos.*, 113, D22303, doi:
1996 22310.21029/22007JD009754, 2008.
- 1997 Chernoff, D. I., and Bertram, A. K.: Effects of sulfate coatings on the ice nucleation
1998 properties of a biological ice nucleus and several types of minerals, *J. Geophys. Res.-Atmos.*,
1999 115, D20205, doi: 20210.21029/22010JD014254, 2010.
- 2000 Clauquin, T., Schulz, M., and Balkanski, Y. J.: Modeling the mineralogy of atmospheric dust
2001 sources, *J. Geophys. Res.-Atmos.*, 104, 22243-22256, 1999.
- 2002 Creamean, J. M., Suski, K. J., Rosenfeld, D., Cazorla, A., DeMott, P. J., Sullivan, R. C.,
2003 White, A. B., Ralph, F. M., Minnis, P., Comstock, J. M., Tomlinson, J. M., and Prather, K.
2004 A.: Dust and Biological Aerosols from the Sahara and Asia Influence Precipitation in the
2005 Western U.S, *Science*, 339, 1572-1578, 2013.
- 2006 Crowley, J. N., Ammann, M., Cox, R. A., Hynes, R. G., Jenkin, M. E., Mellouki, A., Rossi,
2007 M. J., Troe, J., and Wallington, T. J.: Evaluated Kinetic and Photochemical Data for
2008 Atmospheric Chemistry: Volume V - Heterogeneous Reactions on Solid Substrates, *Atmos.*
2009 *Chem. Phys.*, 10, 9059-9223, 2010a.
- 2010 Crowley, J. N., Schuster, G., Pouvesle, N., Parchatka, U., Fischer, H., Bonn, B., Bingemer,
2011 H., and Lelieveld, J.: Nocturnal nitrogen oxides at a rural mountain-site in south-western
2012 Germany, *Atmos. Chem. Phys.*, 10, 2795-2812, 2010b.



- 2013 Crutzen, P. J.: Albedo enhancement by stratospheric sulfur injections: A contribution to
2014 resolve a policy dilemma?, *Clim. Change*, 77, 211-219, 2006.
- 2015 Cwiertny, D. M., Young, M. A., and Grassian, V. H.: Chemistry and photochemistry of
2016 mineral dust aerosol, *Annu. Rev. Phys. Chem.*, 59, 27-51, 2008.
- 2017 Cziczo, D. J., Froyd, K. D., Hoose, C., Jensen, E. J., Diao, M., Zondlo, M. A., Smith, J. B.,
2018 Twohy, C. H., and Murphy, D. M.: Clarifying the Dominant Sources and Mechanisms of
2019 Cirrus Cloud Formation, *Science*, 340, 1320-1324, 2013.
- 2020 Davidovits, P., Kolb, C. E., Williams, L. R., Jayne, J. T., and Worsnop, D. R.: Update 1 of:
2021 Mass Accommodation and Chemical Reactions at Gas-Liquid Interfaces, *Chem. Rev.*, 111,
2022 PR76-PR109, 2011.
- 2023 De Longueville, F., Hountondji, Y.-C., Henry, S., and Ozer, P.: What do we know about
2024 effects of desert dust on air quality and human health in West Africa compared to other
2025 regions?, *Sci. Total Environ.*, 409, 1-8, 2010.
- 2026 de Longueville, F., Ozer, P., Doumbia, S., and Henry, S.: Desert dust impacts on human
2027 health: an alarming worldwide reality and a need for studies in West Africa, *Int. J.*
2028 *Biometeorol.*, 57, 1-19, 2013.
- 2029 de Reus, M., Dentener, F., Thomas, A., Borrmann, S., Strom, J., and Lelieveld, J.: Airborne
2030 observations of dust aerosol over the North Atlantic Ocean during ACE 2: Indications for
2031 heterogeneous ozone destruction, *J. Geophys. Res.-Atmos.*, 105, 15263-15275, 2000.
- 2032 de Reus, M., Fischer, H., Sander, R., Gros, V., Kormann, R., Salisbury, G., Van Dingenen,
2033 R., Williams, J., Zollner, M., and Lelieveld, J.: Observations and model calculations of trace
2034 gas scavenging in a dense Saharan dust plume during MINATROC, *Atmos. Chem. Phys.*, 5,
2035 1787-1803, 2005.
- 2036 DeMott, P. J., Sassen, K., Poellot, M. R., Baumgardner, D., Rogers, D. C., Brooks, S. D.,
2037 Prenni, A. J., and Kreidenweis, S. M.: African dust aerosols as atmospheric ice nuclei,
2038 *Geophys. Res. Lett.*, 30, 1732, doi: 1710.1029/2003gl017410, 2003.
- 2039 DeMott, P. J., Prenni, A. J., McMeeking, G. R., Sullivan, R. C., Petters, M. D., Tobo, Y.,
2040 Niemand, M., Möhler, O., Snider, J. R., Wang, Z., and Kreidenweis, S. M.: Integrating
2041 laboratory and field data to quantify the immersion freezing ice nucleation activity of mineral
2042 dust particles, *Atmos. Chem. Phys.*, 15, 393-409, 2015.
- 2043 Dentener, F. J., and Crutzen, P. J.: Reaction of N₂O₅ on tropospheric aerosols: Impact on the
2044 global distributions of NO_x, O₃, and OH, *J. Geophys. Res.-Atmos.*, 98, 7149-7163, 1993.
- 2045 Dentener, F. J., Carmichael, G. R., Zhang, Y., Lelieveld, J., and Crutzen, P. J.: Role of
2046 Mineral Aerosol as a Reactive Surface in the Global Troposphere, *J. Geophys. Res.-Atmos.*,
2047 101, 22869-22889, 1996.
- 2048 Dhandapani, B., and Oyama, S. T.: Gas phase ozone decomposition catalysts, *Appl. Catal.*,
2049 *B: Environ.*, 11, 129-166, 1997.
- 2050 Ding, A. J., Fu, C. B., Yang, X. Q., Sun, J. N., Zheng, L. F., Xie, Y. N., Herrmann, E., Nie,
2051 W., Petäjä, T., Kerminen, V. M., and Kulmala, M.: Ozone and fine particle in the western
2052 Yangtze River Delta: an overview of 1 yr data at the SORPES station, *Atmos. Chem. Phys.*,
2053 13, 5813-5830, 2013.
- 2054 Donaldson, M. A., Berke, A. E., and Raff, J. D.: Uptake of Gas Phase Nitrous Acid onto
2055 Boundary Layer Soil Surfaces, *Environ. Sci. Technol.*, 48, 375-383, 2014.
- 2056 Dusanter, S., Vimal, D., Stevens, P. S., Volkamer, R., Molina, L. T., Baker, A., Meinardi, S.,
2057 Blake, D., Sheehy, P., Merten, A., Zhang, R., Zheng, J., Fortner, E. C., Junkermann, W.,
2058 Dubey, M., Rahn, T., Eichinger, B., Lewandowski, P., Prueger, J., and Holder, H.:
2059 Measurements of OH and HO₂ concentrations during the MCMA-2006 field campaign - Part
2060 2: Model comparison and radical budget, *Atmos. Chem. Phys.*, 9, 6655-6675, 2009.



- 2061 Duvall, R. M., Majestic, B. J., Shafer, M. M., Chuang, P. Y., Simoneit, B. R. T., and Schauer,
2062 J. J.: The water-soluble fraction of carbon, sulfur, and crustal elements in Asian aerosols and
2063 Asian soils, *Atmos. Environ.*, 42, 5872-5884, 2008.
- 2064 Edwards, P. M., Brown, S. S., Roberts, J. M., Ahmadov, R., Banta, R. M., deGouw, J. A.,
2065 Dube, W. P., Field, R. A., Flynn, J. H., Gilman, J. B., Graus, M., Helmig, D., Koss, A.,
2066 Langford, A. O., Lefer, B. L., Lerner, B. M., Li, R., Li, S.-M., McKeen, S. A., Murphy, S.
2067 M., Parrish, D. D., Senff, C. J., Soltis, J., Stutz, J., Sweeney, C., Thompson, C. R., Trainer,
2068 M. K., Tsai, C., Veres, P. R., Washenfelder, R. A., Warneke, C., Wild, R. J., Young, C. J.,
2069 Yuan, B., and Zamora, R.: High winter ozone pollution from carbonyl photolysis in an oil
2070 and gas basin, *Nature*, 514, 351-354, 2014.
- 2071 Ehhalt, D. H.: Photooxidation of trace gases in the troposphere Plenary Lecture, *Phys. Chem.*
2072 *Chem. Phys.*, 1, 5401-5408, 1999.
- 2073 El Zein, A., and Bedjanian, Y.: Reactive Uptake of HONO to TiO₂ Surface: "Dark" Reaction,
2074 *J. Phys. Chem. A*, 116, 3665-3672, 2012.
- 2075 El Zein, A., Bedjanian, Y., and Romanias, M. N.: Kinetics and products of HONO interaction
2076 with TiO₂ surface under UV irradiation, *Atmos. Environ.*, 67, 203-210, 2013a.
- 2077 El Zein, A., Romanias, M. N., and Bedjanian, Y.: Kinetics and Products of Heterogeneous
2078 Reaction of HONO with Fe₂O₃ and Arizona Test Dust, *Environ. Sci. Technol.*, 47, 6325-
2079 6331, 2013b.
- 2080 El Zein, A., Romanias, M. N., and Bedjanian, Y.: Heterogeneous Interaction of H₂O₂ with
2081 Arizona Test Dust, *J. Phys. Chem. A*, 118, 441-448, 2014.
- 2082 Evans, M. J., and Jacob, D. J.: Impact of new laboratory studies of N₂O₅ hydrolysis on global
2083 model budgets of tropospheric nitrogen oxides, ozone, and OH, *Geophys. Res. Lett.*, 32,
2084 L09813, doi:09810.01029/02005GL022469, 2005.
- 2085 Fitzgerald, E., Ault, A. P., Zauscher, M. D., Mayol-Bracero, O. L., and Prather, K. A.:
2086 Comparison of the mixing state of long-range transported Asian and African mineral dust,
2087 *Atmos. Environ.*, 115, 19-25, 2015.
- 2088 Formenti, P., Schutz, L., Balkanski, Y., Desboeufs, K., Ebert, M., Kandler, K., Petzold, A.,
2089 Scheuven, D., Weinbruch, S., and Zhang, D.: Recent progress in understanding physical and
2090 chemical properties of African and Asian mineral dust, *Atmos. Chem. Phys.*, 11, 8231-8256,
2091 2011.
- 2092 Formenti, P., Caquineau, S., Desboeufs, K., Klaver, A., Chevaillier, S., Journet, E., and Rajot,
2093 J. L.: Mapping the physico-chemical properties of mineral dust in western Africa:
2094 mineralogical composition, *Atmos. Chem. Phys.*, 14, 10663-10686, 2014.
- 2095 Fuller, E. N., Schettle, P. D., and Giddings, J. C.: A new method for prediction of binary gas-
2096 phase diffusion coefficients, *Ind. Eng. Chem.*, 58, 19-27, 1966.
- 2097 Galy-Lacaux, C., Carmichael, G. R., Song, C. H., Lacaux, J. P., Al Ourabi, H., and Modi, A.
2098 I.: Heterogeneous processes involving nitrogenous compounds and Saharan dust inferred
2099 from measurements and model calculations, *J. Geophys. Res.-Atmos.*, 106, 12559-12578,
2100 2001.
- 2101 Gankanda, A., and Grassian, V. H.: Nitrate Photochemistry on Laboratory Proxies of Mineral
2102 Dust Aerosol: Wavelength Dependence and Action Spectra, *J. Phys. Chem. C*, 118, 29117-
2103 29125, 2014.
- 2104 Ge, M. F., Wu, L. Y., Tong, S. R., Liu, Q. F., and Wang, W. G.: Heterogeneous chemistry of
2105 trace atmospheric gases on atmospheric aerosols: an overview, *Science Foundation in China*,
2106 23, 62-80, 2015.
- 2107 Geng, F., Tie, X., Xu, J., Zhou, G., Peng, L., Gao, W., Tang, X., and Zhao, C.:
2108 Characterizations of ozone, NO_x, and VOCs measured in Shanghai, China, *Atmos. Environ.*,
2109 42, 6873-6883, 2008.



- 2110 George, C., Ammann, M., D'Anna, B., Donaldson, D. J., and Nizkorodov, S. A.:
2111 Heterogeneous Photochemistry in the Atmosphere, *Chem. Rev.*, 115, 4218-4258, 2015.
2112 George, C., Beeldens, A., Barmpas, F., Doussin, J.-F., Manganelli, G., Herrmann, H.,
2113 Kleffmann, J., and Mellouki, A.: Impact of photocatalytic remediation of pollutants on urban
2114 air quality, *Front. Environ. Sci. Eng.*, 10, 1-11, 2016.
2115 Gershenson, Y. M., Ivanov, A. V., Kucheryavyi, S. I., and Rozenshtein, V. B.: Annihilation
2116 of OH radicals on the surfaces of substances chemically similar to atmospheric aerosol
2117 particles, *Kinet. Catal.*, 27, 1069-1074, 1986.
2118 Geyer, A., Aliche, B., Konrad, S., Schmitz, T., Stutz, J., and Platt, U.: Chemistry and
2119 oxidation capacity of the nitrate radical in the continental boundary layer near Berlin, *J.*
2120 *Geophys. Res.-Atmos.*, 106, 8013-8025, 2001.
2121 Geyer, A., Bachmann, K., Hofzumahaus, A., Holland, F., Konrad, S., Klupfel, T., Patz, H.
2122 W., Perner, D., Mihelcic, D., Schafer, H. J., Volz-Thomas, A., and Platt, U.: Nighttime
2123 formation of peroxy and hydroxyl radicals during the BERLIOZ campaign: Observations and
2124 modeling studies, *J. Geophys. Res.-Atmos.*, 108, 8249, DOI: 8210.1029/2001JD000656,
2125 2003.
2126 Giannadaki, D., Pozzer, A., and Lelieveld, J.: Modeled global effects of airborne desert dust
2127 on air quality and premature mortality, *Atmos. Chem. Phys.*, 14, 957-968, 2014.
2128 Ginoux, P., Prospero, J. M., Gill, T. E., Hsu, N. C., and Zhao, M.: Global-scale Attribution of
2129 Anthropogenic and Natural Dust Sources and Their Emission Rates Based on MODIS Deep
2130 Blue Aerosol Products, *Rev. Geophys.*, 50, RG3005, doi: 3010.1029/2012RG000388, 2012.
2131 Gobbi, G. P., Barnaba, F., Giorgi, R., and Santacasa, A.: Altitude-resolved properties of a
2132 Saharan dust event over the Mediterranean, *Atmos. Environ.*, 34, 5119-5127, 2000.
2133 Goodman, A. L., Underwood, G. M., and Grassian, V. H.: A Laboratory Study of the
2134 Heterogeneous Reaction of Nitric Acid on Calcium Carbonate Particles, *J. Geophys. Res.-*
2135 *Atmos.*, 105, 29053-29064, 2000.
2136 Graedel, T. E., Mandich, M. L., and Weschler, C. J.: Kinetic model studies of atmospheric
2137 droplet chemistry: 2. Homogeneous transition metal chemistry in raindrops, *J. Geophys. Res.-*
2138 *Atmos.*, 91, 5205-5221, 1986.
2139 Hall, B. D., and Claiborn, C. S.: Measurements of the dry deposition of peroxides to a
2140 Canadian boreal forest, *J. Geophys. Res.-Atmos.*, 102, 29343-29353, 1997.
2141 Hanisch, F., and Crowley, J. N.: Heterogeneous Reactivity of Gaseous Nitric Acid on Al₂O₃,
2142 CaCO₃, and Atmospheric Dust Samples: A Knudsen Cell Study, *J. Phys. Chem. A*, 105,
2143 3096-3106, 2001.
2144 Hanisch, F., and Crowley, J. N.: Ozone decomposition on Saharan dust: an experimental
2145 investigation, *Atmos. Chem. Phys.*, 3, 119-130, 2003a.
2146 Hanisch, F., and Crowley, J. N.: Heterogeneous reactivity of NO and HNO₃ on mineral dust
2147 in the presence of ozone, *Phys. Chem. Chem. Phys.*, 5, 883-887, 2003b.
2148 Hanning-Lee, M. A., Brady, B. B., Martin, L. R., and Syage, J. A.: Ozone decomposition on
2149 alumina: Implications for solid rocket motor exhaust, *Geophys. Res. Lett.*, 23, 1961-1964,
2150 1996.
2151 Harris, E., Sinha, B., Foley, S., Crowley, J. N., Borrmann, S., and Hoppe, P.: Sulfur isotope
2152 fractionation during heterogeneous oxidation of SO₂ on mineral dust, *Atmos. Chem. Phys.*,
2153 12, 4867-4884, 2012.
2154 Harrison, R. M., and Kitto, A. M. N.: EVIDENCE FOR A SURFACE SOURCE OF
2155 ATMOSPHERIC NITROUS-ACID, *Atmos. Environ.*, 28, 1089-1094, 1994.
2156 Harrison, R. M., Peak, J. D., and Collins, G. M.: Tropospheric cycle of nitrous acid, *J.*
2157 *Geophys. Res.-Atmos.*, 101, 14429-14439, 1996.



- 2158 He, H., Wang, Y., Ma, Q., Ma, J., Chu, B., Ji, D., Tang, G., Liu, C., Zhang, H., and Hao, J.:
2159 Mineral Dust and NO_x Promote the Conversion of SO₂ to Sulfate in Heavy Pollution Days,
2160 Sci. Rep., 4, 4172, doi: 4110.1038/srep04172, 2014.
- 2161 Heard, D. E., Carpenter, L. J., Creasey, D. J., Hopkins, J. R., Lee, J. D., Lewis, A. C., Pilling,
2162 M. J., Seakins, P. W., Carslaw, N., and Emmerson, K. M.: High levels of the hydroxyl radical
2163 in the winter urban troposphere, Geophys. Res. Lett., 31, L18112, DOI:
2164 18110.11029/12004GL020544, 2004.
- 2165 Highwood, E., and Ryder, C.: Radiative Effects of Dust, in: Mineral Dust, edited by:
2166 Knippertz, P., and Stuut, J.-B. W., Springer, Netherlands, 267-286, 2014.
- 2167 Hoffman, R. C., Gebel, M. E., Fox, B. S., and Finlayson-Pitts, B. J.: Knudsen cell studies of
2168 the reactions of N₂O₅ and ClONO₂ with NaCl: development and application of a model for
2169 estimating available surface areas and corrected uptake coefficients, Phys. Chem. Chem.
2170 Phys., 5, 1780-1789, 2003a.
- 2171 Hoffman, R. C., Kaleuati, M. A., and Finlayson-Pitts, B. J.: Knudsen cell studies of the
2172 reaction of gaseous HNO₃ with NaCl using less than a single layer of particles at 298 K: A
2173 modified mechanism, J. Phys. Chem. A, 107, 7818-7826, 2003b.
- 2174 Hofzumahaus, A., Rohrer, F., Lu, K. D., Bohn, B., Brauers, T., Chang, C. C., Fuchs, H.,
2175 Holland, F., Kita, K., Kondo, Y., Li, X., Lou, S. R., Shao, M., Zeng, L. M., Wahner, A., and
2176 Zhang, Y. H.: Amplified Trace Gas Removal in the Troposphere, Science, 324, 1702-1704,
2177 2009.
- 2178 Holland, F., Hofzumahaus, A., Schäfer, J., Kraus, A., and Pätz, H.-W.: Measurements of OH
2179 and HO₂ radical concentrations and photolysis frequencies during BERLIOZ, J. Geophys.
2180 Res.-Atmos., 108, 8246, doi: 8210.1029/2001JD001393, 2003.
- 2181 Hoose, C., Kristjansson, J. E., and Burrows, S. M.: How important is biological ice
2182 nucleation in clouds on a global scale?, Environ. Res. Lett., 5, 024009, 2010.
- 2183 Hoose, C., and Moehler, O.: Heterogeneous ice nucleation on atmospheric aerosols: a review
2184 of results from laboratory experiments, Atmos. Chem. Phys., 12, 9817-9854, 2012.
- 2185 Hou, S. Q., Tong, S. R., Zhang, Y., Tan, F., Guo, Y. C., and Ge, M. F.: Heterogeneous uptake
2186 of gas-phase acetic acid on α -Al₂O₃ particle surface: the impact of temperature, Chem. Asian
2187 J., doi: 10.1002/asia.201600402, 2016.
- 2188 Hua, W., Chen, Z. M., Jie, C. Y., Kondo, Y., Hofzumahaus, A., Takegawa, N., Chang, C. C.,
2189 Lu, K. D., Miyazaki, Y., Kita, K., Wang, H. L., Zhang, Y. H., and Hu, M.: Atmospheric
2190 hydrogen peroxide and organic hydroperoxides during PRIDE-PRD'06, China: their
2191 concentration, formation mechanism and contribution to secondary aerosols, Atmos. Chem.
2192 Phys., 8, 6755-6773, 2008.
- 2193 Huang, L., Zhao, Y., Li, H., and Chen, Z.: Kinetics of Heterogeneous Reaction of Sulfur
2194 Dioxide on Authentic Mineral Dust: Effects of Relative Humidity and Hydrogen Peroxide,
2195 Environ. Sci. Technol., 49, 10797-10805, 2015a.
- 2196 Huang, X., Song, Y., Zhao, C., Cai, X., Zhang, H., and Zhu, T.: Direct Radiative Effect by
2197 Multicomponent Aerosol over China, J. Climate, 28, 3472-3495, 2015b.
- 2198 Huff, D. M., Joyce, P. L., Fochesatto, G. J., and Simpson, W. R.: Deposition of dinitrogen
2199 pentoxide, N₂O₅, to the snowpack at high latitudes, Atmos. Chem. Phys., 11, 4929-4938,
2200 2011.
- 2201 Huneus, N., Schulz, M., Balkanski, Y., Griesfeller, J., Prospero, J., Kinne, S., Bauer, S.,
2202 Boucher, O., Chin, M., Dentener, F., Diehl, T., Easter, R., Fillmore, D., Ghan, S., Ginoux, P.,
2203 Grini, A., Horowitz, L., Koch, D., Krol, M. C., Landing, W., Liu, X., Mahowald, N., Miller,
2204 R., Morcrette, J. J., Myhre, G., Penner, J., Perlwitz, J., Stier, P., Takemura, T., and Zender, C.
2205 S.: Global dust model intercomparison in AeroCom phase I, Atmos. Chem. Phys., 11, 7781-
2206 7816, 2011.



- 2207 Ingham, T., Goddard, A., Whalley, L. K., Furneaux, K. L., Edwards, P. M., Seal, C. P., Self,
2208 D. E., Johnson, G. P., Read, K. A., Lee, J. D., and Heard, D. E.: A flow-tube based laser-
2209 induced fluorescence instrument to measure OH reactivity in the troposphere, *Atmos. Meas.*
2210 *Tech.*, 2, 465-477, 2009.
- 2211 Itahashi, S., Uno, I., Irie, H., Kurokawa, J. I., and Ohara, T.: Regional modeling of
2212 tropospheric NO₂ vertical column density over East Asia during the period
2213 2000–2010: comparison with multisatellite observations, *Atmos. Chem. Phys.*, 14, 3623-
2214 3635, 2014.
- 2215 Ito, A., and Xu, L.: Response of acid mobilization of iron-containing mineral dust to
2216 improvement of air quality projected in the future, *Atmos. Chem. Phys.*, 14, 3441-3459,
2217 2014.
- 2218 Jacob, D. J.: Heterogeneous chemistry and tropospheric ozone, *Atmos. Environ.*, 34, 2131-
2219 2159, 2000.
- 2220 James, A. D., Moon, D. R., Feng, W., Lakey, P. S. J., Frankland, V. L., Heard, D. E., and
2221 Plane, J. M. C.: The uptake of HO₂ on meteoric smoke analogues, *J. Geophys. Res.-Atmos.*,
2222 122, 554-565, 2017.
- 2223 Jeong, G. R., and Sokolik, I. N.: Effect of mineral dust aerosols on the photolysis rates in the
2224 clean and polluted marine environments, *J. Geophys. Res.-Atmos.*, 112, D21308, doi:
2225 10.1029/2007jd008442, 2007.
- 2226 Jeong, G. Y.: Bulk and single-particle mineralogy of Asian dust and a comparison with its
2227 source soils, *J. Geophys. Res.-Atmos.*, 113, D02208, doi: 10.1029/2007jd008606,
2228 2008.
- 2229 Jickells, T., Boyd, P., and Hunter, K.: Biogeochemical Impacts of Dust on the Global Carbon
2230 Cycle, in: *Mineral Dust*, edited by: Knippertz, P., and Stuut, J.-B. W., Springer, Netherlands,
2231 359-384, 2014.
- 2232 Jickells, T. D., An, Z. S., Andersen, K. K., Baker, A. R., Bergametti, G., Brooks, N., Cao, J.
2233 J., Boyd, P. W., Duce, R. A., Hunter, K. A., Kawahata, H., Kubilay, N., laRoche, J., Liss, P.
2234 S., Mahowald, N., Prospero, J. M., Ridgwell, A. J., Tegen, I., and Torres, R.: Global Iron
2235 Connections between Desert Dust, Ocean Biogeochemistry, and Climate, *Science*, 308, 67-
2236 71, 2005.
- 2237 Journet, E., Desboeufs, K. V., Caquineau, S., and Colin, J.-L.: Mineralogy as a critical factor
2238 of dust iron solubility, *Geophys. Res. Lett.*, 35, L07805, doi: 10.1029/2007GL031589,
2239 2008.
- 2240 Journet, E., Balkanski, Y., and Harrison, S. P.: A New Data Set of Soil Mineralogy for Dust-
2241 cycle Modeling, *Atmos. Chem. Phys.*, 14, 3801-3816, 2014.
- 2242 Jung, J., Kim, Y. J., Lee, K. Y., Cayetano, M. G., Batmunkh, T., Koo, J. H., and Kim, J.:
2243 Spectral optical properties of long-range transport Asian dust and pollution aerosols over
2244 Northeast Asia in 2007 and 2008, *Atmos. Chem. Phys.*, 10, 5391-5408, 2010.
- 2245 Kaiser, E. W., and Wu, C. H.: A kinetic study of the gas phase formation and decomposition
2246 reactions of nitrous acid, *J. Phys. Chem.*, 81, 1701-1706, 1977.
- 2247 Kanaya, Y., Cao, R., Akimoto, H., Fukuda, M., Komazaki, Y., Yokouchi, Y., Koike, M.,
2248 Tanimoto, H., Takegawa, N., and Kondo, Y.: Urban photochemistry in central Tokyo: 1.
2249 Observed and modeled OH and HO₂ radical concentrations during the winter and summer of
2250 2004, *J. Geophys. Res.-Atmos.*, 112, D21312, doi: 10.1029/2007JD008670, 2007a.
- 2251 Kanaya, Y., Cao, R. Q., Akimoto, H., Fukuda, M., Komazaki, Y., Yokouchi, Y., Koike, M.,
2252 Tanimoto, H., Takegawa, N., and Kondo, Y.: Urban photochemistry in central Tokyo: 1.
2253 Observed and modeled OH and HO₂ radical concentrations during the winter and summer of
2254 2004, *J. Geophys. Res.-Atmos.*, 112, D21312, DOI: 10.1029/2007JD008670, 2007b.
- 2255 Karagulian, F., and Rossi, M. J.: The heterogeneous chemical kinetics of NO₃ on atmospheric
2256 mineral dust surrogates, *Phys. Chem. Chem. Phys.*, 7, 3150-3162, 2005.



- 2257 Karagulian, F., and Rossi, M. J.: The heterogeneous decomposition of ozone on atmospheric
2258 mineral dust surrogates at ambient temperature, *Int. J. Chem. Kinet.*, 38, 407-419, 2006.
- 2259 Karagulian, F., Santschi, C., and Rossi, M. J.: The heterogeneous chemical kinetics of N₂O₅
2260 on CaCO₃ and other atmospheric mineral dust surrogates, *Atmos. Chem. Phys.*, 6, 1373-
2261 1388, 2006.
- 2262 Keyser, L. F., Moore, S. B., and Leu, M. T.: Surface-Reaction and Pore Diffusion in Flow-
2263 Tube Reactors, *J. Phys. Chem.*, 95, 5496-5502, 1991.
- 2264 Keyser, L. F., Leu, M. T., and Moore, S. B.: Comment on porosities of ice films used to
2265 simulate stratospheric cloud surfaces, *J. Phys. Chem.*, 97, 2800-2801, 1993.
- 2266 Koehler, K. A., Kreidenweis, S. M., DeMott, P. J., Petters, M. D., Prenni, A. J., and Carrico,
2267 C. M.: Hygroscopicity and cloud droplet activation of mineral dust aerosol, *Geophys. Res.*
2268 *Let.*, 36, L08805, doi: 08810.01029/02009gl037348, 2009.
- 2269 Kolb, C. E., Cox, R. A., Abbatt, J. P. D., Ammann, M., Davis, E. J., Donaldson, D. J.,
2270 Garrett, B. C., George, C., Griffiths, P. T., Hanson, D. R., Kulmala, M., McFiggans, G.,
2271 Pöschl, U., Riipinen, I., Rossi, M. J., Rudich, Y., Wagner, P. E., Winkler, P. M., Worsnop, D.
2272 R., and O' Dowd, C. D.: An overview of current issues in the uptake of atmospheric trace
2273 gases by aerosols and clouds, *Atmos. Chem. Phys.*, 10, 10561-10605, 2010.
- 2274 Kong, L. D., Zhao, X., Sun, Z. Y., Yang, Y. W., Fu, H. B., Zhang, S. C., Cheng, T. T., Yang,
2275 X., Wang, L., and Chen, J. M.: The effects of nitrate on the heterogeneous uptake of sulfur
2276 dioxide on hematite, *Atmos. Chem. Phys.*, 14, 9451-9467, 2014.
- 2277 Krieger, U. K., Marcolli, C., and Reid, J. P.: Exploring the complexity of aerosol particle
2278 properties and processes using single particle techniques, *Chem. Soc. Rev.*, 41, 6631-6662,
2279 2012.
- 2280 Krueger, B. J., Grassian, V. H., Iedema, M. J., Cowin, J. P., and Laskin, A.: Probing
2281 heterogeneous chemistry of individual atmospheric particles using scanning electron
2282 microscopy and energy-dispersive X-ray analysis, *Anal. Chem.*, 75, 5170-5179, 2003a.
- 2283 Krueger, B. J., Grassian, V. H., Laskin, A., and Cowin, J. P.: The Transformation of Solid
2284 Atmospheric Particles into Liquid Droplets through Heterogeneous Chemistry: Laboratory
2285 Insights into the Processing of Calcium Containing Mineral Dust Aerosol in the Troposphere,
2286 *Geophys. Res. Let.*, 30, 1148, doi: 1110.1029/2002gl016563, 2003b.
- 2287 Kulkarni, G., Zhang, K., Zhao, C., Nandasiri, M., Shutthanandan, V., Liu, X., Fast, J., and
2288 Berg, L.: Ice Formation on Nitric Acid Coated Dust Particles: Laboratory and Modeling
2289 Studies, *J. Geophys. Res.-Atmos.*, 120, 7682-7698, 2015.
- 2290 Kumar, P., Sokolik, I. N., and Nenes, A.: Parameterization of cloud droplet formation for
2291 global and regional models: including adsorption activation from insoluble CCN, *Atmos.*
2292 *Chem. Phys.*, 9, 2517-2532, 2009.
- 2293 Kumar, R., Barth, M. C., Madronich, S., Naja, M., Carmichael, G. R., Pfister, G. G., Knote,
2294 C., Brasseur, G. P., Ojha, N., and Sarangi, T.: Effects of dust aerosols on tropospheric
2295 chemistry during a typical pre-monsoon season dust storm in northern India, *Atmos. Chem.*
2296 *Phys.*, 14, 6813-6834, 2014.
- 2297 Ladino, L. A., Stetzer, O., and Lohmann, U.: Contact freezing: a review of experimental
2298 studies, *Atmos. Chem. Phys.*, 13, 9745-9769, 2013.
- 2299 Lampimäki, M., Zelenay, V., Krepelova, A., Liu, Z., Chang, R., Bluhm, H., and Ammann,
2300 M.: Ozone-Induced Band Bending on Metal-Oxide Surfaces Studied under Environmental
2301 Conditions, *ChemPhysChem*, 14, 2419 – 2425, 2013.
- 2302 Langridge, J. M., Gustafsson, R. J., Griffiths, P. T., Cox, R. A., Lambert, R. M., and Jones, R.
2303 L.: Solar driven nitrous acid formation on building material surfaces containing titanium
2304 dioxide: A concern for air quality in urban areas?, *Atmos. Environ.*, 43, 5128-5131, 2009.



- 2305 Laskin, A., Iedema, M. J., Ichkovich, A., Graber, E. R., Taraniuk, I., and Rudich, Y.: Direct
2306 Observation of Completely Processed Calcium Carbonate Dust Particles, *Faraday Discuss.*,
2307 130, 453-468, 2005a.
- 2308 Laskin, A., Wietsma, T. W., Krueger, B. J., and Grassian, V. H.: Heterogeneous chemistry of
2309 individual mineral dust particles with nitric acid: A combined CCSEM/EDX, ESEM, and
2310 ICP-MS study, *J. Geophys. Res.-Atmos.*, 110, 2005b.
- 2311 Laufs, S., Burgeth, G., Duttlinger, W., Kurtenbach, R., Maban, M., Thomas, C., Wiesen, P.,
2312 and Kleffmann, J.: Conversion of nitrogen oxides on commercial photocatalytic dispersion
2313 paints, *Atmos. Environ.*, 44, 2341-2349, 2010.
- 2314 Lee, A. K. Y., and Chan, C. K.: Heterogeneous Reactions of Linoleic Acid and Linolenic
2315 Acid Particles with Ozone: Reaction Pathways and Changes in Particle Mass,
2316 Hygroscopicity, and Morphology, *J. Phys. Chem. A*, 111, 6285-6295, 2007.
- 2317 Lee, A. K. Y., Ling, T. Y., and Chan, C. K.: Understanding hygroscopic growth and phase
2318 transformation of aerosols using single particle Raman spectroscopy in an electrodynamic
2319 balance, *Faraday Discuss.*, 137, 245-263, 2008.
- 2320 Lelieveld, J., Butler, T. M., Crowley, J. N., Dillon, T. J., Fischer, H., Ganzeveld, L., Harder,
2321 H., Lawrence, M. G., Martinez, M., Taraborrelli, D., and Williams, J.: Atmospheric oxidation
2322 capacity sustained by a tropical forest, *Nature*, 452, 737-740, 2008.
- 2323 Lemaitre, C., Flamant, C., Cuesta, J., Raut, J. C., Chazette, P., Formenti, P., and Pelon, J.:
2324 Radiative heating rates profiles associated with a springtime case of Bodele and Sudan dust
2325 transport over West Africa, *Atmos. Chem. Phys.*, 10, 8131-8150, 2010.
- 2326 Li, G., Su, H., Li, X., Kuhn, U., Meusel, H., Hoffmann, T., Ammann, M., Pöschl, U., Shao,
2327 M., and Cheng, Y. F.: Uptake of gaseous formaldehyde by soil surfaces: a combination of
2328 adsorption/desorption equilibrium and chemical reactions, *Atmos. Chem. Phys.*, 16, 10299-
2329 10311, 2016.
- 2330 Li, H. J., Zhu, T., Zhao, D. F., Zhang, Z. F., and Chen, Z. M.: Kinetics and mechanisms of
2331 heterogeneous reaction of NO₂ on CaCO₃ surfaces under dry and wet conditions, *Atmos.*
2332 *Chem. Phys.*, 10, 463-474, 2010.
- 2333 Li, L., Chen, Z. M., Zhang, Y. H., Zhu, T., Li, J. L., and Ding, J.: Kinetics and mechanism of
2334 heterogeneous oxidation of sulfur dioxide by ozone on surface of calcium carbonate, *Atmos.*
2335 *Chem. Phys.*, 6, 2453-2464, 2006.
- 2336 Li, P., Al-Abadleh, H. A., and Grassian, V. H.: Measuring heterogeneous uptake coefficients
2337 of gases on solid particle surfaces with a Knudsen cell reactor: Complications due to surface
2338 saturation and gas diffusion into underlying layers, *J. Phys. Chem. A*, 106, 1210-1219, 2002.
- 2339 Li, W., Gibbs, G. V., and Oyama, S. T.: Mechanism of ozone decomposition on a manganese
2340 oxide catalyst. I. In situ Raman spectroscopy and ab initio molecular orbital calculations, *J.*
2341 *Am. Chem. Soc.*, 120, 9041-9046, 1998.
- 2342 Li, W., and Oyama, S. T.: Mechanism of ozone decomposition on a manganese oxide
2343 catalyst. 2. Steady-state and transient kinetic studies, *J. Am. Chem. Soc.*, 120, 9047-9052,
2344 1998.
- 2345 Li, W. J., and Shao, L. Y.: Observation of Nitrate Coatings on Atmospheric Mineral Dust
2346 Particles, *Atmos. Chem. Phys.*, 9, 1863-1871, 2009.
- 2347 Li, X., Brauers, T., Haseler, R., Bohn, B., Fuchs, H., Hofzumahaus, A., Holland, F., Lou, S.,
2348 Lu, K. D., Rohrer, F., Hu, M., Zeng, L. M., Zhang, Y. H., Garland, R. M., Su, H., Nowak, A.,
2349 Wiedensohler, A., Takegawa, N., Shao, M., and Wahner, A.: Exploring the atmospheric
2350 chemistry of nitrous acid (HONO) at a rural site in Southern China, *Atmos. Chem. Phys.*, 12,
2351 1497-1513, 2012.
- 2352 Liao, H., Yung, Y. L., and Seinfeld, J. H.: Effects of aerosols on tropospheric photolysis rates
2353 in clear and cloudy atmospheres, *J. Geophys. Res.-Atmos.*, 104, 23697-23707, 1999.



- 2354 Liao, J., Huey, L. G., Liu, Z., Tanner, D. J., Cantrell, C. A., Orlando, J. J., Flocke, F. M.,
2355 Shepson, P. B., Weinheimer, A. J., Hall, S. R., Ullmann, K., Beine, H. J., Wang, Y., Ingall, E.
2356 D., Stephens, C. R., Hornbrook, R. S., Apel, E. C., Riemer, D., Fried, A., Mauldin Iii, R. L.,
2357 Smith, J. N., Staebler, R. M., Neuman, J. A., and Nowak, J. B.: High levels of molecular
2358 chlorine in the Arctic atmosphere, *Nature Geosci.*, 7, 91-94, 2014.
- 2359 Lipfert, F. W.: Atmospheric damage to calcareous stones: Comparison and reconciliation of
2360 recent experimental findings, *Atmos. Environ.*, 23, 415-429, 1989.
- 2361 Liu, C., Ma, Q., Liu, Y., Ma, J., and He, H.: Synergistic reaction between SO₂ and NO₂ on
2362 mineral oxides: a potential formation pathway of sulfate aerosol, *Phys. Chem. Chem. Phys.*,
2363 14, 1668-1676, 2012.
- 2364 Liu, H. M., Lian, Z. W., Ye, X. J., and Shangguan, W. F.: Kinetic analysis of photocatalytic
2365 oxidation of gas-phase formaldehyde over titanium dioxide, *Chemosphere*, 60, 630-635,
2366 2005.
- 2367 Liu, Y., Ma, J., and He, H.: Heterogeneous reactions of carbonyl sulfide on mineral oxides:
2368 mechanism and kinetics study, *Atmos. Chem. Phys.*, 10, 10335-10344, 2010.
- 2369 Liu, Y., Han, C., Ma, J., Bao, X., and He, H.: Influence of relative humidity on heterogeneous
2370 kinetics of NO₂ on kaolin and hematite, *Phys. Chem. Chem. Phys.*, 17, 19424-19431, 2015.
- 2371 Liu, Y. C., He, H., and Mu, Y. J.: Heterogeneous reactivity of carbonyl sulfide on α -Al₂O₃
2372 and γ -Al₂O₃, *Atmos. Environ.*, 42, 960-969, 2008a.
- 2373 Liu, Y. J., Zhu, T., Zhao, D. F., and Zhang, Z. F.: Investigation of the hygroscopic properties
2374 of Ca(NO₃)₂ and internally mixed Ca(NO₃)₂/CaCO₃ particles by micro-Raman spectrometry,
2375 *Atmos. Chem. Phys.*, 8, 7205-7215, 2008b.
- 2376 Lohmann, U., and Feichter, J.: Global indirect aerosol effects: a review, *Atmos. Chem. Phys.*,
2377 5, 715-737, 2005.
- 2378 Lou, S., Holland, F., Rohrer, F., Lu, K., Bohn, B., Brauers, T., Chang, C. C., Fuchs, H.,
2379 Häseler, R., Kita, K., Kondo, Y., Li, X., Shao, M., Zeng, L., Wahner, A., Zhang, Y., Wang,
2380 W., and Hofzumahaus, A.: Atmospheric OH reactivities in the Pearl River Delta – China in
2381 summer 2006: measurement and model results, *Atmos. Chem. Phys.*, 10, 11243-11260, 2010.
- 2382 Lu, K. D., Rohrer, F., Holland, F., Fuchs, H., Bohn, B., Brauers, T., Chang, C. C., Haseler,
2383 R., Hu, M., Kita, K., Kondo, Y., Li, X., Lou, S. R., Nehr, S., Shao, M., Zeng, L. M., Wahner,
2384 A., Zhang, Y. H., and Hofzumahaus, A.: Observation and modelling of OH and HO₂
2385 concentrations in the Pearl River Delta 2006: a missing OH source in a VOC rich
2386 atmosphere, *Atmos. Chem. Phys.*, 12, 1541-1569, 2012.
- 2387 Lu, K. D., Hofzumahaus, A., Holland, F., Bohn, B., Brauers, T., Fuchs, H., Hu, M., Haseler,
2388 R., Kita, K., Kondo, Y., Li, X., Lou, S. R., Oebel, A., Shao, M., Zeng, L. M., Wahner, A.,
2389 Zhu, T., Zhang, Y. H., and Rohrer, F.: Missing OH source in a suburban environment near
2390 Beijing: observed and modelled OH and HO₂ concentrations in summer 2006, *Atmos. Chem.*
2391 *Phys.*, 13, 1057-1080, 2013.
- 2392 Lu, K. D., Rohrer, F., Holland, F., Fuchs, H., Brauers, T., Oebel, A., Dlugi, R., Hu, M., Li,
2393 X., Lou, S. R., Shao, M., Zhu, T., Wahner, A., Zhang, Y. H., and Hofzumahaus, A.:
2394 Nighttime observation and chemistry of HO_x in the Pearl River Delta and Beijing in summer
2395 2006, *Atmos. Chem. Phys.*, 14, 4979-4999, 2014.
- 2396 Ma, Q. X., Liu, Y. C., Liu, C., and He, H.: Heterogeneous Reaction of Acetic Acid on MgO,
2397 α -Al₂O₃, and CaCO₃ and the Effect on the Hygroscopic Behavior of These Particles, *Phys.*
2398 *Chem. Chem. Phys.*, 14, 8403-8409, 2012.
- 2399 Macintyre, H. L., and Evans, M. J.: Sensitivity of a global model to the uptake of N₂O₅ by
2400 tropospheric aerosol, *Atmos. Chem. Phys.*, 10, 7409-7414, 2010.
- 2401 Macintyre, H. L., and Evans, M. J.: Parameterisation and impact of aerosol uptake of HO₂ on
2402 a global tropospheric model, *Atmos. Chem. Phys.*, 11, 10965-10974, 2011.



- 2403 Mahowald, N., Jickells, T. D., Baker, A. R., Artaxo, P., Benitez-Nelson, C. R., Bergametti,
2404 G., Bond, T. C., Chen, Y., Cohen, D. D., Herut, B., Kubilay, N., Losno, R., Luo, C.,
2405 Maenhaut, W., McGee, K. A., Okin, G. S., Siefert, R. L., and Tsukuda, S.: Global distribution
2406 of atmospheric phosphorus sources, concentrations and deposition rates, and anthropogenic
2407 impacts, *Glob. Biogeochem. Cycle*, 22, GB4026, doi: 4010.1029/2008GB003240., 2008.
- 2408 Mahowald, N.: Aerosol Indirect Effect on Biogeochemical Cycles and Climate, *Science*, 334,
2409 794-796, 2011.
- 2410 Mahowald, N. M., Baker, A. R., Bergametti, G., Brooks, N., Duce, R. A., Jickells, T. D.,
2411 Kubilay, N., Prospero, J. M., and Tegen, I.: Atmospheric Global Dust Cycle and Iron Inputs
2412 to the Ocean, *Glob. Biogeochem. Cycle*, 19, GB4025, doi:4010.1029/2004GB002402, 2005.
- 2413 Mahowald, N. M., Ballantine, J. A., Feddesma, J., and Ramankutty, N.: Global trends in
2414 visibility: implications for dust sources, *Atmos. Chem. Phys.*, 7, 3309-3339, 2007.
- 2415 Mao, J., Jacob, D. J., Evans, M. J., Olson, J. R., Ren, X., Brune, W. H., Clair, J. M. S.,
2416 Crouse, J. D., Spencer, K. M., Beaver, M. R., Wennberg, P. O., Cubison, M. J., Jimenez, J.
2417 L., Fried, A., Weibring, P., Walega, J. G., Hall, S. R., Weinheimer, A. J., Cohen, R. C., Chen,
2418 G., Crawford, J. H., McNaughton, C., Clarke, A. D., Jaeglé, L., Fisher, J. A., Yantosca, R.
2419 M., Le Sager, P., and Carouge, C.: Chemistry of hydrogen oxide radicals (HOx) in the Arctic
2420 troposphere in spring, *Atmos. Chem. Phys.*, 10, 5823-5838, 2010a.
- 2421 Mao, J., Ren, X., Chen, S., Brune, W. H., Chen, Z., Martinez, M., Harder, H., Lefter, B.,
2422 Rappenglück, B., Flynn, J., and Leuchner, M.: Atmospheric oxidation capacity in the summer
2423 of Houston 2006: Comparison with summer measurements in other metropolitan studies,
2424 *Atmos. Environ.*, 44, 4107-4115, 2010b.
- 2425 Mao, J., Fan, S., Jacob, D. J., and Travis, K. R.: Radical loss in the atmosphere from Cu-Fe
2426 redox coupling in aerosols, *Atmos. Chem. Phys.*, 12, 509-519, 2013a.
- 2427 Mao, J. Q., Paulot, F., Jacob, D. J., Cohen, R. C., Crouse, J. D., Wennberg, P. O., Keller, C.
2428 A., Hudman, R. C., Barkley, M. P., and Horowitz, L. W.: Ozone and organic nitrates over the
2429 eastern United States: Sensitivity to isoprene chemistry, *J. Geophys. Res.-Atmos.*, 118,
2430 11256-11268, 2013b.
- 2431 Martinez, M., Perner, D., Hackenthal, E. M., Kulzer, S., and Schutz, L.: NO₃ at Helgoland
2432 during the NORDEX campaign in October 1996, *J. Geophys. Res.-Atmos.*, 105, 22685-
2433 22695, 2000.
- 2434 Matsuki, A., Iwasaka, Y., Shi, G. Y., Zhang, D. Z., Trochkin, D., Yamada, M., Kim, Y. S.,
2435 Chen, B., Nagatani, T., Miyazawa, T., Nagatani, M., and Nakata, H.: Morphological and
2436 chemical modification of mineral dust: Observational insight into the heterogeneous uptake
2437 of acidic gases, *Geophys. Res. Lett.*, 32, L22806, doi: 22810.21029/22005gl024176, 2005.
- 2438 Matthews, P. S. J., Baeza-Romero, M. T., Whalley, L. K., and Heard, D. E.: Uptake of HO₂
2439 radicals onto Arizona test dust particles using an aerosol flow tube, *Atmos. Chem. Phys.*, 14,
2440 7397-7408, 2014.
- 2441 Mauldin III, R. L., Berndt, T., Sipila, M., Paasonen, P., Petaja, T., Kim, S., Kurten, T.,
2442 Stratmann, F., Kerminen, V. M., and Kulmala, M.: A new atmospherically relevant oxidant
2443 of sulphur dioxide, *Nature*, 488, 193-196, 2012.
- 2444 Meng, Z., and Lu, B.: Dust events as a risk factor for daily hospitalization for respiratory and
2445 cardiovascular diseases in Minqin, China, *Atmos. Environ.*, 41, 7048-7058, 2007.
- 2446 Meskhidze, N., Chameides, W. L., and Nenes, A.: Dust and pollution: A recipe for enhanced
2447 ocean fertilization?, *J. Geophys. Res.-Atmos.*, 110, D03301, doi:
2448 03310.01029/02004jd005082, 2005.
- 2449 Michel, A. E., Usher, C. R., and Grassian, V. H.: Heterogeneous and catalytic uptake of
2450 ozone on mineral oxides and dusts: A Knudsen cell investigation, *Geophys. Res. Lett.*, 29,
2451 1665, 10.1029/2002gl014896, 2002.



- 2452 Michel, A. E., Usher, C. R., and Grassian, V. H.: Reactive uptake of ozone on mineral oxides
2453 and mineral dusts, *Atmos. Environ.*, 37, 3201-3211, 2003.
- 2454 Mihelcic, D., Holland, F., Hofzumahaus, A., Hoppe, L., Konrad, S., Müsgen, P., Pätz, H. W.,
2455 Schäfer, H. J., Schmitz, T., Volz-Thomas, A., Bächmann, K., Schlomski, S., Platt, U., Geyer,
2456 A., Alicke, B., and Moortgat, G. K.: Peroxy radicals during BERLIOZ at Pabstthum:
2457 Measurements, radical budgets and ozone production, *J. Geophys. Res.-Atmos.*, 108, 8254,
2458 doi: 8210.1029/2001JD001014, 2003.
- 2459 Mogili, P. K., Kleiber, P. D., Young, M. A., and Grassian, V. H.: Heterogeneous uptake of
2460 ozone on reactive components of mineral dust aerosol: An environmental aerosol reaction
2461 chamber study, *J. Phys. Chem. A*, 110, 13799-13807, 2006a.
- 2462 Mogili, P. K., Kleiber, P. D., Young, M. A., and Grassian, V. H.: N₂O₅ hydrolysis on the
2463 components of mineral dust and sea salt aerosol: Comparison study in an environmental
2464 aerosol reaction chamber, *Atmos. Environ.*, 40, 7401-7408, 2006b.
- 2465 Morgan, W. T., Ouyang, B., Allan, J. D., Aruffo, E., Di Carlo, P., Kennedy, O. J., Lowe, D.,
2466 Flynn, M. J., Rosenberg, P. D., Williams, P. I., Jones, R., McFiggans, G. B., and Coe, H.:
2467 Influence of aerosol chemical composition on N₂O₅ uptake: airborne regional measurements
2468 in northwestern Europe, *Atmos. Chem. Phys.*, 15, 973-990, 2015.
- 2469 Morman, S., and Plumlee, G.: Dust and Human Health, in: *Mineral Dust*, edited by:
2470 Knippertz, P., and Stuut, J.-B. W., Springer, Netherlands, 385-409, 2014.
- 2471 Murray, B. J., O'Sullivan, D., Atkinson, J. D., and Webb, M. E.: Ice nucleation by particles
2472 immersed in supercooled cloud droplets, *Chem. Soc. Rev.*, 41, 6519-6554, 2012.
- 2473 Nölscher, A. C., Williams, J., Sinha, V., Custer, T., Song, W., Johnson, A. M., Axinte, R.,
2474 Bozem, H., Fischer, H., Pouvesle, N., Phillips, G., Crowley, J. N., Rantala, P., Rinne, J.,
2475 Kulmala, M., Gonzales, D., Valverde-Canossa, J., Vogel, A., Hoffmann, T., Ouwersloot, H.
2476 G., Vilà-Guerau de Arellano, J., and Lelieveld, J.: Summertime total OH reactivity
2477 measurements from boreal forest during HUMPPA-COPEC 2010, *Atmos. Chem. Phys.*, 12,
2478 8257-8270, 2012.
- 2479 Nanayakkara, C. E., Jayaweera, P. M., Rubasinghege, G., Baltrusaitis, J., and Grassian, V.
2480 H.: Surface Photochemistry of Adsorbed Nitrate: The Role of Adsorbed Water in the
2481 Formation of Reduced Nitrogen Species on α -Fe₂O₃ Particle Surfaces, *J. Phys. Chem. A*,
2482 118, 158-166, 2013.
- 2483 Nanayakkara, C. E., Dillon, J. K., and Grassian, V. H.: Surface Adsorption and
2484 Photochemistry of Gas-Phase Formic Acid on TiO₂ Nanoparticles: The Role of Adsorbed
2485 Water in Surface Coordination, Adsorption Kinetics, and Rate of Photoproduct Formation, *J.*
2486 *Phys. Chem. C*, 118, 25487-25495, 2014.
- 2487 Ndour, M., Nicolas, M., D'Anna, B., Ka, O., and George, C.: Photoreactivity of NO₂ on
2488 mineral dusts originating from different locations of the Sahara desert, *Phys. Chem. Chem.*
2489 *Phys.*, 11, 1312-1319, 2009.
- 2490 Nenes, A., Krom, M. D., Mihalopoulos, N., Van Cappellen, P., Shi, Z., Bougiatioti, A.,
2491 Zarnpas, P., and Herut, B.: Atmospheric acidification of mineral aerosols: a source of
2492 bioavailable phosphorus for the oceans, *Atmos. Chem. Phys.*, 11, 6265-6272, 2011.
- 2493 Nickovic, S., Vukovic, A., Vujadinovic, M., Djurdjevic, V., and Pejanovic, G.: Technical
2494 Note: High-resolution mineralogical database of dust-productive soils for atmospheric dust
2495 modeling, *Atmos. Chem. Phys.*, 12, 845-855, 2012.
- 2496 Nicolas, M., Ndour, M., Ka, O., D'anna, B., and George, C.: Photochemistry of Atmospheric
2497 Dust: Ozone Decomposition on Illuminated Titanium Dioxide, *Environ. Sci. Technol.*, 43,
2498 7347-7442, 2009.
- 2499 Nie, W., Ding, A., Wang, T., Kerminen, V.-M., George, C., Xue, L., Wang, W., Zhang, Q.,
2500 Petaja, T., Qi, X., Gao, X., Wang, X., Yang, X., Fu, C., and Kulmala, M.: Polluted dust



- 2501 promotes new particle formation and growth, *Sci. Rep.*, 4, 6634, doi: 6610.1038/srep06634,
2502 2014.
- 2503 Noguchi, T., Fujishima, A., Sawunyama, P., and Hashimoto, K.: Photocatalytic Degradation
2504 of Gaseous Formaldehyde Using TiO₂ Film, *Environ. Sci. Technol.*, 32, 3831-3833, 1998.
- 2505 Obee, T. N., and Brown, R. T.: TiO₂ Photocatalysis for Indoor Air Applications: Effects of
2506 Humidity and Trace Contaminant Levels on the Oxidation Rates of Formaldehyde, Toluene,
2507 and 1,3-Butadiene, *Environ. Sci. Technol.*, 29, 1223-1231, 1995.
- 2508 Osthoff, H. D., Roberts, J. M., Ravishankara, A. R., Williams, E. J., Lerner, B. M.,
2509 Sommariva, R., Bates, T. S., Coffman, D., Quinn, P. K., Dibb, J. E., Stark, H., Burkholder, J.
2510 B., Talukdar, R. K., Meagher, J., Fehsenfeld, F. C., and Brown, S. S.: High levels of nitryl
2511 chloride in the polluted subtropical marine boundary layer, *Nature Geosci.*, 1, 324-328, 2008.
- 2512 Ouyang, B., McLeod, M. W., Jones, R. L., and Bloss, W. J.: NO₃ radical production from the
2513 reaction between the Criegee intermediate CH₂OO and NO₂, *Phys. Chem. Chem. Phys.*, 15,
2514 17070-17075, 2013.
- 2515 Pöschl, U., Rudich, Y., and Ammann, M.: Kinetic model framework for aerosol and cloud
2516 surface chemistry and gas-phase interaction-Part 1: General equation, parameters, and
2517 terminology, *Atmos. Chem. Phys.*, 7, 5989-6023, 2007.
- 2518 Pöschl, U.: Gas-particle interactions of tropospheric aerosols: Kinetic and thermodynamic
2519 perspectives of multiphase chemical reactions, amorphous organic substances, and the
2520 activation of cloud condensation nuclei, *Atmos. Res.*, 101, 562-573, 2011.
- 2521 Pöschl, U., and Shiraiwa, M.: Multiphase Chemistry at the Atmosphere-Biosphere Interface
2522 Influencing Climate and Public Health in the Anthropocene, *Chem. Rev.*, 115, 4440-4475,
2523 2015.
- 2524 Park, J.-H., Ivanov, A. V., and Molina, M. J.: Effect of Relative Humidity on OH Uptake by
2525 Surfaces of Atmospheric Importance, *J. Phys. Chem. A*, 112, 6968-6977, 2008.
- 2526 Percival, C. J., Welz, O., Eskola, A. J., Savee, J. D., Osborn, D. L., Topping, D. O., Lowe, D.,
2527 Utembe, S. R., Bacak, A., McFiggans, G., Cooke, M. C., Xiao, P., Archibald, A. T., Jenkin,
2528 M. E., Derwent, R. G., Riipinen, I., Mok, D. W. K., Lee, E. P. F., Dyke, J. M., Taatjes, C. A.,
2529 and Shallcross, D. E.: Regional and global impacts of Criegee intermediates on atmospheric
2530 sulphuric acid concentrations and first steps of aerosol formation, *Faraday Discuss.*, 165, 45-
2531 73, 2013.
- 2532 Phillips, G. J., Tang, M. J., Thieser, J., Brickwedde, B., Schuster, G., Bohn, B., Lelieveld, J.,
2533 and Crowley, J. N.: Significant concentrations of nitryl chloride observed in rural continental
2534 Europe associated with the influence of sea salt chloride and anthropogenic emissions,
2535 *Geophys. Res. Lett.*, 39, L10811, 10.1029/2012gl051912, 2012.
- 2536 Phillips, G. J., Thieser, J., Tang, M. J., Sobanski, N., Schuster, G., Fachinger, J., Drewnick,
2537 F., Borrmann, S., Bingemer, H., Lelieveld, J., and Crowley, J. N.: Estimating N₂O₅ uptake
2538 coefficients using ambient measurements of NO₃, N₂O₅, ClNO₂ and particle-phase nitrate,
2539 *Atmos. Chem. Phys. Discuss.*, 2016, 1-34, 10.5194/acp-2016-693, 2016.
- 2540 Pope, F. D., Dennis-Smith, B. J., Griffiths, P. T., Clegg, S. L., and Cox, R. A.: Studies of
2541 Single Aerosol Particles Containing Malonic Acid, Glutaric Acid, and Their Mixtures with
2542 Sodium Chloride. I. Hygroscopic Growth, *J. Phys. Chem. A*, 114, 5335-5341, 2010.
- 2543 Pope, F. D., Braesicke, P., Grainger, R. G., Kalberer, M., Watson, I. M., Davidson, P. J., and
2544 Cox, R. A.: Stratospheric aerosol particles and solar-radiation management, *Nature Clim.
2545 Change*, 2, 713-719, 2012.
- 2546 Pradhan, M., Kalberer, M., Griffiths, P. T., Braban, C. F., Pope, F. D., Cox, R. A., and
2547 Lambert, R. M.: Uptake of Gaseous Hydrogen Peroxide by Submicrometer Titanium Dioxide
2548 Aerosol as a Function of Relative Humidity, *Environ. Sci. Technol.*, 44, 1360-1365, 2010a.
- 2549 Pradhan, M., Kyriakou, G., Archibald, A. T., Papageorgiou, A. C., Kalberer, M., and
2550 Lambert, R. M.: Heterogeneous uptake of gaseous hydrogen peroxide by Gobi and Saharan



- 2551 dust aerosols: a potential missing sink for H₂O₂ in the troposphere, *Atmos. Chem. Phys.*, 10,
2552 7127-7136, 2010b.
- 2553 Prospero, J. M.: Mineral and sea salt aerosol concentrations in various ocean regions, *J.*
2554 *Geophys. Res.-Atmos.*, 84, 725-731, 1979.
- 2555 Prospero, J. M.: Long-range Transport of Mineral Dust in the Global Atmosphere: Impact of
2556 African Dust on the Environment of the Southeastern United States, *Proc. Natl. Acad. Sci. U.*
2557 *S. A.*, 96, 3396-3403, 1999.
- 2558 Raff, J. D., Njegic, B., Chang, W. L., Gordon, M. S., Dabdub, D., Gerber, R. B., and
2559 Finlayson-Pitts, B. J.: Chlorine Activation Indoors and Outdoors via Surface-mediated
2560 Reactions of Nitrogen Oxides with Hydrogen Chloride, *Proc. Natl. Acad. Sci. U. S. A.*, 106,
2561 13647-13654, 2009.
- 2562 Real, E., and Sartelet, K.: Modeling of photolysis rates over Europe: impact on chemical
2563 gaseous species and aerosols, *Atmos. Chem. Phys.*, 11, 1711-1727, 2011.
- 2564 Ren, X., Harder, H., Martinez, M., Leshner, R. L., Oligier, A., Simpas, J. B., Brune, W. H.,
2565 Schwab, J. J., Demerjian, K. L., He, Y., Zhou, X., and Gao, H.: OH and HO₂ Chemistry in
2566 the urban atmosphere of New York City, *Atmos. Environ.*, 37, 3639-3651, 2003.
- 2567 Rkhouak, L., Tang, M. J., Camp, J. C. J., McGregor, J., Watson, I. M., Cox, R. A., Kalberer,
2568 M., Ward, A. D., and Pope, F. D.: Optical trapping and Raman Spectroscopy of solid aerosol
2569 particles, *Phys. Chem. Chem. Phys.*, 16, 11426-11434, 2014.
- 2570 Ro, C. U., Hwang, H., Chun, Y., and Van Grieken, R.: Single-particle characterization of four
2571 "Asian Dust" samples collected in Korea, using low-Z particle electron probe X-ray
2572 microanalysis, *Environ. Sci. Technol.*, 39, 1409-1419, 2005.
- 2573 Rohrer, F., Lu, K. D., Hofzumahaus, A., Bohn, B., Brauers, T., Chang, C. C., Fuchs, H.,
2574 Haseler, R., Holland, F., Hu, M., Kita, K., Kondo, Y., Li, X., Lou, S. R., Oebel, A., Shao, M.,
2575 Zeng, L. M., Zhu, T., Zhang, Y. H., and Wahner, A.: Maximum efficiency in the hydroxyl-
2576 radical-based self-cleansing of the troposphere, *Nature Geoscience*, 7, 559-563, 2014.
- 2577 Romanias, M. N., El Zein, A., and Bedjanian, Y.: Reactive uptake of HONO on aluminium
2578 oxide surface, *J. Photochem. Photobiol. A-Chem.*, 250, 50-57, 2012a.
- 2579 Romanias, M. N., El Zein, A., and Bedjanian, Y.: Heterogeneous Interaction of H₂O₂ with
2580 TiO₂ Surface under Dark and UV Light Irradiation Conditions, *J. Phys. Chem. A*, 116, 8191-
2581 8200, 2012b.
- 2582 Romanias, M. N., El Zein, A., and Bedjanian, Y.: Uptake of hydrogen peroxide on the
2583 surface of Al₂O₃ and Fe₂O₃, *Atmos. Environ.*, 77, 1-8, 2013.
- 2584 Roscoe, J. M., and Abbatt, J. P. D.: Diffuse reflectance FTIR study of the interaction of
2585 alumina surfaces with ozone and water vapor, *J. Phys. Chem. A*, 109, 9028-9034, 2005.
- 2586 Rosenfeld, D., Rudich, Y., and Lahav, R.: Desert dust suppressing precipitation: A possible
2587 desertification feedback loop, *Proc. Natl. Acad. Sci. U. S. A.*, 98, 5975-5980, 2001.
- 2588 Rosenfeld, D., Lohmann, U., Raga, G. B., O'Dowd, C. D., Kulmala, M., Fuzzi, S., Reissell,
2589 A., and Andreae, M. O.: Flood or drought: How do aerosols affect precipitation?, *Science*,
2590 321, 1309-1313, 2008.
- 2591 Rubasinghege, G., and Grassian, V. H.: Surface-Catalyzed Chlorine and Nitrogen Activation:
2592 Mechanisms for the Heterogeneous Formation of ClNO, NO, NO₂, HONO, and N₂O from
2593 HNO₃ and HCl on Aluminum Oxide Particle Surfaces, *J. Phys. Chem. A*, 116, 5180-5192,
2594 2012.
- 2595 Rubasinghege, G., and Grassian, V. H.: Role(s) of Adsorbed Water in the Surface Chemistry
2596 of Environmental Interfaces, *Chem. Commun.*, 49, 3071-3094, 2013.
- 2597 Ryder, O. S., Ault, A. P., Cahill, J. F., Guasco, T. L., Riedel, T. P., Cuadra-Rodriguez, L. A.,
2598 Gaston, C. J., Fitzgerald, E., Lee, C., Prather, K. A., and Bertram, T. H.: On the Role of
2599 Particle Inorganic Mixing State in the Reactive Uptake of N₂O₅ to Ambient Aerosol
2600 Particles, *Environ. Sci. Technol.*, 10.1021/es4042622, 2014.



- 2601 Sassine, M., Burel, L., D'Anna, B., and George, C.: Kinetics of the tropospheric
2602 formaldehyde loss onto mineral dust and urban surfaces, *Atmos. Environ.*, 44, 5468-5475,
2603 2010.
- 2604 Scanza, R. A., Mahowald, N., Ghan, S., Zender, C. S., Kok, J. F., Liu, X., Zhang, Y., and
2605 Albani, S.: Modeling Dust as Component Minerals in the Community Atmosphere Model:
2606 Development of Framework and Impact on Radiative Forcing, *Atmos. Chem. Phys.*, 15, 537-
2607 561, 2015.
- 2608 Scheuven, D., Schütz, L., Kandler, K., Ebert, M., and Weinbruch, S.: Bulk composition of
2609 northern African dust and its source sediments - A compilation, *Earth-Sci. Rev.*, 116, 170-
2610 194, 2013.
- 2611 Schulz, M., Prospero, J. M., Baker, A. R., Dentener, F., Ickes, L., Liss, P. S., Mahowald, N.
2612 M., Nickovic, S., García-Pando, C. P., Rodríguez, S., Sarin, M., Tegen, I., and Duce, R. A.:
2613 Atmospheric Transport and Deposition of Mineral Dust to the Ocean: Implications for
2614 Research Needs, *Environ. Sci. Technol.*, 46, 10390-10404, 2012.
- 2615 Seinfeld, J. H., Carmichael, G. R., Arimoto, R., Conant, W. C., Brechtel, F. J., Bates, T. S.,
2616 Cahill, T. A., Clarke, A. D., Doherty, S. J., Flatau, P. J., Huebert, B. J., Kim, J., Markowicz,
2617 K. M., Quinn, P. K., Russell, L. M., Russell, P. B., Shimizu, A., Shinozuka, Y., Song, C. H.,
2618 Tang, Y., Uno, I., Vogelmann, A. M., Weber, R. J., Woo, J.-H., and Zhang, X. Y.: ACE-
2619 ASIA: Regional Climatic and Atmospheric Chemical Effects of Asian Dust and Pollution,
2620 *Bull. Amer. Meteorol. Soc.*, 85, 367-380, 2004.
- 2621 Seinfeld, J. H., and Pandis, S. N.: *Atmospheric Chemistry and Physics: From Air Pollution to*
2622 *Climate Change*, Wiley Interscience, New York, 2006.
- 2623 Seisel, S., Borensen, C., Vogt, R., and Zellner, R.: Kinetics and Mechanism of the Uptake of
2624 N₂O₅ on Mineral Dust at 298 K, *Atmos. Chem. Phys.*, 5, 3423-3432, 2005.
- 2625 Seyfioglu, R., Odabasi, M., and Cetin, E.: Wet and dry deposition of formaldehyde in Izmir,
2626 Turkey, *Sci. Total Environ.*, 366, 809-818, 2006.
- 2627 Shao, M., Zhang, Y., Zeng, L., Tang, X., Zhang, J., Zhong, L., and Wang, B.: Ground-level
2628 ozone in the Pearl River Delta and the roles of VOC and NO_x in its production, *Journal of*
2629 *Environmental Management*, 90, 512-518, 2009.
- 2630 Shen, X., Zhao, Y., Chen, Z., and Huang, D.: Heterogeneous reactions of volatile organic
2631 compounds in the atmosphere, *Atmos. Environ.*, 68, 297-314, 2013.
- 2632 Shi, Z., Zhang, D., Hayashi, M., Ogata, H., Ji, H., and Fujie, W.: Influences of sulfate and
2633 nitrate on the hygroscopic behaviour of coarse dust particles, *Atmos. Environ.*, 42, 822-827,
2634 2008.
- 2635 Shi, Z. B., Krom, M. D., Jickells, T. D., Bonneville, S., Carslaw, K. S., Mihalopoulos, N.,
2636 Baker, A. R., and Benning, L. G.: Impacts on iron solubility in the mineral dust by processes
2637 in the source region and the atmosphere: A review, *Aeolian Res.*, 5, 21-42, 2012.
- 2638 Shiraiwa, M., Ammann, M., Koop, T., and Pöschl, U.: Gas uptake and chemical aging of
2639 semisolid organic aerosol particles, *Proc. Natl. Acad. Sci. U. S. A.*, 108, 11003-11008, 2011.
- 2640 Shiraiwa, M., Pfrang, C., Koop, T., and Pöschl, U.: Kinetic multi-layer model of gas-particle
2641 interactions in aerosols and clouds (KM-GAP): linking condensation, evaporation and
2642 chemical reactions of organics, oxidants and water, *Atmos. Chem. Phys.*, 12, 2777-2794,
2643 2012.
- 2644 Shirley, T. R., Brune, W. H., Ren, X., Mao, J., Leshner, R., Cardenas, B., Volkamer, R.,
2645 Molina, L. T., Molina, M. J., Lamb, B., Velasco, E., Jobson, T., and Alexander, M.:
2646 Atmospheric oxidation in the Mexico City Metropolitan Area (MCMA) during April 2003,
2647 *Atmos. Chem. Phys.*, 6, 2753-2765, 2006.
- 2648 Sihvonen, S. K., Schill, G. P., Lykтей, N. A., Veghte, D. P., Tolbert, M. A., and Freedman,
2649 M. A.: Chemical and Physical Transformations of Aluminosilicate Clay Minerals Due to



- 2650 Acid Treatment and Consequences for Heterogeneous Ice Nucleation, *J. Phys. Chem. A*, 118,
2651 8787-8796, 2014.
- 2652 Simpson, W. R., Brown, S. S., Saiz-Lopez, A., Thornton, J. A., and Glasow, R. v.:
2653 Tropospheric Halogen Chemistry: Sources, Cycling, and Impacts, *Chem. Rev.*, 115, 4035-
2654 4062, 2015.
- 2655 Sinha, V., Williams, J., Crowley, J. N., and Lelieveld, J.: The Comparative Reactivity
2656 Method ‐ a new tool to measure total OH Reactivity in ambient air, *Atmos. Chem.*
2657 *Phys.*, 8, 2213-2227, 2008.
- 2658 Sobanski, N., Tang, M. J., Thieser, J., Schuster, G., Pöhler, D., Fischer, H., Song, W.,
2659 Sauvage, C., Williams, J., Fachinger, J., Berkes, F., Hoor, P., Platt, U., Lelieveld, J., and
2660 Crowley, J. N.: Chemical and meteorological influences on the lifetime of NO₃ at a semi-
2661 rural mountain site during PARADE, *Atmos. Chem. Phys.*, 16, 4867-4883, 2016.
- 2662 Song, C. H., Kim, C. M., Lee, Y. J., Carmichael, G. R., Lee, B. K., and Lee, D. S.: An
2663 evaluation of reaction probabilities of sulfate and nitrate precursors onto East Asian dust
2664 particles, *J. Geophys. Res.-Atmos.*, 112, D18206, 10.1029/2006jd008092, 2007.
- 2665 Spicer, C. W., Chapman, E. G., Finlayson-Pitts, B. J., Plastringe, R. A., Hubbe, J. M., Fast, J.
2666 D., and Berkowitz, C. M.: Unexpectedly high concentrations of molecular chlorine in coastal
2667 air, *Nature*, 394, 353-356, 1998.
- 2668 Stockwell, W. R.: On the HO₂+HO₂ reaction: its misapplication in atmospheric chemistry
2669 models, *J. Geophys. Res.-Atmos.*, 100, 11695-11698, 10.1029/94jd03107, 1995.
- 2670 Stockwell, W. R., Kirchner, F., Kuhn, M., and Seefeld, S.: A new mechanism for regional
2671 atmospheric chemistry modeling, *J. Geophys. Res.-Atmos.*, 102, 25847-25879, 1997.
- 2672 Stone, D., Whalley, L. K., and Heard, D. E.: Tropospheric OH and HO₂ radicals: field
2673 measurements and model comparisons, *Chem. Soc. Rev.*, 41, 6348-6404, 2012.
- 2674 Striegel, M. F., Bede Guin, E., Hallett, K., Sandoval, D., Swingle, R., Knox, K., Best, F., and
2675 Fornea, S.: Air pollution, coatings, and cultural resources, *Progress in Organic Coatings*, 48,
2676 281-288, 2003.
- 2677 Stutz, J., Alicke, B., and Neftel, A.: Nitrous acid formation in the urban atmosphere: Gradient
2678 measurements of NO₂ and HONO over grass in Milan, Italy, *J. Geophys. Res.-Atmos.*, 107,
2679 8192, doi: 8110.1029/2001jd000390, 2002.
- 2680 Su, H., Cheng, Y. F., Shao, M., Gao, D. F., Yu, Z. Y., Zeng, L. M., Slanina, J., Zhang, Y. H.,
2681 and Wiedensohler, A.: Nitrous acid (HONO) and its daytime sources at a rural site during the
2682 2004 PRIDE-PRD experiment in China, *J. Geophys. Res.-Atmos.*, 113, D14312, doi:
2683 14310.11029/12007jd009060, 2008.
- 2684 Suh, M., Bagus, P. S., Pak, S., Rosynek, M. P., and Lunsford, J. H.: Reactions of hydroxyl
2685 radicals on titania, silica, alumina, and gold surfaces, *J. Phys. Chem. B*, 104, 2736-2742,
2686 2000.
- 2687 Sullivan, R. C., Thornberry, T., and Abbatt, J. P. D.: Ozone decomposition kinetics on
2688 alumina: effects of ozone partial pressure, relative humidity and repeated oxidation cycles,
2689 *Atmos. Chem. Phys.*, 4, 1301-1310, 2004.
- 2690 Sullivan, R. C., Guazzotti, S. A., Sodeman, D. A., and Prather, K. A.: Direct Observations of
2691 the Atmospheric Processing of Asian Mineral Dust, *Atmos. Chem. Phys.*, 7, 1213-1236,
2692 2007.
- 2693 Sullivan, R. C., Moore, M. J. K., Petters, M. D., Kreidenweis, S. M., Roberts, G. C., and
2694 Prather, K. A.: Timescale for Hygroscopic Conversion of Calcite Mineral Particles through
2695 Heterogeneous Reaction with Nitric Acid, *Phys. Chem. Chem. Phys.*, 11, 7826-7837, 2009a.
- 2696 Sullivan, R. C., Moore, M. J. K., Petters, M. D., Kreidenweis, S. M., Roberts, G. C., and
2697 Prather, K. A.: Effect of Chemical Mixing State on the Hygroscopicity and Cloud Nucleation
2698 Properties of Calcium Mineral Dust Particles, *Atmos. Chem. Phys.*, 9, 3303-3316, 2009b.



- 2699 Sun, S., Ding, J., Bao, J., Gao, C., Qi, Z., and Li, C.: Photocatalytic Oxidation of Gaseous
2700 Formaldehyde on TiO₂: An In Situ DRIFTS Study, *Catal. Lett.*, 137, 239-246, 2010.
- 2701 Syomin, D. A., and Finlayson-Pitts, B. J.: HONO decomposition on borosilicate glass
2702 surfaces: implications for environmental chamber studies and field experiments, *Phys. Chem.*
2703 *Chem. Phys.*, 5, 5236-5242, 2003.
- 2704 Ta, W. Q., Xiao, Z., Qu, J. J., Yang, G. S., and Wang, T.: Characteristics of dust particles
2705 from the desert/Gobi area of northwestern China during dust-storm periods, *Environmental*
2706 *Geology*, 43, 667-679, 2003.
- 2707 Taatjes, C. A., Welz, O., Eskola, A. J., Savee, J. D., Scheer, A. M., Shallcross, D. E.,
2708 Rotavera, B., Lee, E. P. F., Dyke, J. M., Mok, D. K. W., Osborn, D. L., and Percival, C. J.:
2709 Direct Measurements of Conformer-Dependent Reactivity of the Criegee Intermediate
2710 CH₃CHOO, *Science*, 340, 177-180, 2013.
- 2711 Taatjes, C. A., Shallcross, D. E., and Percival, C. J.: Research frontiers in the chemistry of
2712 Criegee intermediates and tropospheric ozonolysis, *Phys. Chem. Chem. Phys.*, 16, 1704-
2713 1718, 2014.
- 2714 Tang, M. J., Thieser, J., Schuster, G., and Crowley, J. N.: Uptake of NO₃ and N₂O₅ to
2715 Saharan dust, ambient urban aerosol and soot: a relative rate study, *Atmos. Chem. Phys.*, 10,
2716 2965-2974, 2010.
- 2717 Tang, M. J., Thieser, J., Schuster, G., and Crowley, J. N.: Kinetics and Mechanism of the
2718 Heterogeneous Reaction of N₂O₅ with Mineral Dust Particles, *Phys. Chem. Chem. Phys.*, 14,
2719 8551-8561, 2012.
- 2720 Tang, M. J., Camp, J. C. J., Rkiouak, L., McGregor, J., Watson, I. M., Cox, R. A., Kalberer,
2721 M., Ward, A. D., and Pope, F. D.: Heterogeneous Interaction of SiO₂ with N₂O₅: Aerosol
2722 Flow Tube and Single Particle Optical Levitation-Raman Spectroscopy Studies, *J. Phys.*
2723 *Chem. A*, 118, 8817-8827, 2014a.
- 2724 Tang, M. J., Cox, R. A., and Kalberer, M.: Compilation and Evaluation of Gas Phase
2725 Diffusion Coefficients of Reactive Trace Gases in the Atmosphere: Volume 1. Inorganic
2726 Compounds, *Atmos. Chem. Phys.*, 14, 9233-9247, 2014b.
- 2727 Tang, M. J., Schuster, G., and Crowley, J. N.: Heterogeneous Reaction of N₂O₅ with Illite
2728 and Arizona Test Dust Particles, *Atmos. Chem. Phys.*, 14, 245-254, 2014c.
- 2729 Tang, M. J., Telford, P. J., Pope, F. D., Rkiouak, L., Abraham, N. L., Archibald, A. T.,
2730 Braesicke, P., Pyle, J. A., McGregor, J., Watson, I. M., Cox, R. A., and Kalberer, M.:
2731 Corrigendum to "Heterogeneous reaction of N₂O₅ with airborne TiO₂ particles and its
2732 implication for stratospheric particle injection" published in *Atmos. Chem. Phys.*, 14, 6035-
2733 6048, 2014, *Atmos. Chem. Phys.*, 14, 8233-8234, 10.5194/acp-14-8233-2014, 2014d.
- 2734 Tang, M. J., Telford, P. J., Pope, F. D., Rkiouak, L., Abraham, N. L., Archibald, A. T.,
2735 Braesicke, P., Pyle, J. A., McGregor, J., Watson, I. M., Cox, R. A., and Kalberer, M.:
2736 Heterogeneous reaction of N₂O₅ with airborne TiO₂ particles and its implication for
2737 stratospheric particle injection, *Atmos. Chem. Phys.*, 14, 6035-6048, 2014e.
- 2738 Tang, M. J., Shiraiwa, M., Pöschl, U., Cox, R. A., and Kalberer, M.: Compilation and
2739 evaluation of gas phase diffusion coefficients of reactive trace gases in the atmosphere:
2740 Volume 2. Diffusivities of organic compounds, pressure-normalised mean free paths, and
2741 average Knudsen numbers for gas uptake calculations, *Atmos. Chem. Phys.*, 15, 5585-5598,
2742 2015.
- 2743 Tang, M. J., Cziczo, D. J., and Grassian, V. H.: Interactions of Water with Mineral Dust
2744 Aerosol: Water Adsorption, Hygroscopicity, Cloud Condensation and Ice Nucleation, *Chem.*
2745 *Rev.*, 116, 4205-4259, 2016a.
- 2746 Tang, M. J., Keeble, J., Telford, P. J., Pope, F. D., Braesicke, P., Griffiths, P. T., Abraham, N.
2747 L., McGregor, J., Watson, I. M., Cox, R. A., Pyle, J. A., and Kalberer, M.: Heterogeneous



- 2748 reaction of ClONO₂ with TiO₂ and SiO₂ aerosol particles: implications for stratospheric
2749 particle injection for climate engineering, *Atmos. Chem. Phys.*, 16, 15397-15412, 2016b.
- 2750 Tang, Y., Carmichael, G. R., Kurata, G., Uno, I., Weber, R. J., Song, C. H., Guttikunda, S.
2751 K., Woo, J. H., Streets, D. G., Wei, C., Clarke, A. D., Huebert, B., and Anderson, T. L.:
2752 Impacts of Dust on Regional Tropospheric Chemistry during the ACE-Asia Experiment: a
2753 Model Study with Observations, *J. Geophys. Res.*, 109, D19s21, doi: 10.1029/2003jd003806,
2754 2004.
- 2755 Ten Brink, H. M., and Spoelstra, H.: The dark decay of hono in environmental (SMOG)
2756 chambers, *Atmos. Environ.*, 32, 247-251, 1998.
- 2757 Textor, C., Schulz, M., Guibert, S., Kinne, S., Balkanski, Y., Bauer, S., Berntsen, T., Berglen,
2758 T., Boucher, O., Chin, M., Dentener, F., Diehl, T., Easter, R., Feichter, H., Fillmore, D.,
2759 Ghan, S., Ginoux, P., Gong, S., Grini, A., Hendricks, J., Horowitz, L., Huang, P., Isaksen, I.,
2760 Iversen, I., Kloster, S., Koch, D., Kirkevåg, A., Kristjansson, J. E., Krol, M., Lauer, A.,
2761 Lamarque, J. F., Liu, X., Montanaro, V., Myhre, G., Penner, J., Pitari, G., Reddy, S., Seland,
2762 Ø., Stier, P., Takemura, T., and Tie, X.: Analysis and Quantification of the Diversities of
2763 Aerosol Life Cycles within AeroCom, *Atmos. Chem. Phys.*, 6, 1777-1813, 2006.
- 2764 Tham, Y. J., Wang, Z., Li, Q., Yun, H., Wang, W., Wang, X., Xue, L., Lu, K., Ma, N., Bohn,
2765 B., Li, X., Kecorius, S., Größ, J., Shao, M., Wiedensohler, A., Zhang, Y., and Wang, T.:
2766 Significant concentrations of nitryl chloride sustained in the morning: investigations of the
2767 causes and impacts on ozone production in a polluted region of northern China, *Atmos.*
2768 *Chem. Phys.*, 16, 14959-14977, 2016.
- 2769 Thornton, J., and Abbatt, J. P. D.: Measurements of HO₂ uptake to aqueous aerosol: Mass
2770 accommodation coefficients and net reactive loss, *J. Geophys. Res.-Atmos.*, 110, D08309,
2771 doi: 08310.01029/02004JD005402, 2005.
- 2772 Thornton, J. A., Kercher, J. P., Riedel, T. P., Wagner, N. L., Cozic, J., Holloway, J., S., Dube,
2773 W. P., Wolfe, G. M., Quinn, P. K., Middlebrook, A. M., Alexander, B., and Brown, S. S.: A
2774 large atomic chlorine source inferred from mid-continental reactive nitrogen chemistry,
2775 *Nature*, 464, 271-174, 2010.
- 2776 Tobo, Y., DeMott, P. J., Raddatz, M., Niedermeier, D., Hartmann, S., Kreidenweis, S. M.,
2777 Stratmann, F., and Wex, H.: Impacts of chemical reactivity on ice nucleation of kaolinite
2778 particles: A case study of levoglucosan and sulfuric acid, *Geophys. Res. Lett.*, 39, L19803,
2779 doi: 19810.11029/12012gl053007, 2012.
- 2780 Tong, H. J., Reid, J. P., Bones, D. L., Luo, B. P., and Krieger, U. K.: Measurements of the
2781 timescales for the mass transfer of water in glassy aerosol at low relative humidity and
2782 ambient temperature, *Atmos. Chem. Phys.*, 11, 4739-4754, 2011.
- 2783 Tong, S. R., Wu, L. Y., Ge, M. F., Wang, W. G., and Pu, Z. F.: Heterogeneous Chemistry of
2784 Monocarboxylic Acids on α -Al₂O₃ at Different Relative Humidities, *Atmos. Chem. Phys.*, 10,
2785 7561-7574, 2010.
- 2786 Twohy, C. H., Kreidenweis, S. M., Eidhammer, T., Browell, E. V., Heymsfield, A. J.,
2787 Bansemer, A. R., Anderson, B. E., Chen, G., Ismail, S., DeMott, P. J., and Van den Heever,
2788 S. C.: Saharan Dust Particles Nucleate Droplets in Eastern Atlantic Clouds, *Geophys. Res.*
2789 *Lett.*, 36, L01807, doi: 01810.01029/02008gl035846, 2009.
- 2790 Ullerstam, M., Vogt, R., Langer, S., and Ljungstrom, E.: The kinetics and mechanism of SO₂
2791 oxidation by O₃ on mineral dust, *Phys. Chem. Chem. Phys.*, 4, 4694-4699, 2002.
- 2792 Umann, B., Arnold, F., Schaal, C., Hanke, M., Uecker, J., Aufmhoff, H., Balkanski, Y., and
2793 Van Dingenen, R.: Interaction of mineral dust with gas phase nitric acid and sulfur dioxide
2794 during the MINATROC II field campaign: First estimate of the uptake coefficient
2795 gamma(HNO₃) from atmospheric data, *J. Geophys. Res.-Atmos.*, 110, D22306,
2796 10.1029/2005jd005906, 2005.



- 2797 Underwood, G. M., Li, P., Usher, C. R., and Grassian, V. H.: Determining accurate kinetic
2798 parameters of potentially important heterogeneous atmospheric reactions on solid particle
2799 surfaces with a Knudsen cell reactor, *J. Phys. Chem. A*, 104, 819-829, 2000.
- 2800 Underwood, G. M., Li, P., Al-Abadleh, H., and Grassian, V. H.: A Knudsen Cell Study of the
2801 Heterogeneous Reactivity of Nitric Acid on Oxide and Mineral Dust Particles, *J. Phys. Chem.*
2802 *A*, 105, 6609-6620, 2001.
- 2803 Uno, I., Eguchi, K., Yumimoto, K., Takemura, T., Shimizu, A., Uematsu, M., Liu, Z., Wang,
2804 Z., Hara, Y., and Sugimoto, N.: Asian Dust Transported One Full Circuit around the Globe,
2805 *Nature Geosci.*, 2, 557-560, 2009.
- 2806 Usher, C. R., Michel, A. E., and Grassian, V. H.: Reactions on Mineral Dust, *Chem. Rev.*,
2807 103, 4883-4939, 2003a.
- 2808 Usher, C. R., Michel, A. E., Stec, D., and Grassian, V. H.: Laboratory studies of ozone uptake
2809 on processed mineral dust, *Atmos. Environ.*, 37, 5337-5347, 2003b.
- 2810 Vlasenko, A., Sjogren, S., Weingartner, E., Stemmler, K., Gaggeler, H. W., and Ammann,
2811 M.: Effect of Humidity on Nitric Acid Uptake to Mineral Dust Aerosol Particles, *Atmos.*
2812 *Chem. Phys.*, 6, 2147-2160, 2006.
- 2813 Vlasenko, A., Huthwelker, T., Gaggeler, H. W., and Ammann, M.: Kinetics of the
2814 heterogeneous reaction of nitric acid with mineral dust particles: an aerosol flow tube study,
2815 *Phys. Chem. Chem. Phys.*, 11, 7921-7930, 2009.
- 2816 Wagner, C., Hanisch, F., Holmes, N., de Coninck, H., Schuster, G., and Crowley, J. N.: The
2817 interaction of N₂O₅ with mineral dust: aerosol flow tube and Knudsen reactor studies, *Atmos.*
2818 *Chem. Phys.*, 8, 91-109, 2008.
- 2819 Wagner, C., Schuster, G., and Crowley, J. N.: An aerosol flow tube study of the interaction of
2820 N₂O₅ with calcite, Arizona dust and quartz, *Atmos. Environ.*, 43, 5001-5008, 2009.
- 2821 Wahner, A., Mentel, T. F., and Sohn, M.: Gas-phase reaction of N₂O₅ with water vapor:
2822 Importance of heterogeneous hydrolysis of N₂O₅ and surface desorption of HNO₃ in a large
2823 teflon chamber, *Geophys. Res. Lett.*, 25, 2169-2172, 1998.
- 2824 Walker, R. A., Wilson, K., Lee, A. F., Woodford, J., Grassian, V. H., Baltrusaitis, J.,
2825 Rubasinghege, G., Cibirin, G., and Dent, A.: Preservation of York Minster historic limestone
2826 by hydrophobic surface coatings, *Sci. Rep.*, 2, 880, doi: 810.1038/srep00880, 2012.
- 2827 Wang, K., Zhang, Y., Nenes, A., and Fountoukis, C.: Implementation of Dust Emission and
2828 Chemistry into the Community Multiscale Air Quality Modeling System and Initial
2829 Application to an Asian Dust Storm Episode, *Atmos. Chem. Phys.*, 12, 10209-10237, 2012.
- 2830 Wang, T., Tham, Y. J., Xue, L., Li, Q., Zha, Q., Wang, Z., Poon, S. C. N., Dubé, W. P.,
2831 Blake, D. R., Louie, P. K. K., Luk, C. W. Y., Tsui, W., and Brown, S. S.: Observations of
2832 nitryl chloride and modeling its source and effect on ozone in the planetary boundary layer of
2833 southern China, *J. Geophys. Res.-Atmos.*, 121, 2476-2489, 2016.
- 2834 Wang, W. G., Ge, M. F., and Sun, Q.: Heterogeneous Uptake of Hydrogen Peroxide on
2835 Mineral Oxides, *Chin. J. Chem. Phys.*, 24, 515-520, 2011.
- 2836 Wang, Y. H., and Jacob, D. J.: Anthropogenic forcing on tropospheric ozone and OH since
2837 preindustrial times, *J. Geophys. Res.-Atmos.*, 103, 31123-31135, 1998.
- 2838 Wayne, R. P., Barnes, I., Biggs, P., Burrows, J. P., Canosamas, C. E., Hjorth, J., Lebras, G.,
2839 Moortgat, G. K., Perner, D., Poulet, G., Restelli, G., and Sidebottom, H.: The nitrate radical-
2840 physics, chemistry, and the atmosphere, *Atmos. Environ.*, 25A, 1-203, 1991.
- 2841 Webb, A. H., Bawden, R. J., Busby, A. K., and Hopkins, J. N.: Studies on the effects of air
2842 pollution on limestone degradation in Great Britain, *Atmos. Environ.*, 26, 165-181, 1992.
- 2843 Weisenstein, D. K., Keith, D. W., and Dykema, J. A.: Solar geoengineering using solid
2844 aerosol in the stratosphere, *Atmos. Chem. Phys.*, 15, 11835-11859, 2015.



- 2845 Welz, O., Savee, J. D., Osborn, D. L., Vasu, S. S., Percival, C. J., Shallcross, D. E., and
 2846 Taatjes, C. A.: Direct Kinetic Measurements of Criegee Intermediate (CH₂OO) Formed by
 2847 Reaction of CH₂I with O₂, *Science*, 335, 204-207, 2012.
- 2848 Wesely, M. L., and Hicks, B. B.: A review of the current status of knowledge on dry
 2849 deposition, *Atmos. Environ.*, 34, 2261-2282, 2000.
- 2850 Wex, H., DeMott, P. J., Tobo, Y., Hartmann, S., Rösch, M., Clauss, T., Tomsche, L.,
 2851 Niedermeier, D., and Stratmann, F.: Kaolinite particles as ice nuclei: learning from the use of
 2852 different kaolinite samples and different coatings, *Atmos. Chem. Phys.*, 14, 5529-5546, 2014.
- 2853 Whalley, L. K., Edwards, P. M., Furneaux, K. L., Goddard, A., Ingham, T., Evans, M. J.,
 2854 Stone, D., Hopkins, J. R., Jones, C. E., Karunaharan, A., Lee, J. D., Lewis, A. C., Monks, P.
 2855 S., Moller, S. J., and Heard, D. E.: Quantifying the magnitude of a missing hydroxyl radical
 2856 source in a tropical rainforest, *Atmos. Chem. Phys.*, 11, 7223-7233, 2011.
- 2857 Wood, E. C., Bertram, T. H., Wooldridge, P. J., and Cohen, R. C.: Measurements of N₂O₅,
 2858 NO₂, and O₃ east of the San Francisco Bay, *Atmos. Chem. Phys.*, 5, 483-491, 2005.
- 2859 Wu, L.-Y., Tong, S.-R., Zhou, L., Wang, W.-G., and Ge, M.-F.: Synergistic Effects between
 2860 SO₂ and HCOOH on α -Fe₂O₃, *J. Phys. Chem. A*, 117, 3972-3979, 2013a.
- 2861 Wu, L., Tong, S., and Ge, M.: Heterogeneous Reaction of NO₂ on Al₂O₃: The Effect of
 2862 Temperature on the Nitrite and Nitrate Formation, *J. Phys. Chem. A*, 117, 4937-4944, 2013b.
- 2863 Wu, L. Y., Tong, S. R., Wang, W. G., and Ge, M. F.: Effects of temperature on the
 2864 heterogeneous oxidation of sulfur dioxide by ozone on calcium carbonate, *Atmos. Chem.*
 2865 *Phys.*, 11, 6593-6605, 2011.
- 2866 Xu, B. Y., Zhu, T., Tang, X. Y., Ding, J., and Li, H. J.: Heterogeneous reaction of
 2867 formaldehyde on surface of α -Al₂O₃ particles, *Chemical Journal of Chinese Universities-*
 2868 *Chinese*, 27, 1912-1917, 2006.
- 2869 Xu, B. Y., Zhu, T., Tang, X. Y., and Shang, J.: Heterogeneous reaction of formaldehyde on
 2870 the surface of TiO₂ particles, *Sci. China-Chem.*, 53, 2644-2651, 2010.
- 2871 Xu, B. Y., Shang, J., Zhu, T., and Tang, X. Y.: Heterogeneous reaction of formaldehyde on
 2872 the surface of γ -Al₂O₃ particles, *Atmos. Environ.*, 45, 3569-3575, 2011.
- 2873 Yang, W. W., He, H., Ma, Q. X., Ma, J. Z., Liu, Y. C., Liu, P. F., and Mu, Y. J.: Synergistic
 2874 formation of sulfate and ammonium resulting from reaction between SO₂ and NH₃ on typical
 2875 mineral dust, *Phys. Chem. Chem. Phys.*, 18, 956-964, 2016a.
- 2876 Yang, Y., Shao, M., Wang, X., Nölscher, A. C., Kessel, S., Guenther, A., and Williams, J.:
 2877 Towards a quantitative understanding of total OH reactivity: A review, *Atmos. Environ.*, 134,
 2878 147-161, 2016b.
- 2879 Yi, J., Bahrini, C., Schoemaeker, C., Fittschen, C., and Choi, W.: Photocatalytic
 2880 Decomposition of H₂O₂ on Different TiO₂ Surfaces Along with the Concurrent Generation of
 2881 HO₂ Radicals Monitored Using Cavity Ring Down Spectroscopy, *J. Phys. Chem. C*, 116,
 2882 10090-10097, 2012.
- 2883 Zhang, Q., Streets, D. G., He, K., Wang, Y., Richter, A., Burrows, J. P., Uno, I., Jang, C. J.,
 2884 Chen, D., Yao, Z., and Lei, Y.: NO_x emission trends for China, 1995–2004: The view from
 2885 the ground and the view from space, *J. Geophys. Res.-Atmos.*, 112, D22306, doi:
 2886 10.1029/2007JD008684, 2007.
- 2887 Zhang, X. Y., Gong, S. L., Shen, Z. X., Mei, F. M., Xi, X. X., Liu, L. C., Zhou, Z. J., Wang,
 2888 D., Wang, Y. Q., and Cheng, Y.: Characterization of soil dust aerosol in China and its
 2889 transport and distribution during 2001 ACE-Asia: 1. Network observations, *J. Geophys. Res.-*
 2890 *Atmos.*, 108, 4206, doi: 10.1029/2002jd002632, 2003.
- 2891 Zhang, Y., Young, S. W., Kotamarthi, V., and Carmichael, G. R.: Photochemical Oxidant
 2892 Processes in the Presence of Dust: An Evaluation of the Impact of Dust on Particulate Nitrate
 2893 and Ozone Formation, *J. Appl. Met.*, 33, 813-824, 1994.



- 2894 Zhao, D. F., Zhu, T., Chen, Q., Liu, Y. J., and Zhang, Z. F.: Raman micro-spectrometry as a
2895 technique for investigating heterogeneous reactions on individual atmospheric particles, *Sci.*
2896 *China-Chem.*, 54, 154-160, 2011a.
- 2897 Zhao, X., Kong, L. D., Sun, Z. Y., Ding, X. X., Cheng, T. T., Yang, X., and Chen, J. M.:
2898 Interactions between Heterogeneous Uptake and Adsorption of Sulfur Dioxide and
2899 Acetaldehyde on Hematite, *J. Phys. Chem. A*, 119, 4001-4008, 2015.
- 2900 Zhao, Y., Chen, Z. M., Shen, X. L., and Zhang, X. A.: Kinetics and Mechanisms of
2901 Heterogeneous Reaction of Gaseous Hydrogen Peroxide on Mineral Oxide Particles, *Environ.*
2902 *Sci. Technol.*, 45, 3317-3324, 2011b.
- 2903 Zhao, Y., Chen, Z. M., Shen, X. L., and Huang, D.: Heterogeneous reactions of gaseous
2904 hydrogen peroxide on pristine and acidic gas-processed calcium carbonate particles: Effects
2905 of relative humidity and surface coverage of coating, *Atmos. Environ.*, 67, 63-72, 2013.
- 2906 Zhou, L., Wang, W. G., and Ge, M. F.: Temperature Dependence of Heterogeneous Uptake
2907 of Hydrogen Peroxide on Silicon Dioxide and Calcium Carbonate, *J. Phys. Chem. A*, 116,
2908 7959-7964, 2012.
- 2909 Zhou, L., Wang, W. G., Gai, Y. B., and Ge, M. F.: Knudsen cell and smog chamber study of
2910 the heterogeneous uptake of sulfur dioxide on Chinese mineral dust, *J. Environ. Sci.*, 26,
2911 2423-2433, 2014.
- 2912 Zhou, L., Wang, W. G., Ge, M. F., and Tong, S. R.: Heterogeneous uptake of gaseous
2913 hydrogen peroxide on mineral dust, *J. Environ. Sci.*, 28, 44-50, 2016.
- 2914 Zhu, S., Butler, T., Sander, R., Ma, J., and Lawrence, M. G.: Impact of Dust on Tropospheric
2915 Chemistry over Polluted Regions: a Case Study of the Beijing Megacity, *Atmos. Chem.*
2916 *Phys.*, 10, 3855-3873, 2010.
- 2917 Zhu, T., Shang, J., and Zhao, D. F.: The roles of heterogeneous chemical processes in the
2918 formation of an air pollution complex and gray haze, *Sci. China-Chem.*, 54, 145-153, 2011.
2919